A citrullination-deficient zebrafish model reveals a

role for Padi2 in fin regeneration

By

Netta Golenberg

A dissertation submitted in partial fulfillment of

the requirements for the degree of

Doctor of Philosophy

(Cellular and Molecular Biology)

at the

UNIVERSITY OF WISCONSIN-MADISON

2019

Date of final oral examination: 6/25/2019

This dissertation is approved by the following members of the Final Oral Committee:

Arash Bashirullah, Associate Professor, Pharmaceutical Sciences

William M. Bement, Professor, Integrative Biology

Anna Huttenlocher, Professor, Pediatrics and Medical Microbiology & Immunology

Phillip A. Newmark, Professor, Integrative Biology

Rupa Sridharan, Assistant Professor, Cell and Regenerative Biology

Table of Contents

Abstract

The study of regenerative medicine is essential to identify both common cellular pathways activated during efficient regeneration and the detrimental responses that are responsible for poor regeneration in human wound healing. Mammals have limited regenerative capacity with wound healing resulting in the maintenance of structural integrity, but the loss of organ/tissue function. Mammalian wounds have persistent leukocyte recruitment and the deposition of a fibrin-rich scar. Conversely, a hallmark of efficient regeneration in multiple regenerative model organisms is the presence of a mesenchymal-cell signaling center called the blastema which is responsible for promoting cell proliferation. In simpler vertebrate models of regeneration, early signals have been identified that are required for late-stage regeneration including early calcium signaling. However, the mechanism by which early calcium flux promotes late regeneration is unknown. This dissertation focuses on the function of the calcium-dependent enzyme, Peptidylarginine deiminase-2 (Padi2) and its enzymatic activity, citrullination. PADI enzymes are known to play a pathogenic role in autoimmune disorders and have recently been associated with pluripotency in stem cells. We first sought to develop a loss-of-function mutant for zebrafish Padi2 and demonstrated that although Padi2 mutant zebrafish lack citrullination, the mutants are viable and fertile. Examination of cellular development revealed that *padi2*-mutant larvae have increased neuromuscular junctions. We characterized the role of citrullination during regeneration and discovered a localized group of cells with citrullinated histones activated upon wounding. Loss of Padi2 in our mutant resulted in the absence of wound-induced citrullination of histones and impaired fin regeneration after tail transection. During

regeneration, Padi2-mutants had increased and persistent neutrophil recruitment to the wound and decreased wound proliferation when compared to wildtype larvae. We have demonstrated a positive role of citrullination in regeneration, potentially through the promotion of a stem-cell like state within the premature blastema. Together, our results demonstrate that citrullination plays a role in neuromuscular development and in the regenerative wound response. These findings identify a new role for citrullination in wound healing and has implications to citrullination-related diseases including autoimmune disorders and cancers.

Acknowledgements

I first want to thank Dr. Anna Huttenlocher, my graduate advisor, for welcoming me into her lab. Her mentorship and guidance allowed me to grow as a scientist and become an independent thinker. Thank you for the many professional experiences and opportunities throughout the years and the support with my work.

I would also like to thank my thesis committee members- Dr. Bill Bement, Dr. Rupa Sridharan, Dr. Arash Bashirullah, and Dr. Phillip Newmark - for their time, input, and scientific and professional guidance. Additionally, I need to thank Dr. Christina Hull who provided me not only with an amazing opportunity to develop my scientific communication skills through MBTG, but also invaluable personal support and professional mentorship.

My time in Madison has brought some wonderful friendships into my life. I was lucky to start my graduate career with an amazing cohort that became instant friends. I particularly want to thank Tricia and Ray; I have been spoiled with delicious food and drinks throughout the years and unending support from them.

A wonderful surprise, has been the family I have gained with my lab mates. The hours spent at the lab and the critical environment that science requires can make for an intense work environment. Despite these pressures, the Hutt labbers have been a main source of my sanity. I owe a huge appreciation to David and Julie, for not only making the lab run smoothly, but both for being integral in the completion of my work. A special thank you to Beth and Will who welcomed me into the lab early on. The long conversations I've had with them outside the lab have reminded me of the importance of

work/life balance. They are examples that success and happiness are not mutually exclusive.

To all the post-docs and my team of lab ladies, thank you, I could not have completed this work without your encouragement, discussions, editing, and friendships. Sofia, thank you for your warmth and for welcoming me into your family. To Laurel, for being the designated fun coordinator and Madison liaison. They both gave me many hours of their time to discuss results, edit many drafts, and gave me endless encouragement. And I owe a huge acknowledgement to Emily. She is a brilliant scientist and I am so lucky to have gotten her input on my work. She was pivotal to my project especially during the long stretches of extended difficulties and disappointments. Emily, thank you for the time you always made for me in and outside the lab. And finally, to my classmate, labmate, deskmate, and friend, Francisco. We started this together and I find no better way to finish this journey than with him. I am so proud of the scientist he has become and look forward to seeing the success he will achieve in the future. He has been an unwavering source of positivity through my grumpiness in the office. Francisco, thank you for your tolerance and for answering all my stupid fish questions.

Thank you to my family. To my siblings, Lavie and Nurit, I have always looked up to both of you and the success you both have found in your lives. Thank you for growing our family with both of yours; they are a constant reminder to laugh and love. I want to particularly thank my parents. You both have instilled a strong sense of integrity in my life and I believe that has driven me academically throughout the years. Your love and support has been unyielding during my time in graduate school. Abba, thank you for your thoughtful input on my work, your constant encouragement, and professional

accountability; you have always been my secret weapon. Ima, you always emphasized the importance of friendship and family and putting my work in perspective of how it feeds my soul. It is because of your encouragement and understanding of what makes us tick that I felt the freedom to explore my passions. Your constant love and support have driven my confidence in who I have become and who I want to be outside the lab. You have always been my biggest cheerleader.

To my loving partner, Eli, I could have never accomplished this without your encouragement. You listened through all the tears and made me laugh after bad days. You were the first to celebrate even the smallest of wins and never failed to tell me how proud you were of me. Thank you for your patience and love over these years.

Chapter 1

Introduction

Regeneration

Regeneration-clinical impact

Regeneration is considered the regrowth or replacement of lost cells, tissues, and organs. The degree to which different organisms and even different tissues can regenerate is variable. Harnessing diverse animal models with a range of regenerative abilities allows for the dissection of the differences and similarities in regenerative capabilities and key mechanisms to enhance our understanding of human wound healing. Humans have poor regenerative capacity, where commonly, humans heal a wound with the excessive recruitment of immune cell and the formation of a collagen-rich scar [1]. In severe wounds, humans replace the lost tissue or organ with fibrotic tissue which can lead to detrimental consequences such congestive heart failure or loss of a limb [2]. This makes the understanding of wound healing and regeneration of clinical importance. Mammalian regeneration is known to occur in select organs, including juvenile digit tips, the liver, and the intestine. The mammalian regenerative mechanism in these organs rely heavily on multipotent stem cells in the regenerating tissue. Interestingly, mammalian digit regeneration has key cellular requirements first described in *Xenopus* [3, 4]. Full understanding of the regenerative mechanism can only be gained through the *in vivo* study of complex multicellular tissues. Insight from diverse model systems for common regenerative processes in efficient regenerators can provide the biomedical understanding to potentially improve human healing.

Zebrafish models for regeneration

Zebrafish (*Danio rerio*) are an optimal model for the study of regeneration as they have a high regenerative capacity for most of their tissues and organs and maintain this regenerative ability in adulthood. Zebrafish models have been established to study some of the most important clinical challenges in the regeneration field such as the spinal cord and brain tissue, heart, liver, and optic nerves [5]. The finding of several common signaling pathways that are necessary for proper regeneration in both the heart and fin [6] allows for the possibility of a general regenerative response mechanism and is a powerful tool when applied to understand why mammals do not regeneration most tissues.

Zebrafish brood sizes are large, develop quickly, and require low maintenance. At larval stages, fish are small and transparent and easily immobilized for live imaging. Zebrafish are genetically amenable to the production of mutant lines and transgenics or transient knockdown with morpholino and have a nearly completely sequenced genome with orthologues for approximately 70% of the human genome [7]. They can easily be used for large drug screens by simply bathing the larvae in pharmaceutical-containing water. Finally, zebrafish have a highly conserved immune system [8] that allows for the study of the innate immune system without the presence of the adaptive immune system which develops at 10 days post fertilization (dpf).

The larval fin fold is a particularly simple and convenient model for studying limb regeneration. The larval fin fold when transected around 2-3 dpf will fully regenerate within 3-4 days post wounding (dpw) [9]. While less developed than the adult regeneration caudal fin model, the time and convenience of the larval fin model make it advantageous to study as it has been shown to use similar mechanisms for

regeneration as adult fin regeneration [9, 10]. At this stage of development, this tissue is relatively simple, with the epidermis being two cell-layers thick, supported by collagen-rich structural fibers [11]. In association with these structural fibers are mesenchymal cells in the center of the fin fold [11]. Also found scattered in the fin fold are sensory neurons, leukocytes, and pigment cells. The fin regeneration model has been modified to include the study of tail excisions, which includes the removal and regeneration of the neural tube, notochord, muscle, and blood vessels [12]. This wound results in a group of cells called the notochord bead [13], which has also been described in tadpole tail regeneration [14], making this simple tissue an excellent model of mammalian skin wounds and limb or digit regeneration.

Epimorphic fin fold regeneration overview

Zebrafish exhibit a type of regeneration called epimorphic regeneration which is characterized by the presence of a mass of proliferative, pluripotent mesenchymal cells called the blastema [5, 15]. Regeneration can be divided into three stages: wound healing (~seconds-hours), blastema formation (~hours-2 dpa), and regenerative outgrowth (~ until 4 dpa) (Fig 1.1).

Early wound signals

Upon wounding, early signals are released to ensure proper wound closure and even late stage signaling. The earliest damage associated molecular pattern (DAMP) is the release of ATP potentially through mechanical stress or by the damaged cells [16]. Within seconds, calcium is elevated intracellularly particularly at the wound edge and in the keratinocytes [17] and remains elevated for an extended period of time up to an

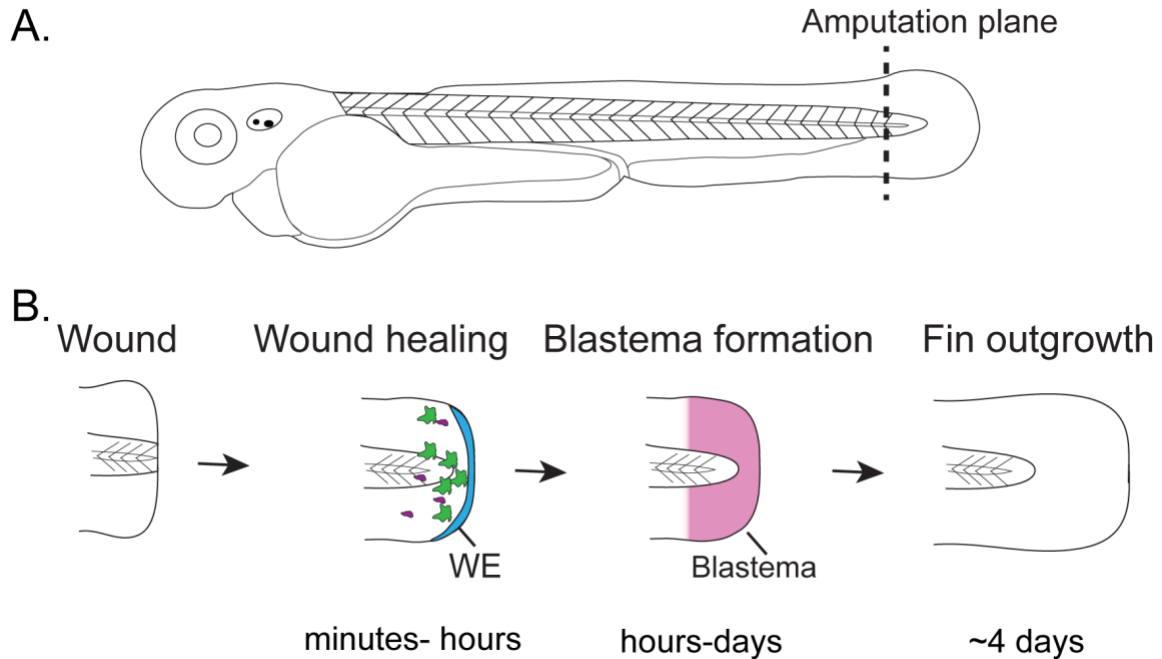**Fig 1.1: Stages of fin regeneration.** (A) Diagram of caudal fin tail amputation. The amputation plane is designated by a dashed line. (B) Stages of regeneration. Wound healing: formation of the wound epithelium (WE-blue) and leukocyte recruitment (neutrophils in purple and macrophages in green). Blastema formation: The immature blastema is labeled in pink. Fin outgrowth: Proliferation promotes restoration of the fin tissue.

hour. Within minutes of wounding, there is a release of reactive oxygen species (ROS) such as H_2O_2 [18, 19]. Some have suggested that these signals act within a sequence with ATP released from damaged cells activating purinergic receptors in neighboring cells to cause the increase of intracellular calcium concentrations, which in turn activates DUOX for the synthesis and release of ROS [16, 20]. The following sections will incorporate the downstream effects of these early signals (Fig 1.2).

Wound healing

In the initial wound healing stage of regeneration, within 10 minutes after wounding, the fin begins to contract. This contraction is driven by the formation of an actomyosin cable [9, 11]. Previous work in *Xenopus laevis* oocytes and *C. elegans* epithelial cells propose that early wound calcium may drive this contraction through Rho GTPases (Fig 1.2) [21, 22]. This contraction promotes epithelial cells to migrate over the wound to form the wound epithelium, also called the apical epithelial cap (AEC), marked by *dlx* expression (Fig 1.1) [9, 23]. This is a proliferation independent event, driven by migration with the eventual thickening of this epithelial region [23-25]. This acts as a clot sealing the wounded tissue and occurs simultaneously with leukocyte recruitment [25].

Wound healing is marked by inflammation with the infiltration of innate immune cells, neutrophils and macrophages, to the site of damage [26]. Leukocyte migration to an injury is observed within minutes of wounding with neutrophil recruitment occurring first and macrophages arriving later [27]. Early wound ROS recruits leukocytes to a wound by activating the Src family kinase, Lyn, and through the establishment of a Cxcl8 gradient (Fig 1.2) [18, 19, 28]. Neutrophils resolve quickly and are absent from the damaged tissue by 12 hpw, while macrophages remain at the wound for an
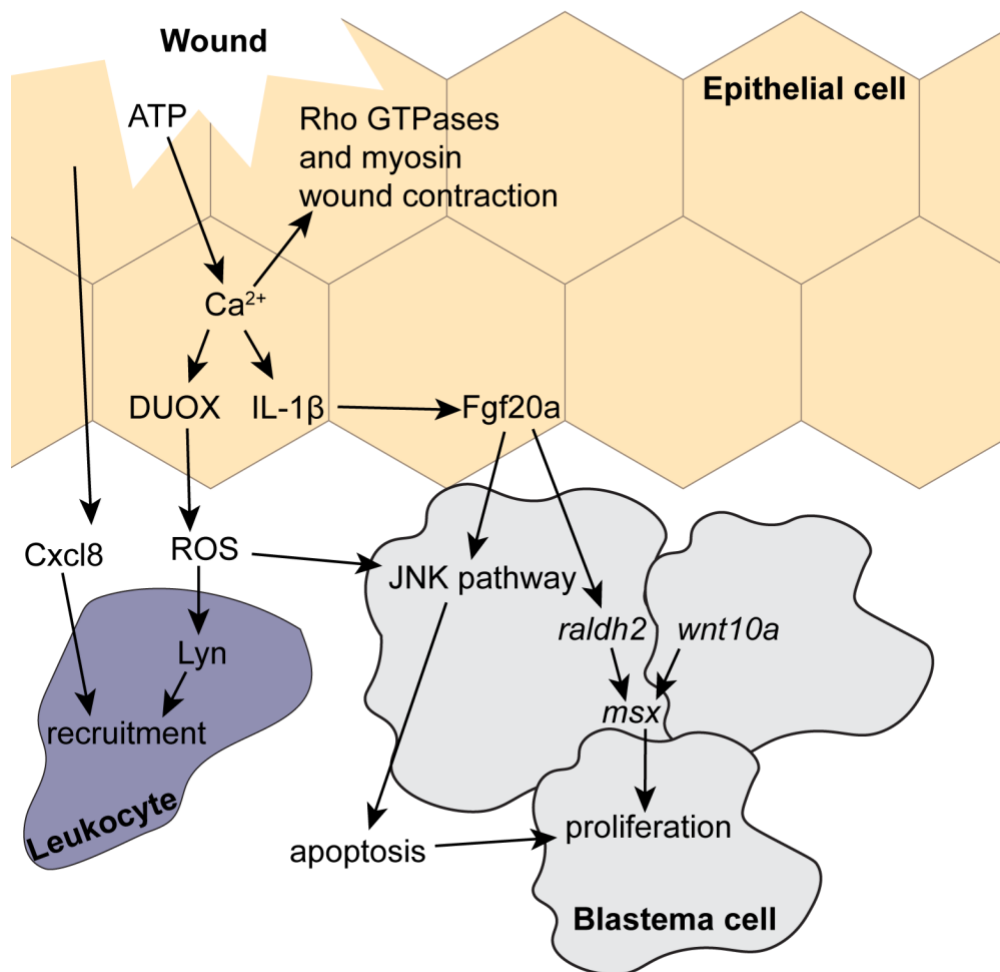
Fig 1.2: Signaling network during fin regeneration. Early wound signals such as ATP, calcium, and ROS activate wound closure, leukocyte recruitment, blastema formation, and proliferation during regeneration. Details in text. Adapted from Roehl, H. H., 2017.

extended period [27]. These differences in response reflect each leukocyte's role during wound healing. Neutrophils are necessary for microbial clearance from a wound, macrophage recruitment, and dampening of further neutrophil chemotactic cues [29]. In contrast, macrophages are essential for wound healing as they remove cellular debris from the healing tissue [30]. This is further confirmed by studies indicating that macrophages promote regeneration [31-33]. These studies support a model in which leukocytes contribute to the regulation of damage cues rather than directly initiating regeneration. Work from the Kawakami lab showed that macrophages release a diffusible signal that is required for dampening interleukin-1beta (IL-1β) expression, a signal necessary to promote proliferation, but when inappropriately maintained induces apoptosis [34, 35]. In contrast to macrophages, neutrophils are thought to be deleterious to regeneration [31]. This zebrafish work, is in agreement with clinical observation of improper, excessive, or sustained neutrophil response being associated with delayed or failed wound healing [36].

Blastema formation

The wound epithelium signals to underlying cells for the proliferation and organization of underlying mesenchymal cells to form the blastema (Fig 1.1) [9]. Cells that give rise to the blastema originate around the notochord [11], although it is still unclear the exact source of these cells; whether they form from dedifferentiation, lineage restricted cells or from the activation of quiescent pluripotent stem cells as conflicting mechanisms have been reported in multiple organisms and tissues [5, 37-40]. The wound epithelium signals to the underlying cells through developmental signaling pathways Wnt and Fgf to activate the expression of msh-homeobox family of

transcription factors (*msx*), retinoic acid synthesis gene *raldh2*, and activation of the

JNK stress response pathway for the reorganization of mesenchymal cells (Fig 1.2) [41-

44]. Interestingly, *msxb/c* are orthologues of the mammalian *Msx1* gene, an inducer and

maintainer of dedifferentiation in mammalian cells supporting the establishment of the

blastema through dedifferentiation [5].

Following injury and the formation of an immature blastema there is an induction

of proliferation in the distal most region of the fin (*msx* expressing region). Early calcium

induced IL-1β in the epidermis induce wound proliferation through expression of Fgf20

and Junba (JNK pathway) [17, 34, 45]. Epithelial ROS is also essential for stimulating

proliferation, again by stimulating the JNK pathway, blastema-activated apoptosis, SFK

signaling, and essential axon regeneration (Fig 1.2) [17, 46, 47]. As the regenerative

process shifts from blastema formation to fin outgrowth, the blastema segregates into

the highly proliferative proximal blastema, and the distal blastema marked by non-

proliferative or slow-dividing cells (Fig 1.3) [9, 10].

Regenerative outgrowth

The transition from blastema formation to outgrowth is marked by an increase in

the cell cycle rate of the blastema compared to the slow proliferation observed during

blastema formation [5, 24]. The outgrowth phase is also marked by the

compartmentalization of the blastema into the distal blastema directly adjacent to the

wound epithelium and the proximal blastema. *msxb* expression becomes restricted to

the distal blastema and is necessary for the maintenance of undifferentiated progenitor

cells. Anterior to the distal blastema is the proximal blastema marked by a proliferation

gradient [24]. Adjacent to the proximal blastema is a region of little proliferation known
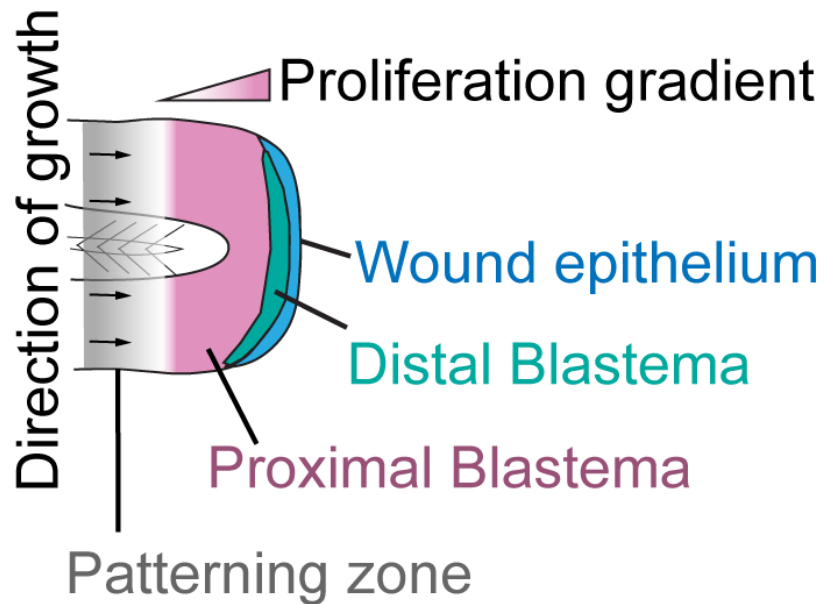
Fig 1.3: Maturation of the blastema during regenerative outgrowth. The premature

blastema segregates into the distal blastema in green and the proliferating proximal

blastema in pink. The patterning zone is in grey.

as the patterning zone (Fig1.3) [24]. This points to a mechanism where regenerating

tissue is pushed out by the proximal tissue patterning. Additionally, ROS-dependent

vimentin expression is required for collagen fiber projection formation during regenerate

outgrowth [48]. Lebert *et al*'s work provides structural evidence of this proximal pushing

of the regenerating fins, as collagen projections were associated with epithelial

projections.

Epigenetic regulation of fin regeneration

Epigenetic regulation plays a crucial role in proper zebrafish fin regeneration. In

the adult caudal fin model, DNA methylation is reduced in the blastema and

reestablished by the late-stage expression of three DNA methyltransferases once

regeneration is completed [49, 50]. The exact role of DNA methylation in fin

regeneration is not known. Epigenetic histone modifications are also dynamic during

regeneration as Saxena *et al*. reported an increase in the activating histone H3 lysine

(H3K4) methylation and (H3K9K14) acetylation. Repressive Histone H3K9 and H4K20

methylation were observed to be slightly delayed [51]. Loss of the repressive H3K27

methylation is required for regeneration as a loss-of-function mutation of H3K27me^3

demethylase results in impaired regeneration [52]. Conversely, inhibition of the EZH2

histone H3K27 methylation also resulted in impaired regeneration [53]. Corresponding

to dynamic histone modifications, components of the nucleosome remodeling and

deacetylase complex (NuRD) are upregulated in the blastema and are required for

redifferentiation [54]. These studies indicate that dynamic epigenetic modifications act

as a regulatory mechanism of transcription during regeneration.

The human proteome is larger than the number of human genes [55]. Protein diversity is required to perform an expansive number of tightly controlled cell functions. In addition to alternative mRNA splicing to account for this difference, another source of expansion of the function of proteins is through post-translational modifications. Post-translational modifications can affect a protein's physical conformation, stability and proteolytic susceptibility, activity, and binding partners. The need to quickly respond to damage by activating wound response pathways leads us to explore the role of protein modifications on the pool of available proteins within the cell. This work will focus on a single post-translational modification, citrullination. With its role in pluripotency and inflammation regulation, we explore a potential role for protein citrullination in wound healing and regeneration.

Citrullination

Free citrulline was first isolated from watermelon (*Citrullus*) in the 1930s lending to its name. It was not until the 1960's that peptidyl-citrulline was discovered within hair follicles [56]. There is no tRNA for citrulline; therefore, peptidyl-citrulline must be produced post-translationally. This post-translational modification is known as citrullination. Citrullination is catalyzed by a family of calcium-dependent enzymes called peptidylarginine deiminases (PADIs or PADs). PADIs are unable to produce free citrulline. Instead, citrulline is naturally formed as an intermediate in the urea cycle and is a byproduct in the production of nitric oxide. Citrullination is the conversion of a peptidyl-arginine to peptidyl-citrulline through hydrolysis and a release of ammonia (Fig 1.4). This deimination of an arginine results in a less than one Dalton increase in the
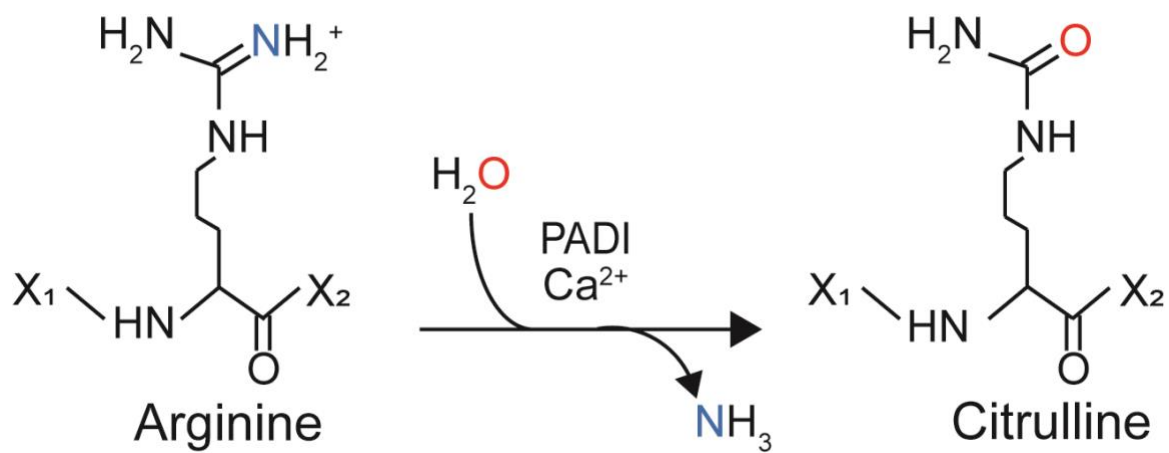
Fig 1.4: Citrullination of peptidyl-arginine by PADI.

molecular mass but, more importantly, alters the positively charged amino acid into a neutrally charged non-standard amino acid [57].

Background of PADIs

PADIs are present in the vertebrate lineage and have been identified in mammals, chickens, frogs, and boney fish. There are five mammalian PADI enzymes within a gene cluster on chromosome 1 in humans. They share 50-70% sequence similarity and function as head-to-tail homodimers [58]. These five isozymes are believed to be the result of gene duplications and mutations, leading to their tissue-specific expression patterns and substrate specialization (Fig 1.5). Fungal and bacterial "PADI" enzymes have been isolated although the relation to mammalian PADIs is in question because of differences in their calcium-dependence and free vs peptidyl-arginine preferences [59, 60].

While there is no single consensus sequence for all the diverse PADI targets, trends for the preferences of deimination have been reported, with primary and secondary structure of the substrate being determinates of deimination susceptibility. Flanking residues of arginine determine susceptibility, with arginine flanked by prolines or glutamic acid impeding citrullination and arginine followed by another arginine, aspartic acid, or glycine resulting in rapid citrullination [61]. The position within the protein will also determine the prevalence of citrullination with arginine near either terminus having low deimination efficiency [62]. Citrullination is affected by the secondary structure of substrates where citrullination of arginine in Beta turns and disordered protein regions is favored as opposed to in alpha helices where deimination

	Tissue distribution	Substrates	Physiological functions	Pathology
PADI1	Epidermis, stomach, uterus	Keratin, Filaggrin	Skin keratinization, skin moisturizing factor	Psoriasis
PADI2	Epidermis, CNS, immune cells, uterus, kidney	Histones, MBP, GFAP, Vimentin, RNA Pol II	Gene regulation, myelin formation, immunity	Multiple sclerosis, Alzheimer's disease
PADI3	Hair follicles, epidermis	Trichohyalin, Filaggrin	Structural maintenance in hair and skin	
PADI4	Immune cells	Histones, Collagen type I, Vimentin, Fibrin, HP1γ	Gene regulation, NET formation, immunity	Rheumatoid arthritis, multiple sclerosis, cancer
PADI6	Ovary, oocytes, embryo, testis	Unknown	Embryonic development	Female infertility

Fig 1.5: Tissue localization, substrates, and functions of mammalian PADI isozymes. Adapted from Amin, B. and Voelter, W., 2017.

is rare [63]. These are, however, reported preferred substrates rather than strict rules, exemplified by human PADI4 having a higher substrate flanking amino acid specificity than human PADI2 [57].

Five mammalian PADI enzymes

PADI1

PADI1 is expressed in the epidermis, stomach, and uterus [64, 65]. Its main substrates are keratin and filaggrin with deimination leading to the maturation and structural network of the epidermis [66]. Filaggrin has a net-positive charge which is necessary to form tight bundles with negatively-charged keratin intermediate filaments [63]. Deimination of filaggrin results in a loss of the positive charge leading to its dissociation and subsequent degradation. Due to this process, the skin produces a natural moisturizing factor that is necessary for the epidermal barrier functions [67, 68]. Loss of PADI1 citrullination of keratin K1 has been linked to psoriasis [69]. PADI1 exists as a monomer rather than a homodimer as observed with PADI2-4 [70].

PADI2

PADI2 is thought to be the ancestral PADI enzyme and has the broadest tissue expression, with distribution in many tissues including the skin, central nervous system, hematopoietic cells, uterus, and kidney [71]. PADI2 is localized primarily in the cytoplasm and lacks a nuclear localization signal, although there has been evidence of nuclear localization and citrullination of Histones H3 and H4 by PADI2 [72, 73]. Below the role of PADI2 in regulating gene expression is discussed in detail. In the brain, two major targets for citrullination are myelin basic protein, a component of the protective myelin sheaths of axons, and glial fibrillary acidic protein, a component of the

intermediate filament expressed in glial cells [71]. Interestingly, the degree of MBP citrullination correlates with brain plasticity as almost all MBP is deiminated in children under two years old while in adults about 20% of MBP is citrullinated in the brain [74, 75]. Hyper citrullination of MBP and GFAP are associated with MS and Alzheimer's disease [76-78]. In macrophages and skeletal muscle, the intermediate filament, vimentin, is a natural substrate of PADI2 [79]. Citrullination of Vimentin causes a collapse of the vimentin cytoskeleton in apoptotic macrophages [80].

PADI3

PADI3 is the only PADI enzyme expressed in the hair follicles and is also localized within the epidermis [81, 82]. Citrullination by PADI3 of trichohyalin in the hair follicles alters its secondary structure making it able to efficiently cross-link with keratin filaments [82]. This structural matrix provides a guide for directional hair fiber growth.

PADI4

PADI4 is mainly expressed in immune cells which accounts for its detection in a number of tissues, including the brain and joints [71]. PADI4 is the only PADI isozyme with a classic nuclear localization signal [83]. PADI4 substrates include histones, collagen type I, vimentin, and fibrin [62]. PADI4 has been implicated in the initiation of a unique form of cell death called NETosis [84], discussed further below. Human PADI4 was initially named PADI5, but was later renamed when data confirmed its relationship to rodent PADI4 [71]. PADI4's role in inflammation implicates citrullination in rheumatoid arthritis (RA), MS, and cancer [61, 85, 86].

PADI6

PADI6 is localized to the ovary, oocytes, embryo, and testis. PADI6 is necessary for the organization of cytoskeletal sheets [87] and the formation of proper cytoplasmic lattices in the oocyte and developing embryo [88]. PADI6 is essential for female fertility, as mutations in PADI6 lead to female sterility [89-92]. Interestingly, PADI6 lacks several calcium-binding residues and the essential catalytic cysteine. Indeed, PADI6 isolated from mouse ovaries had no enzymatic activity [93], suggesting that its role is not through citrullination or that it requires other factors for its enzymatic activity.

Catalytic mechanism of activity

With the exception of PADI6, PADIs have five conserved calcium binding sites with a sixth identified calcium-coordination site in PADI2. In the PADI enzymes, calcium binding orders unstructured, acidic regions to form an ordered N-terminal calcium-binding region and the C-terminal active site cleft [94, 95]. PADIs exhibit cooperative calcium binding as calcium coordination leads to conformational changes necessary for structural stability, substrate binding, and catalysis. Calcium 3, 4, 5, and 6 binding sites reside in the N-terminal domain, while Ca1 and Ca2 are located in the active cleft in the C-terminal domain and are essential for catalysis [96]. The PADI2 apoenzyme has Ca1 and Ca6 binding sites occupied [96]. Binding of Ca3, Ca4, and Ca5 act as a "calcium switch", by causing the conformational change that stabilizes the structure and induces movement of the "gatekeeping" amino acid (human PADI2 R347) which sterically obstructs the active site [96]. Binding of Ca3 and Ca4, while distal from the active site play a crucial non-catalytic role on the full activation of the enzyme by stabilizing the proper geometry of the active site [95]. The C-terminal domain of a calcium-free PADI is

a concave-acidic surface which becomes ordered to form the active site cleft upon binding of Ca2 [94, 96]. Both Ca1 and Ca2 are required for catalysis as they move the catalytic resides into the active site.

The catalytic residues conserved within PADI enzymes are 2 aspartates, a histidine and a cysteine. Upon binding of the substrate, citrullination begins with a nucleophilic attack of the Cζ atom of substrate's peptidyl-arginine which is stabilized by the two catalytic aspartates. The C-N bond is then cleaved with the release of ammonia. An activated water molecule performs the second nucleophilic attack for the final product of peptidyl-citrulline (Fig 1.6) [94].

Regulation of PADI enzymes

Calcium-dependence of PADIs

As discussed above, the key regulator of PADIs is calcium. Activity *in vivo* occurs at a calcium concentration 100-fold higher than normal physiological cytosolic concentrations (10^{-8}-10^{-6} M) [97]. This high level of calcium would indicate activation of PADIs occurs only in extreme conditions such as apoptosis in which PADIs have been implicated [98]. However, it is also known that PADIs are involved in many different homeostatic cellular processes including gene regulation [84]. This begs the question, what other factors are involved in the activation of PADIs in homeostatic calcium concentrations in the cell? Reports have shown that citrullination can be regulated at the transcriptional level, by calcium and estrogen hormone, as well as through the auto-deimination of PADI homodimers.
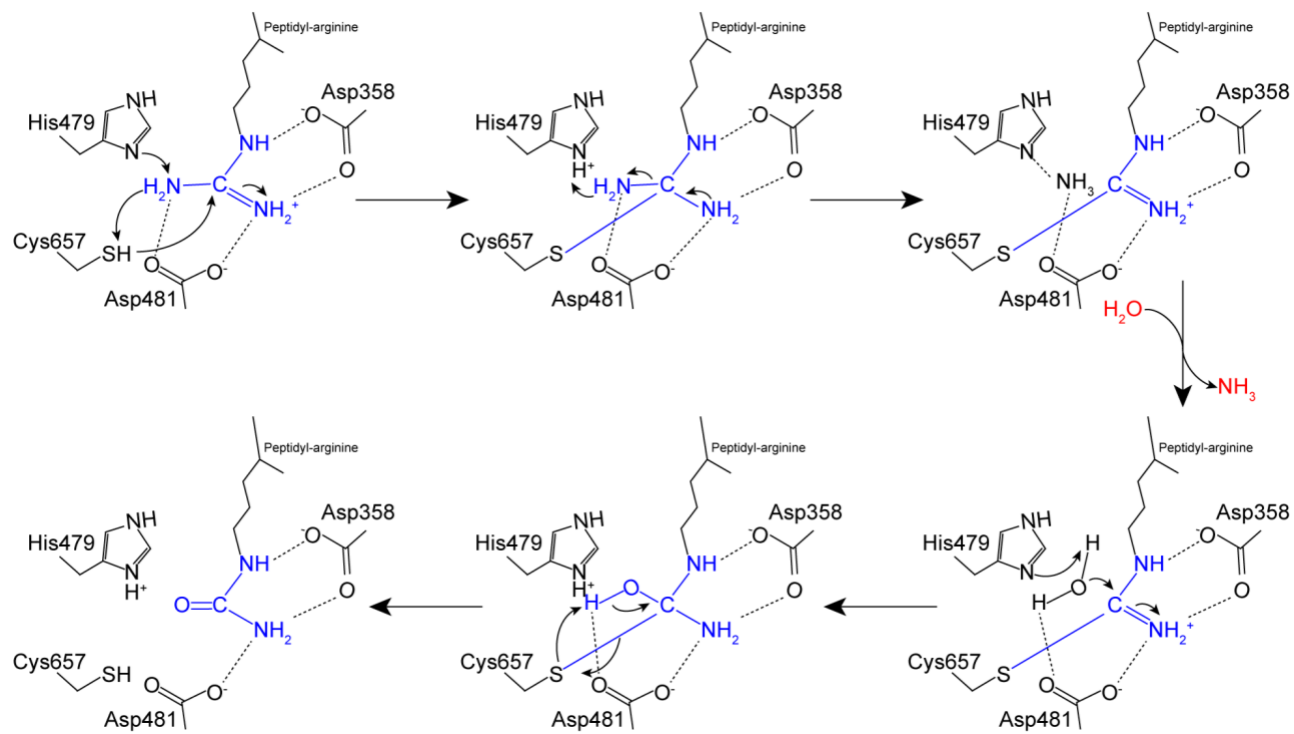
Fig 1.6: Proposed mechanism of catalysis. Adapted from Arita, K. *et al.*, 2004

Transcriptional Regulation

Interestingly, calcium may have a role in promoting citrullination through the transcriptional control of *Padi* genes. *Padi1-3* in human keratinocytes have regulatory elements in their promoter regions. Binding of the ubiquitous Sp-family transcription factors and Myeloid Zinc Finger 1 transcription factor have been reported to drive *Padi*s' expression during keratinocyte differentiation, a process marked by high calcium [99-102]. Increased intracellular calcium levels may promote transcription factor occupancy to the promoter regions and contribute to PADI subcellular localization and activity. In the disease state of multiple sclerosis (MS) where a high level of citrullination is observed, the *Padi2* promoter region is hypomethylated in these neurons, a modification generally associated with active expression [103].

Hormonal Regulation

At the transcriptional level, the hormone estrogen regulates *Padi* expression in the uterus via the direct binding of the estrogen receptor (ER) with estrogen response elements (ERE) in the *Padi4* promoter and through the stabilization of transcription factors and enhancers in that region [104]. Estrogen regulates the subcellular localization of PADIs, stimulating PADI2 activity and citrullination of histone H3 in breast cancer cells [72, 73]. Estrogen activation leads to the association of ER with PADI2 and facilitates PADI2's translocation into the nucleus. Once inside the nucleus, PADI2 citrullinates histones, leading to a decondensed chromatin. ER subsequently can access EREs to promote the expression of estrogen target genes [72, 105].

Auto-citrullination

PADIs exist as a dimer; therefore, auto-citrullination is another attractive mechanism of regulation of PADIs' activity. PADI2 and PADI4 are known to be auto-citrullinated [106-108]. Padi4 has 10 citrullinated arginines in three distinct regions, including in the active site cleft. Citrullination of arginine within this region inactivates the enzyme [107]. While work on auto-citrullination has been conducted primarily *in vitro*, auto-citrullination does provide an attractive mechanism for further regulation of this post-translational modification.

Downstream consequences of citrullination

PADI2 in gene regulation

Evidence of histone citrullination in breast cancer cells points to a role of PADIs in gene expression and transcriptional regulation. There is direct evidence for citrullination of H1R54, H3R17, H3R26, and H4R3 [109-111], where deimination and loss of the positively-charged arginine in the DNA binding domain leads to disassociation from negatively-charged DNA and a less compact chromatin state. As discussed above, PADI2 acts as a transcriptional coactivator in response to estrogen stimulation in breast cancer cells [72, 105]. Similarly, H3cit26 inhibits H3K27 methylation through the recruitment of demethylases to chromatin. The methylation of H3K27 is also able to slow H3R26 citrullination. The citrullination and methylation of histones oppose each other leading to a mechanism of gene regulation with H3K27me repressing gene expression and H3cit26 activating gene expression [112]. In addition to epigenetic regulation of gene expression, PADI2 citrullinates the C-terminal domain of RNA polymerase II. This citrullination is needed for the recruitment of the positive

transcription elongation factor b kinase complex that releases paused RNA polymerase II for transcriptional elongation [113].

Citrullination regulates pluripotency

Studies of citrullination as a regulator of gene expression suggests the functional importance of citrullination as a chromatin modifier to regulate pluripotency. The first evidence for a role for citrullination in maintaining pluripotency was in 2014 when PADI4 was shown to be specifically expressed in pluripotent stem cells rather than multipotent stem cells and differentiated cells [109]. Christophorou et al. proposed that the citrullination of histones H1 and H3 negatively regulate chromatin compaction for the maintenance of pluripotency [109]. Histone citrullination has also been shown to antagonize histone H3K9me^3 mediated heterochromatin compaction [110, 111]. Recognition of H3cit26 by SMARCAD1 targets the suppression of H3K9me3 heterochromatin formation to maintain naïve pluripotency [114]. Similarly, PADI4 recruitment to specific genomic loci in stem cells facilitates the citrullination of the reader protein HP1γ and reduces its affinity to chromatin. Conversely, with the loss of PADI4 expression and HP1γ citrullination during differentiation, HP1γ can associate with H3K9me3 to facilitate either chromatin compaction or gene expression (Fig 1.7) [115].

Citrullination modulates migration

Neutrophils are recruited to the site of a wound or infection by multiple pro-inflammatory factors including chemokines, which are small-secreted proteins that bind G-protein coupled receptors to induce migration. Once activated at the site of injury,
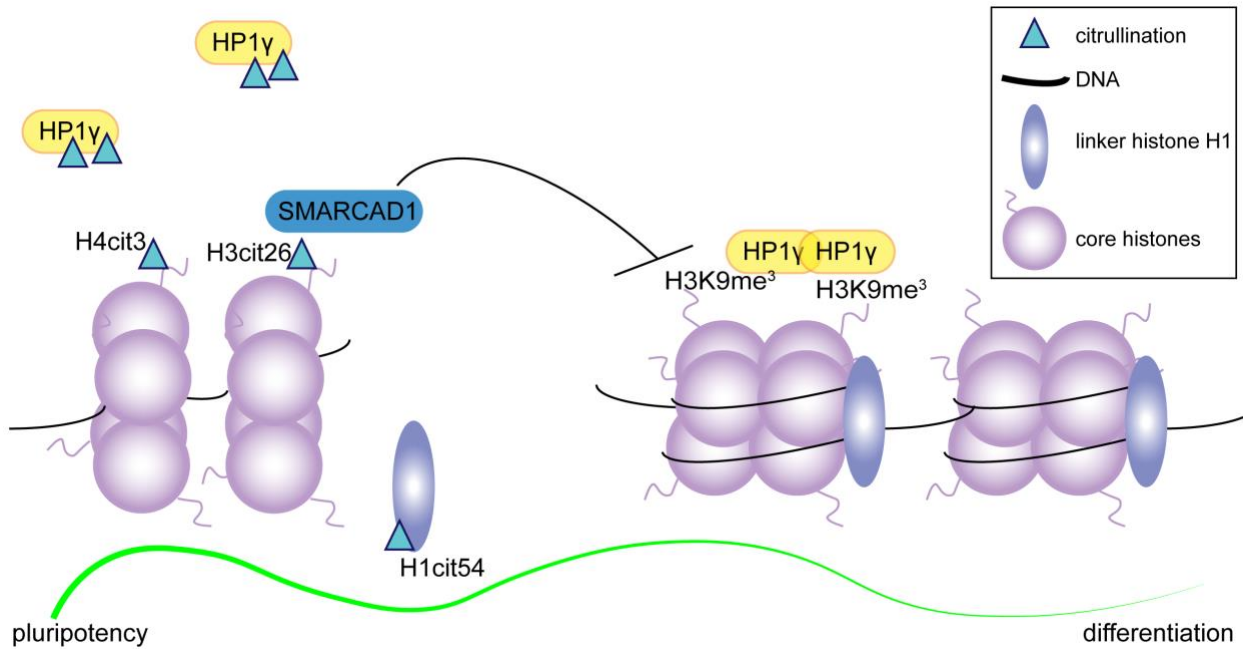
Fig 1.7: Citrullination as a chromatin modifier to promote pluripotency. In

pluripotent stem cells, citrullination of histones causes a weaker association with DNA

and recruits SMARCAD1 to inhibit histone methylation and promote a localized open

chromatin state. Citrullination of HP1γ also reduces its affinity to chromatin. An open

chromatin conformation on specific gene loci allow for expression of pluripotency genes.

Upon differentiation, PADI enzyme and citrullination levels decrease, leading to

chromatin compaction and a change in gene expression.

neutrophils are essential for microbe clearance achieved through the release of antimicrobial peptides, production of reactive oxygen species, and phagocytosis of bacteria [36]. Citrullination of chemokines acts as another mechanism to temporally control chemotactic cues to the site of an infection or wound. The chemokine CXCL8 is known to be one of the most potent neutrophil chemoattractants [116, 117]. CXCL8, when bound to its receptors CXCR1 or CXCR2, activates a signaling cascade leading to the reorganization of the actin cytoskeleton and migration [118, 119]. Deimination of human CXCL8 dampens the inflammatory response by preventing cleavage to its most potent form, reducing its binding affinity to glycosaminoglycans (GAGs), as well as to CXCR2 [120]. Injection of citrullinated CXCL8 failed to recruit neutrophils in mice [120]. Citrullinated CXCL8 may be unable to induce migration due to its loss of the direct binding to CXCR2 and signaling on neutrophils or rather due to its failure to form a chemotactic gradient through the binding to GAGs [120]. Conversely, further work from the same group found that citrullinated CXCL8 increased neutrophil recruitment into the blood circulation from the blood marrow. This occurred due to the increase in L-selectin shedding required for transendothelial migration and increased β-integrin CD11b surface expression [121]. Deiminated CXCL8 has lower binding affinity for the scavenging receptor, Duffy antigen/receptor for chemokines, delaying CXCL8 clearance in the blood stream [121].

Citrullination as a mode of regulation of cell migration may be universal as citrullination of chemokines for the activation of other immune cells have been reported. Citrullination of the neutrophil chemokine, CXCL5, converts the previously non-monocyte recruiting factor to now stimulate monocyte chemotaxis [122]. Citrullination of

T-cell chemokines CXCL10 and CXCL11 reduced the chemoattracting capacity of theses ligands and decreased binding affinity to GAGs [123]. *In vitro* studies of lymphocyte chemokine CXCL12 citrullination confirmed a loss of chemoattraction after citrullination potentially through the altered binding efficiencies of citrullinated CXCL12 to its two receptors, CXCR4 and CXCR7 [124]. The universality of chemoattraction dampening via post-translational modifications has great implications for therapeutic approaches in chronic inflammatory diseases such as rheumatoid arthritis, MS, and in infection.

Citrullination of integrin-binding motifs of extracellular matrix (ECM) components is another mechanism of time-based modulation of cell migration. Integrins play a pivotal role in mediating the interactions between the ECM and the cell's cytoskeleton during cell migration [125]. Citrullination of collagen lowers integrin-binding and results in decreased migration in mesenchymal stem cells and colorectal cancer cells [126, 127]. Citrullination of another major ECM protein, fibronectin, impaired the migration of synovial fibroblasts [128]. Extensive citrullination of ECM proteins has been reported in the inflamed joints of rheumatoid arthritis patients with the extent of citrullination corelating to the intensity of inflammation [129].

Neutrophil Extracellular Traps

Only 14 years ago, the observation of neutrophil extracellular traps (NETS) in response to bacterial infection was reported [130]. In this phenomenon, there is a breakdown of the nuclear envelope and a global decompaction and release of DNA into the extracellular space [131]. This extracellular DNA is entwined with cytoplasmic proteases and anti-bacterial peptides including myeloperoxidase, neutrophil elastase,

and cathepsin G [130, 132]. NETs respond to infection both by entrapping large pathogens that are too big to be phagocytosed by macrophages and by participating in direct killing by creating a highly concentrated anti-microbial environment. There is thought to be a suicidal, reactive oxygen species (ROS)-dependent NETosis which is activated in response to *Aspergillus fumigatus* and HIV [133, 134] or ROS-independent vital NETosis in which there is a chromatin decompaction and release but the cell is still able to chemotax to and phagocytize nearby microbes (seen in response to *Candida albicans* and *Staphylococcus aureus*) [135].

Recent debate has sparked about the necessity of citrullinated histones as a catalyst for NET formation. PADI4-deficient mice had impaired NET formation and were more susceptible to *Staphylococcus aureus* infection [136], while other reports demonstrated normal NET formation in these mice [137]. While citrullinated histones on extracellular DNA was previously considered a hallmark of NETs, now it is believed that not all NETs are PADI4-dependent. Different stimuli induce NETs with differing levels of citrullinated DNA with PADI4, but not PADI2, being required for highly-citrullinated NETs [138].

PADIs in disease

With PADI's broad tissue expression and role in many cellular processes, improper or dysregulated activity unsurprisingly implicates PADIs and citrullination in a number of diseases, a select few are discussed below. The most highly associated disease with citrullination is RA, a systemic autoimmune disease with chronic inflammation of the joints. RA patients have increased citrullinated proteins in the joints

and produce autoantibodies against citrullinated proteins, which are pathological and increase the immune response to the afflicted synovium [139]. Citrullination is increased in inflamed tissues [140]. Again, citrullinated proteins were found in ulcerative colitis (UC) patients and PADI4 haplotypes have been correlated with increased risk of both RA and UC in Japanese populations [141, 142].

In the brain, the presence of citrullination has been correlated with the destruction of the myelin sheath and chronic inflammation observed in MS patient brains. The protective myelin sheath on axons contains myelin basic protein (MBP) in complex with phospholipids. MS patients have 45% of their total MBP citrullinated compared to 18% in healthy adults [77]. This citrullination causes partial unfolding of the MBP, weakening the interaction with the phospholipids of the myelin sheath, causing them to become less densely packed, and susceptible to degradation [143]. In another neurodegenerative disease, Alzheimer's disease (AD), the presence of PADI2 and citrullinated proteins in the hippocampus of AD patients contributes to activation of the immune response [78, 144].

PADI overexpression and activity have been linked to multiple cancers including, breast, liver, lung, and ovarian [86]. In these patient sample tumors, PADI4 levels were elevated similar to samples from patients with autoimmune disorders like RA and UC, but increased expression was not observed in benign tumors and chronic inflamed tissues [86]. Overexpression of PADI2 in transgenic mice promoted the rapid progression of skin tumors and increased immune cell infiltration [145]. Many citrullinated proteins have been identified in tumors suggesting that the mechanism by which citrullination promotes tumorigenesis is likely to be complex. Overall, the

dysregulation of PADI enzymes and citrullination have major implications on the immune response lending themselves as therapeutic targets for many leukocyte-driven disorders including autoimmune diseases and cancer.

PADI4 in wound healing

There has been very little work done examining a role for citrullination in wound healing. The first evidence was reported in 2011 in the mouse cutaneous wound healing model [146]. The authors reported the expression of PADI1 and PADI3 in the newly formed epidermis and differentiating keratinocytes, aligning with their roles in skin homeostasis. PADI4 and citrullinated-fibrin were found specifically within the clot-derived scab [146]. The unhealthy buildup of scar tissue (and fibrin) are thought to be responsible for poor wound healing in mammals. Similarly, PADI4-dependent NETs were observed in skin wounds, and the inhibition of both NETs and PADI4 resulted in improved wound healing [147]. The mechanism by which diabetes primes neutrophils to undergo NETosis, may partly contribute to the poor wound healing observed in diabetic patients [147]. During retina injury, PADI4 is also upregulated, with inhibition of PADI4 attenuating the pathological upregulation of the cytoskeletal protein GFAP [148]. Taken together, these studies implicate PADI4 expression and activity during wound healing, although the direct mechanism and citrullination targets during injury remain unknown.

References

1.   White ES, Mantovani AR. Inflammation, wound repair, and fibrosis: reassessing the spectrum of tissue injury and resolution. J Pathol. 2013;229(2):141-4.

2.   Uygur A, Lee RT. Mechanisms of Cardiac Regeneration. Dev Cell. 2016;36(4):362-74.

3.   Han M, Yang X, Farrington JE, Muneoka K. Digit regeneration is regulated by Msx1 and BMP4 in fetal mice. Development. 2003;130(21):5123-32.

4.   Beck CW, Christen B, Slack JM. Molecular pathways needed for regeneration of spinal cord and muscle in a vertebrate. Dev Cell. 2003;5(3):429-39.

5.   Poss KD, Keating MT, Nechiporuk A. Tales of regeneration in zebrafish. Dev Dyn. 2003;226(2):202-10.

6.   Tal TL, Franzosa JA, Tanguay RL. Molecular signaling networks that choreograph epimorphic fin regeneration in zebrafish - a mini-review. Gerontology. 2010;56(2):231-40.

7.   Howe K, Clark MD, Torroja CF, Torrance J, Berthelot C, Muffato M, et al. The zebrafish reference genome sequence and its relationship to the human genome. Nature. 2013;496(7446):498-503.

8.   Renshaw SA, Trede NS. A model 450 million years in the making: zebrafish and vertebrate immunity. Dis Model Mech. 2012;5(1):38-47.

9.   Kawakami A, Fukazawa T, Takeda H. Early fin primordia of zebrafish larvae regenerate by a similar growth control mechanism with adult regeneration. Dev Dyn. 2004;231(4):693-9.

10.   Yoshinari N, Ishida T, Kudo A, Kawakami A. Gene expression and functional analysis of zebrafish larval fin fold regeneration. Dev Biol. 2009;325(1):71-81.

11.   Mateus R, Pereira T, Sousa S, de Lima JE, Pascoal S, Saude L, et al. In vivo cell and tissue dynamics underlying zebrafish fin fold regeneration. PLoS One. 2012;7(12):e51766.

12.   Rojas-Munoz A, Rajadhyksha S, Gilmour D, van Bebber F, Antos C, Rodriguez Esteban C, et al. ErbB2 and ErbB3 regulate amputation-induced proliferation and migration during vertebrate regeneration. Dev Biol. 2009;327(1):177-90.

13.   Romero MMG, McCathie G, Jankun P, Roehl HH. Damage-induced reactive oxygen species enable zebrafish tail regeneration by repositioning of Hedgehog expressing cells. Nat Commun. 2018;9(1):4010.

14.   Taniguchi Y, Watanabe K, Mochii M. Notochord-derived hedgehog is essential for tail regeneration in Xenopus tadpole. BMC Dev Biol. 2014;14:27.

15.   Poss KD, Nechiporuk A, Hillam AM, Johnson SL, Keating MT. Mps1 defines a proximal blastemal proliferative compartment essential for zebrafish fin regeneration. Development. 2002;129(22):5141-9.

16.   de Oliveira S, Lopez-Munoz A, Candel S, Pelegrin P, Calado A, Mulero V. ATP modulates acute inflammation in vivo through dual oxidase 1-derived H2O2 production and NF-kappaB activation. J Immunol. 2014;192(12):5710-9.

17.   Yoo SK, Freisinger CM, LeBert DC, Huttenlocher A. Early redox, Src family kinase, and calcium signaling integrate wound responses and tissue regeneration in zebrafish. J Cell Biol. 2012;199(2):225-34.

18.   Yoo SK, Starnes TW, Deng Q, Huttenlocher A. Lyn is a redox sensor that mediates leukocyte wound attraction in vivo. Nature. 2011;480(7375):109-12.

19.   Niethammer P, Grabher C, Look AT, Mitchison TJ. A tissue-scale gradient of hydrogen peroxide mediates rapid wound detection in zebrafish. Nature. 2009;459(7249):996-9.

20.   Niethammer P. The early wound signals. Curr Opin Genet Dev. 2016;40:17-22.

21.   Benink HA, Bement WM. Concentric zones of active RhoA and Cdc42 around single cell wounds. J Cell Biol. 2005;168(3):429-39.

22.   Xu S, Chisholm AD. A Galphaq-Ca(2)(+) signaling pathway promotes actin-mediated epidermal wound closure in C. elegans. Curr Biol. 2011;21(23):1960-7.

23.   Poleo G, Brown CW, Laforest L, Akimenko MA. Cell proliferation and movement during early fin regeneration in zebrafish. Dev Dyn. 2001;221(4):380-90.

24.   Nechiporuk A, Keating MT. A proliferation gradient between proximal and msxb-expressing distal blastema directs zebrafish fin regeneration. Development. 2002;129(11):2607-17.

25.   Santos-Ruiz L, Santamaria JA, Ruiz-Sanchez J, Becerra J. Cell proliferation during blastema formation in the regenerating teleost fin. Dev Dyn. 2002;223(2):262-72.

26.   Lieschke GJ, Oates AC, Crowhurst MO, Ward AC, Layton JE. Morphologic and functional characterization of granulocytes and macrophages in embryonic and adult zebrafish. Blood. 2001;98(10):3087-96.

27.   Tauzin S, Starnes TW, Becker FB, Lam PY, Huttenlocher A. Redox and Src family kinase signaling control leukocyte wound attraction and neutrophil reverse migration. J Cell Biol. 2014;207(5):589-98.

28.   de Oliveira S, Boudinot P, Calado A, Mulero V. Duox1-derived H2O2 modulates Cxcl8 expression and neutrophil recruitment via JNK/c-JUN/AP-1 signaling and chromatin modifications. J Immunol. 2015;194(4):1523-33.

29.   Nathan C. Neutrophils and immunity: challenges and opportunities. Nat Rev Immunol. 2006;6(3):173-82.

30.   van Furth R. Monocyte production during inflammation. Comp Immunol Microbiol Infect Dis. 1985;8(2):205-11.

31.   Li L, Yan B, Shi YQ, Zhang WQ, Wen ZL. Live imaging reveals differing roles of macrophages and neutrophils during zebrafish tail fin regeneration. J Biol Chem. 2012;287(30):25353-60.

32.   Petrie TA, Strand NS, Yang CT, Rabinowitz JS, Moon RT. Macrophages modulate adult zebrafish tail fin regeneration. Development. 2014;141(13):2581-91.

33.   Morales RA, Allende ML. Peripheral Macrophages Promote Tissue Regeneration in Zebrafish by Fine-Tuning the Inflammatory Response. Front Immunol. 2019;10:253.

34.   Hasegawa T, Hall CJ, Crosier PS, Abe G, Kawakami K, Kudo A, et al. Transient inflammatory response mediated by interleukin-1beta is required for proper regeneration in zebrafish fin fold. Elife. 2017;6.

35.   Hasegawa T, Nakajima T, Ishida T, Kudo A, Kawakami A. A diffusible signal derived from hematopoietic cells supports the survival and proliferation of regenerative cells during zebrafish fin fold regeneration. Dev Biol. 2015;399(1):80-90.

36.   Wilgus TA, Roy S, McDaniel JC. Neutrophils and Wound Repair: Positive Actions and Negative Reactions. Adv Wound Care (New Rochelle). 2013;2(7):379-88.

37.   Brockes JP, Kumar A. Comparative aspects of animal regeneration. Annu Rev Cell Dev Biol. 2008;24:525-49.

38.   Knopf F, Hammond C, Chekuru A, Kurth T, Hans S, Weber CW, et al. Bone regenerates via dedifferentiation of osteoblasts in the zebrafish fin. Dev Cell. 2011;20(5):713-24.

39.   Tu S, Johnson SL. Fate restriction in the growing and regenerating zebrafish fin. Dev Cell. 2011;20(5):725-32.

40. Singh SP, Holdway JE, Poss KD. Regeneration of amputated zebrafish fin rays from de novo osteoblasts. Dev Cell. 2012;22(4):879-86.

41. Poss KD, Shen J, Nechiporuk A, McMahon G, Thisse B, Thisse C, et al. Roles for Fgf signaling during zebrafish fin regeneration. Dev Biol. 2000;222(2):347-58.

42. Whitehead GG, Makino S, Lien CL, Keating MT. fgf20 is essential for initiating zebrafish fin regeneration. Science. 2005;310(5756):1957-60.

43. Kawakami Y, Rodriguez Esteban C, Raya M, Kawakami H, Marti M, Dubova I, et al. Wnt/beta-catenin signaling regulates vertebrate limb regeneration. Genes Dev. 2006;20(23):3232-7.

44. Mathew LK, Sengupta S, Franzosa JA, Perry J, La Du J, Andreasen EA, et al. Comparative expression profiling reveals an essential role for raldh2 in epimorphic regeneration. J Biol Chem. 2009;284(48):33642-53.

45. Roehl HH. Linking wound response and inflammation to regeneration in the zebrafish larval fin. Int J Dev Biol. 2018;62(6-7-8):473-7.

46. Gauron C, Rampon C, Bouzaffour M, Ipendey E, Teillon J, Volovitch M, et al. Sustained production of ROS triggers compensatory proliferation and is required for regeneration to proceed. Sci Rep. 2013;3:2084.

47. Rieger S, Sagasti A. Hydrogen peroxide promotes injury-induced peripheral sensory axon regeneration in the zebrafish skin. PLoS Biol. 2011;9(5):e1000621.

48. LeBert D, Squirrell JM, Freisinger C, Rindy J, Golenberg N, Frecentese G, et al. Damage-induced reactive oxygen species regulate vimentin and dynamic collagen-based projections to mediate wound repair. Elife. 2018;7.

49. Hirose K, Shimoda N, Kikuchi Y. Transient reduction of 5-methylcytosine and 5-hydroxymethylcytosine is associated with active DNA demethylation during regeneration of zebrafish fin. Epigenetics. 2013;8(9):899-906.

50. Takayama K, Shimoda N, Takanaga S, Hozumi S, Kikuchi Y. Expression patterns of dnmt3aa, dnmt3ab, and dnmt4 during development and fin regeneration in zebrafish. Gene Expr Patterns. 2014;14(2):105-10.

51. Saxena S, Purushothaman S, Meghah V, Bhatti B, Poruri A, Meena Lakshmi MG, et al. Role of annexin gene and its regulation during zebrafish caudal fin regeneration. Wound Repair Regen. 2016;24(3):551-9.

52. Stewart S, Tsun ZY, Izpisua Belmonte JC. A histone demethylase is necessary for regeneration in zebrafish. Proc Natl Acad Sci U S A. 2009;106(47):19889-94.

53.   Dupret B, Volkel P, Vennin C, Toillon RA, Le Bourhis X, Angrand PO. The histone lysine methyltransferase Ezh2 is required for maintenance of the intestine integrity and for caudal fin regeneration in zebrafish. Biochim Biophys Acta Gene Regul Mech. 2017;1860(10):1079-93.

54.   Pfefferli C, Muller F, Jazwinska A, Wicky C. Specific NuRD components are required for fin regeneration in zebrafish. BMC Biol. 2014;12:30.

55.   Roth MJ, Forbes AJ, Boyne MT, 2nd, Kim YB, Robinson DE, Kelleher NL. Precise and parallel characterization of coding polymorphisms, alternative splicing, and modifications in human proteins by mass spectrometry. Mol Cell Proteomics. 2005;4(7):1002-8.

56.   Rogers GE. Occurrence of citrulline in proteins. Nature. 1962;194:1149-51.

57.   Hensen SM, Pruijn GJ. Methods for the detection of peptidylarginine deiminase (PAD) activity and protein citrullination. Mol Cell Proteomics. 2014;13(2):388-96.

58.   Liu YL, Chiang YH, Liu GY, Hung HC. Functional role of dimerization of human peptidylarginine deiminase 4 (PAD4). PLoS One. 2011;6(6):e21314.

59.   El-Sayed ASA, Shindia AA, AbouZaid AA, Yassin AM, Ali GS, Sitohy MZ. Biochemical characterization of peptidylarginine deiminase-like orthologs from thermotolerant Emericella dentata and Aspergillus nidulans. Enzyme Microb Technol. 2019;124:41-53.

60.   McGraw WT, Potempa J, Farley D, Travis J. Purification, characterization, and sequence analysis of a potential virulence factor from Porphyromonas gingivalis, peptidylarginine deiminase. Infect Immun. 1999;67(7):3248-56.

61.   Gyorgy B, Toth E, Tarcsa E, Falus A, Buzas EI. Citrullination: a posttranslational modification in health and disease. Int J Biochem Cell Biol. 2006;38(10):1662-77.

62.   Amin B, Voelter W. Human Deiminases: Isoforms, Substrate Specificities, Kinetics, and Detection. Prog Chem Org Nat Prod. 2017;106:203-40.

63.   Tarcsa E, Marekov LN, Mei G, Melino G, Lee SC, Steinert PM. Protein unfolding by peptidylarginine deiminase. Substrate specificity and structural relationships of the natural substrates trichohyalin and filaggrin. J Biol Chem. 1996;271(48):30709-16.

64.   Rus'd AA, Ikejiri Y, Ono H, Yonekawa T, Shiraiwa M, Kawada A, et al. Molecular cloning of cDNAs of mouse peptidylarginine deiminase type I, type III and type IV, and the expression pattern of type I in mouse. Eur J Biochem. 1999;259(3):660-9.

65.	Guerrin M, Ishigami A, Mechin MC, Nachat R, Valmary S, Sebbag M, et al. cDNA cloning, gene organization and expression analysis of human peptidylarginine deiminase type I. Biochem J. 2003;370(Pt 1):167-74.

66.	Ishida-Yamamoto A, Senshu T, Eady RA, Takahashi H, Shimizu H, Akiyama M, et al. Sequential reorganization of cornified cell keratin filaments involving filaggrin-mediated compaction and keratin 1 deimination. J Invest Dermatol. 2002;118(2):282-7.

67.	Hsu CY, Henry J, Raymond AA, Mechin MC, Pendaries V, Nassar D, et al. Deimination of human filaggrin-2 promotes its proteolysis by calpain 1. J Biol Chem. 2011;286(26):23222-33.

68.	Chavanas S, Mechin MC, Nachat R, Adoue V, Coudane F, Serre G, et al. Peptidylarginine deiminases and deimination in biology and pathology: relevance to skin homeostasis. J Dermatol Sci. 2006;44(2):63-72.

69.	Ishida-Yamamoto A, Senshu T, Takahashi H, Akiyama K, Nomura K, Iizuka H. Decreased deiminated keratin K1 in psoriatic hyperproliferative epidermis. J Invest Dermatol. 2000;114(4):701-5.

70.	Saijo S, Nagai A, Kinjo S, Mashimo R, Akimoto M, Kizawa K, et al. Monomeric Form of Peptidylarginine Deiminase Type I Revealed by X-ray Crystallography and Small-Angle X-ray Scattering. J Mol Biol. 2016;428(15):3058-73.

71.	Vossenaar ER, Zendman AJ, van Venrooij WJ, Pruijn GJ. PAD, a growing family of citrullinating enzymes: genes, features and involvement in disease. Bioessays. 2003;25(11):1106-18.

72.	Zhang X, Bolt M, Guertin MJ, Chen W, Zhang S, Cherrington BD, et al. Peptidylarginine deiminase 2-catalyzed histone H3 arginine 26 citrullination facilitates estrogen receptor alpha target gene activation. Proc Natl Acad Sci U S A. 2012;109(33):13331-6.

73.	Cherrington BD, Morency E, Struble AM, Coonrod SA, Wakshlag JJ. Potential role for peptidylarginine deiminase 2 (PAD2) in citrullination of canine mammary epithelial cell histones. PLoS One. 2010;5(7):e11768.

74.	Moscarello MA, Wood DD, Ackerley C, Boulias C. Myelin in multiple sclerosis is developmentally immature. J Clin Invest. 1994;94(1):146-54.

75.	Moscarello MA, Pritzker L, Mastronardi FG, Wood DD. Peptidylarginine deiminase: a candidate factor in demyelinating disease. J Neurochem. 2002;81(2):335-43.

76.   Moscarello MA, Mastronardi FG, Wood DD. The role of citrullinated proteins suggests a novel mechanism in the pathogenesis of multiple sclerosis. Neurochem Res. 2007;32(2):251-6.

77.   Wood DD, Bilbao JM, O'Connors P, Moscarello MA. Acute multiple sclerosis (Marburg type) is associated with developmentally immature myelin basic protein. Ann Neurol. 1996;40(1):18-24.

78.   Ishigami A, Ohsawa T, Hiratsuka M, Taguchi H, Kobayashi S, Saito Y, et al. Abnormal accumulation of citrullinated proteins catalyzed by peptidylarginine deiminase in hippocampal extracts from patients with Alzheimer's disease. J Neurosci Res. 2005;80(1):120-8.

79.   Inagaki M, Takahara H, Nishi Y, Sugawara K, Sato C. Ca2+-dependent deimination-induced disassembly of intermediate filaments involves specific modification of the amino-terminal head domain. J Biol Chem. 1989;264(30):18119-27.

80.   Asaga H, Yamada M, Senshu T. Selective deimination of vimentin in calcium ionophore-induced apoptosis of mouse peritoneal macrophages. Biochem Biophys Res Commun. 1998;243(3):641-6.

81.   Kanno T, Kawada A, Yamanouchi J, Yosida-Noro C, Yoshiki A, Shiraiwa M, et al. Human peptidylarginine deiminase type III: molecular cloning and nucleotide sequence of the cDNA, properties of the recombinant enzyme, and immunohistochemical localization in human skin. J Invest Dermatol. 2000;115(5):813-23.

82.   Rogers G, Winter B, McLaughlan C, Powell B, Nesci T. Peptidylarginine deiminase of the hair follicle: characterization, localization, and function in keratinizing tissues. J Invest Dermatol. 1997;108(5):700-7.

83.   Nakashima K, Hagiwara T, Yamada M. Nuclear localization of peptidylarginine deiminase V and histone deimination in granulocytes. J Biol Chem. 2002;277(51):49562-8.

84.   Witalison EE, Thompson PR, Hofseth LJ. Protein Arginine Deiminases and Associated Citrullination: Physiological Functions and Diseases Associated with Dysregulation. Curr Drug Targets. 2015;16(7):700-10.

85.   Spengler J, Lugonja B, Ytterberg AJ, Zubarev RA, Creese AJ, Pearson MJ, et al. Release of Active Peptidyl Arginine Deiminases by Neutrophils Can Explain Production of Extracellular Citrullinated Autoantigens in Rheumatoid Arthritis Synovial Fluid. Arthritis Rheumatol. 2015;67(12):3135-45.

86.   Chang X, Han J, Pang L, Zhao Y, Yang Y, Shen Z. Increased PADI4 expression in blood and tissues of patients with malignant tumors. BMC Cancer. 2009;9:40.

87.   Esposito G, Vitale AM, Leijten FP, Strik AM, Koonen-Reemst AM, Yurttas P, et al. Peptidylarginine deiminase (PAD) 6 is essential for oocyte cytoskeletal sheet formation and female fertility. Mol Cell Endocrinol. 2007;273(1-2):25-31.

88.   Yurttas P, Vitale AM, Fitzhenry RJ, Cohen-Gould L, Wu W, Gossen JA, et al. Role for PADI6 and the cytoplasmic lattices in ribosomal storage in oocytes and translational control in the early mouse embryo. Development. 2008;135(15):2627-36.

89.   Xu Y, Shi Y, Fu J, Yu M, Feng R, Sang Q, et al. Mutations in PADI6 Cause Female Infertility Characterized by Early Embryonic Arrest. Am J Hum Genet. 2016;99(3):744-52.

90.   Qian J, Nguyen NMP, Rezaei M, Huang B, Tao Y, Zhang X, et al. Biallelic PADI6 variants linking infertility, miscarriages, and hydatidiform moles. Eur J Hum Genet. 2018;26(7):1007-13.

91.   Maddirevula S, Coskun S, Awartani K, Alsaif H, Abdulwahab FM, Alkuraya FS. The human knockout phenotype of PADI6 is female sterility caused by cleavage failure of their fertilized eggs. Clin Genet. 2017;91(2):344-5.

92.   Wang X, Song D, Mykytenko D, Kuang Y, Lv Q, Li B, et al. Novel mutations in genes encoding subcortical maternal complex proteins may cause human embryonic developmental arrest. Reprod Biomed Online. 2018;36(6):698-704.

93.   Raijmakers R, Zendman AJ, Egberts WV, Vossenaar ER, Raats J, Soede-Huijbregts C, et al. Methylation of arginine residues interferes with citrullination by peptidylarginine deiminases in vitro. J Mol Biol. 2007;367(4):1118-29.

94.   Arita K, Hashimoto H, Shimizu T, Nakashima K, Yamada M, Sato M. Structural basis for Ca(2+)-induced activation of human PAD4. Nat Struct Mol Biol. 2004;11(8):777-83.

95.   Liu YL, Tsai IC, Chang CW, Liao YF, Liu GY, Hung HC. Functional roles of the non-catalytic calcium-binding sites in the N-terminal domain of human peptidylarginine deiminase 4. PLoS One. 2013;8(1):e51660.

96.   Slade DJ, Fang P, Dreyton CJ, Zhang Y, Fuhrmann J, Rempel D, et al. Protein arginine deiminase 2 binds calcium in an ordered fashion: implications for inhibitor design. ACS Chem Biol. 2015;10(4):1043-53.

97.   Nakayama-Hamada M, Suzuki A, Kubota K, Takazawa T, Ohsaka M, Kawaida R, et al. Comparison of enzymatic properties between hPADI2 and hPADI4. Biochem Biophys Res Commun. 2005;327(1):192-200.

98.   Hsu PC, Liao YF, Lin CL, Lin WH, Liu GY, Hung HC. Vimentin is involved in peptidylarginine deiminase 2-induced apoptosis of activated Jurkat cells. Mol Cells. 2014;37(5):426-34.

99.   Ying S, Dong S, Kawada A, Kojima T, Chavanas S, Mechin MC, et al. Transcriptional regulation of peptidylarginine deiminase expression in human keratinocytes. J Dermatol Sci. 2009;53(1):2-9.

100.   Dong S, Ying S, Kojima T, Shiraiwa M, Kawada A, Mechin MC, et al. Crucial roles of MZF1 and Sp1 in the transcriptional regulation of the peptidylarginine deiminase type I gene (PADI1) in human keratinocytes. J Invest Dermatol. 2008;128(3):549-57.

101.   Chavanas S, Adoue V, Mechin MC, Ying S, Dong S, Duplan H, et al. Long-range enhancer associated with chromatin looping allows AP-1 regulation of the peptidylarginine deiminase 3 gene in differentiated keratinocyte. PLoS One. 2008;3(10):e3408.

102.   Adoue V, Chavanas S, Coudane F, Mechin MC, Caubet C, Ying S, et al. Long-range enhancer differentially regulated by c-Jun and JunD controls peptidylarginine deiminase-3 gene in keratinocytes. J Mol Biol. 2008;384(5):1048-57.

103.   Mastronardi FG, Noor A, Wood DD, Paton T, Moscarello MA. Peptidyl argininedeiminase 2 CpG island in multiple sclerosis white matter is hypomethylated. J Neurosci Res. 2007;85(9):2006-16.

104.   Dong S, Zhang Z, Takahara H. Estrogen-enhanced peptidylarginine deiminase type IV gene (PADI4) expression in MCF-7 cells is mediated by estrogen receptor-alpha-promoted transfactors activator protein-1, nuclear factor-Y, and Sp1. Mol Endocrinol. 2007;21(7):1617-29.

105.   Guertin MJ, Zhang X, Anguish L, Kim S, Varticovski L, Lis JT, et al. Targeted H3R26 deimination specifically facilitates estrogen receptor binding by modifying nucleosome structure. PLoS Genet. 2014;10(9):e1004613.

106.   Lewallen DM, Bicker KL, Subramanian V, Clancy KW, Slade DJ, Martell J, et al. Chemical Proteomic Platform To Identify Citrullinated Proteins. ACS Chem Biol. 2015;10(11):2520-8.

107.   Andrade F, Darrah E, Gucek M, Cole RN, Rosen A, Zhu X. Autocitrullination of human peptidyl arginine deiminase type 4 regulates protein citrullination during cell activation. Arthritis Rheum. 2010;62(6):1630-40.

108.   Sarmento OF, Digilio LC, Wang Y, Perlin J, Herr JC, Allis CD, et al. Dynamic alterations of specific histone modifications during early murine development. J Cell Sci. 2004;117(Pt 19):4449-59.

109.   Christophorou MA, Castelo-Branco G, Halley-Stott RP, Oliveira CS, Loos R, Radzisheuskaya A, et al. Citrullination regulates pluripotency and histone H1 binding to chromatin. Nature. 2014;507(7490):104-8.

110.   Wang Y, Wysocka J, Sayegh J, Lee YH, Perlin JR, Leonelli L, et al. Human PAD4 regulates histone arginine methylation levels via demethylimination. Science. 2004;306(5694):279-83.

111.   Cuthbert GL, Daujat S, Snowden AW, Erdjument-Bromage H, Hagiwara T, Yamada M, et al. Histone deimination antagonizes arginine methylation. Cell. 2004;118(5):545-53.

112.   Clancy KW, Russell AM, Subramanian V, Nguyen H, Qian Y, Campbell RM, et al. Citrullination/Methylation Crosstalk on Histone H3 Regulates ER-Target Gene Transcription. ACS Chem Biol. 2017;12(6):1691-702.

113.   Sharma P, Lioutas A, Fernandez-Fuentes N, Quilez J, Carbonell-Caballero J, Wright RHG, et al. Arginine Citrullination at the C-Terminal Domain Controls RNA Polymerase II Transcription. Mol Cell. 2019;73(1):84-96 e7.

114.   Xiao S, Lu J, Sridhar B, Cao X, Yu P, Zhao T, et al. SMARCAD1 Contributes to the Regulation of Naive Pluripotency by Interacting with Histone Citrullination. Cell Rep. 2017;18(13):3117-28.

115.   Wiese M, Bannister AJ, Basu S, Boucher W, Wohlfahrt K, Christophorou MA, et al. Citrullination of HP1gamma chromodomain affects association with chromatin. Epigenetics Chromatin. 2019;12(1):21.

116.   de Oliveira S, Reyes-Aldasoro CC, Candel S, Renshaw SA, Mulero V, Calado A. Cxcl8 (IL-8) mediates neutrophil recruitment and behavior in the zebrafish inflammatory response. J Immunol. 2013;190(8):4349-59.

117.   Matsushima K, Morishita K, Yoshimura T, Lavu S, Kobayashi Y, Lew W, et al. Molecular cloning of a human monocyte-derived neutrophil chemotactic factor (MDNCF) and the induction of MDNCF mRNA by interleukin 1 and tumor necrosis factor. J Exp Med. 1988;167(6):1883-93.

118.   Jones SA, Wolf M, Qin S, Mackay CR, Baggiolini M. Different functions for the interleukin 8 receptors (IL-8R) of human neutrophil leukocytes: NADPH oxidase and phospholipase D are activated through IL-8R1 but not IL-8R2. Proc Natl Acad Sci U S A. 1996;93(13):6682-6.

119.   de Oliveira S, Rosowski EE, Huttenlocher A. Neutrophil migration in infection and wound repair: going forward in reverse. Nat Rev Immunol. 2016;16(6):378-91.

120. Proost P, Loos T, Mortier A, Schutyser E, Gouwy M, Noppen S, et al. Citrullination of CXCL8 by peptidylarginine deiminase alters receptor usage, prevents proteolysis, and dampens tissue inflammation. J Exp Med. 2008;205(9):2085-97.

121. Loos T, Opdenakker G, Van Damme J, Proost P. Citrullination of CXCL8 increases this chemokine's ability to mobilize neutrophils into the blood circulation. Haematologica. 2009;94(10):1346-53.

122. Yoshida K, Korchynskyi O, Tak PP, Isozaki T, Ruth JH, Campbell PL, et al. Citrullination of epithelial neutrophil-activating peptide 78/CXCL5 results in conversion from a non-monocyte-recruiting chemokine to a monocyte-recruiting chemokine. Arthritis Rheumatol. 2014;66(10):2716-27.

123. Loos T, Mortier A, Gouwy M, Ronsse I, Put W, Lenaerts JP, et al. Citrullination of CXCL10 and CXCL11 by peptidylarginine deiminase: a naturally occurring posttranslational modification of chemokines and new dimension of immunoregulation. Blood. 2008;112(7):2648-56.

124. Struyf S, Noppen S, Loos T, Mortier A, Gouwy M, Verbeke H, et al. Citrullination of CXCL12 differentially reduces CXCR4 and CXCR7 binding with loss of inflammatory and anti-HIV-1 activity via CXCR4. J Immunol. 2009;182(1):666-74.

125. Huttenlocher A, Horwitz AR. Integrins in cell migration. Cold Spring Harb Perspect Biol. 2011;3(9):a005074.

126. Sipila K, Haag S, Denessiouk K, Kapyla J, Peters EC, Denesyuk A, et al. Citrullination of collagen II affects integrin-mediated cell adhesion in a receptor-specific manner. FASEB J. 2014;28(8):3758-68.

127. Yuzhalin AE, Gordon-Weeks AN, Tognoli ML, Jones K, Markelc B, Konietzny R, et al. Colorectal cancer liver metastatic growth depends on PAD4-driven citrullination of the extracellular matrix. Nat Commun. 2018;9(1):4783.

128. Shelef MA, Bennin DA, Mosher DF, Huttenlocher A. Citrullination of fibronectin modulates synovial fibroblast behavior. Arthritis Res Ther. 2012;14(6):R240.

129. Sipila KH, Ranga V, Rappu P, Mali M, Pirila L, Heino I, et al. Joint inflammation related citrullination of functional arginines in extracellular proteins. Sci Rep. 2017;7(1):8246.

130. Brinkmann V, Reichard U, Goosmann C, Fauler B, Uhlemann Y, Weiss DS, et al. Neutrophil extracellular traps kill bacteria. Science. 2004;303(5663):1532-5.

131. Fuchs TA, Abed U, Goosmann C, Hurwitz R, Schulze I, Wahn V, et al. Novel cell death program leads to neutrophil extracellular traps. J Cell Biol. 2007;176(2):231-41.

132.   Li RHL, Tablin F. A Comparative Review of Neutrophil Extracellular Traps in Sepsis. Front Vet Sci. 2018;5:291.

133.   Bruns S, Kniemeyer O, Hasenberg M, Aimanianda V, Nietzsche S, Thywissen A, et al. Production of extracellular traps against Aspergillus fumigatus in vitro and in infected lung tissue is dependent on invading neutrophils and influenced by hydrophobin RodA. PLoS Pathog. 2010;6(4):e1000873.

134.   Yipp BG, Kubes P. NETosis: how vital is it? Blood. 2013;122(16):2784-94.

135.   Yipp BG, Petri B, Salina D, Jenne CN, Scott BN, Zbytnuik LD, et al. Infection-induced NETosis is a dynamic process involving neutrophil multitasking in vivo. Nat Med. 2012;18(9):1386-93.

136.   Thammavongsa V, Missiakas DM, Schneewind O. Staphylococcus aureus degrades neutrophil extracellular traps to promote immune cell death. Science. 2013;342(6160):863-6.

137.   Kenny EF, Herzig A, Kruger R, Muth A, Mondal S, Thompson PR, et al. Diverse stimuli engage different neutrophil extracellular trap pathways. Elife. 2017;6.

138.   Holmes CL, Shim D, Kernien J, Johnson CJ, Nett JE, Shelef MA. Insight into Neutrophil Extracellular Traps through Systematic Evaluation of Citrullination and Peptidylarginine Deiminases. J Immunol Res. 2019;2019:2160192.

139.   Schellekens GA, de Jong BA, van den Hoogen FH, van de Putte LB, van Venrooij WJ. Citrulline is an essential constituent of antigenic determinants recognized by rheumatoid arthritis-specific autoantibodies. J Clin Invest. 1998;101(1):273-81.

140.   Makrygiannakis D, af Klint E, Lundberg IE, Lofberg R, Ulfgren AK, Klareskog L, et al. Citrullination is an inflammation-dependent process. Ann Rheum Dis. 2006;65(9):1219-22.

141.   Chumanevich AA, Causey CP, Knuckley BA, Jones JE, Poudyal D, Chumanevich AP, et al. Suppression of colitis in mice by Cl-amidine: a novel peptidylarginine deiminase inhibitor. Am J Physiol Gastrointest Liver Physiol. 2011;300(6):G929-38.

142.   Chen CC, Isomoto H, Narumi Y, Sato K, Oishi Y, Kobayashi T, et al. Haplotypes of PADI4 susceptible to rheumatoid arthritis are also associated with ulcerative colitis in the Japanese population. Clin Immunol. 2008;126(2):165-71.

143.   Pritzker LB, Joshi S, Gowan JJ, Harauz G, Moscarello MA. Deimination of myelin basic protein. 1. Effect of deimination of arginyl residues of myelin basic protein on its structure and susceptibility to digestion by cathepsin D. Biochemistry. 2000;39(18):5374-81.

144.   Acharya NK, Nagele EP, Han M, Coretti NJ, DeMarshall C, Kosciuk MC, et al. Neuronal PAD4 expression and protein citrullination: possible role in production of autoantibodies associated with neurodegenerative disease. J Autoimmun. 2012;38(4):369-80.

145.   Mohanan S, Horibata S, Anguish LJ, Mukai C, Sams K, McElwee JL, et al. PAD2 overexpression in transgenic mice augments malignancy and tumor-associated inflammation in chemically initiated skin tumors. Cell Tissue Res. 2017;370(2):275-83.

146.   Coudane F, Mechin MC, Huchenq A, Henry J, Nachat R, Ishigami A, et al. Deimination and expression of peptidylarginine deiminases during cutaneous wound healing in mice. Eur J Dermatol. 2011;21(3):376-84.

147.   Wong SL, Demers M, Martinod K, Gallant M, Wang Y, Goldfine AB, et al. Diabetes primes neutrophils to undergo NETosis, which impairs wound healing. Nat Med. 2015;21(7):815-9.

148.   Wizeman JW, Mohan R. Expression of peptidylarginine deiminase 4 in an alkali injury model of retinal gliosis. Biochem Biophys Res Commun. 2017;487(1):134-9.

Chapter 2

Development and characterization of a peptidylarginine deiminase-deficient zebrafish model

Netta Golenberg, David A. Bennin, Paige E. Pistono, Miriam A. Shelef, and Anna Huttenlocher.

Author contributions: NG designed, performed, and analyzed experiments, and wrote the manuscript. DAB performed *in vitro* assays and protein purifications. PEP imaged larvae used in Figure 2.5A and B. AH and MAS designed experiments and edited the manuscript.

Abstract

Peptidylarginine deiminases (PADIs or PADs) are a family of enzymes that catalyze citrullination, a post-translational modification that has been implicated in a wide variety of diseases, including autoimmune disorders and Alzheimer's disease. The mechanisms by which PADIs contribute to development, physiology, and disease remain unclear. While PADIs have been widely studied in mammalian models, the presence of multiple PADI isoforms and functional redundancies make it challenging to dissect the functional roles of the mammalian PADI isozymes. Zebrafish have only one known ancestral *padi* gene, *padi2*. We generated a *padi2* zebrafish mutant line that has undetectable calcium-dependent citrullination and no evidence of compensation from unannotated Padi enzymes. The *padi2* mutants develop normally, but have increased numbers of neuromuscular synapses with normal muscle architecture at the larval stage. The *padi2* mutant zebrafish will provide a useful tool to study the role of citrullination both during development and in the context of zebrafish disease models.

Introduction

      Citrullination, or deimination, is the process by which a peptidyl-arginine is converted to a peptidyl-citrulline [1, 2]. Proteins belonging to the peptidylarginine deiminase (PADIs, also called PADs) family catalyze this posttranslational modification in a calcium-dependent manner [2, 3]. There are five mammalian isozymes (PADI1, 2, 3, 4, and 6), each with tissue-specific localization, function, and substrates, with PADI2 having the broadest tissue distribution and substrates [1, 4]. Citrullination results in a loss of a positively charged amino acid and has profound effects on the structure and function of its diverse substrates. PADIs function in a wide variety of processes including apoptosis, regulation of gene expression, pluripotency, and the immune response [5].

      Citrullination by PADI enzymes has also been implicated in a number of diseases including rheumatoid arthritis, multiple sclerosis (MS), cancer, and neurodegenerative diseases [6-8]. Patients with rheumatoid arthritis show increased PADI2 and PADI4 protein levels, increased citrullination, and pathologic autoantibodies against citrullinated proteins [7, 9-11]. Deletion of either PADI2 or PADI4 in a murine model of rheumatoid arthritis reduces arthritis severity, but does not abrogate disease completely, potentially due to compensation from other PADI enzymes [12, 13]. In MS, excessive citrullination of myelin basic protein (MBP) may contribute to MBP degradation and the demyelination that results in disease [7, 14, 15]. Overexpression of PADI2 in mice under the control of the MBP promoter was sufficient to drive myelin degradation [16]. However, the *Padi2* knockout was not sufficient to attenuate disease in a mouse model of MS [17], potentially due to the remaining citrullination activity of

other PADIs [18, 19]. Further investigation into the mechanisms by which citrullination contributes to these and other diseases may provide a putative target for therapeutic purposes. However, these investigations are difficult in existing mammalian models because of potential compensation by other *Padi* genes.

Here we generated a Padi2-deficient zebrafish to dissect the role of citrullination during development. Zebrafish, *Danio rerio*, have one highly-conserved copy of a *padi* gene, *padi2*, that shares canonical mammalian PADI features, with conserved enzymatic activity and calcium dependence. We generated a *padi2* mutant zebrafish line that lacks detectable calcium-dependent citrullination activity, providing the first reported model of a citrullination-deficient vertebrate. Padi2-deficient zebrafish are viable and fertile, without obvious developmental defects. In particular, we were interested in the potential neurodevelepmental defects in *padi2* mutants, given the role of citrullination in diseases of the nervous system. We found that Padi2-deficient zebrafish have altered formation of neuromuscular synapses. The Padi2-deficient zebrafish will provide a powerful tool to examine the role of citrullination in development, physiology, and disease models.

Results

Characterization of zebrafish peptidylarginine deiminases

To study Padi function in zebrafish, we first determined which transcripts were produced from the one predicted *padi* gene, *padi2*. Both a full-length (16 exons-ENSDART00000064842.6) and a short-length (7 exons-ENSDART00000140943.3) transcript have been predicted. Additionally, two alternative start sites are annotated.

Predicted transcripts and differences between annotations in the GRCz10 and GRCz11

genome assemblies are shown in Fig 2.1A. To determine the full-length transcripts

present in zebrafish larvae, we amplified *padi2* transcripts from cDNA using primers

complementary to the annotated stop site and the two proposed start sites. We

identified two full length splice variants, referred to here as 001 and 002 (Fig 2.1A).

These transcripts have a different start site and different first exon, but of note, both

splice variants have a shared full-length exon 10, contrary to the genome assembly

predictions. These transcripts are highly conserved with the human PADIs (Fig 2.1B).

Specifically, when aligned to human PADI2, catalytic, substrate-binding, and calcium-

coordinating amino acids are conserved in both variants and have approximately 55%

amino acid identity and 69% similarity to human PADI2 [20] (Fig 2.2A and Fig 2.1B).

Next, to characterize Padi2 protein expression in larval zebrafish, we generated a

polyclonal zebrafish anti-Padi2 antibody. This antibody was first characterized using

western blotting of whole larvae lysates which yielded a doublet at 75-80 kDA, providing

further evidence for two full length zebrafish *padi2* splice variants (Fig 2.2B). Notably,

this antibody did not detect a protein of equivalent size to the predicted short transcript

(Fig 2.1C). Absence of this doublet with pre-immune serum demonstrates the

specificity of the antibody (Fig 2.1D).

To confirm that zebrafish Padi2 has citrullination activity, we assayed protein

from both transcripts expressed in bacteria and employed a colorimetric *in vitro*

citrullination activity assay [21]. Both products can efficiently catalyze the citrullination of

the substrate (Fig 2.2C). Mammalian PADIs bind 5-6 calcium ions for proper structure
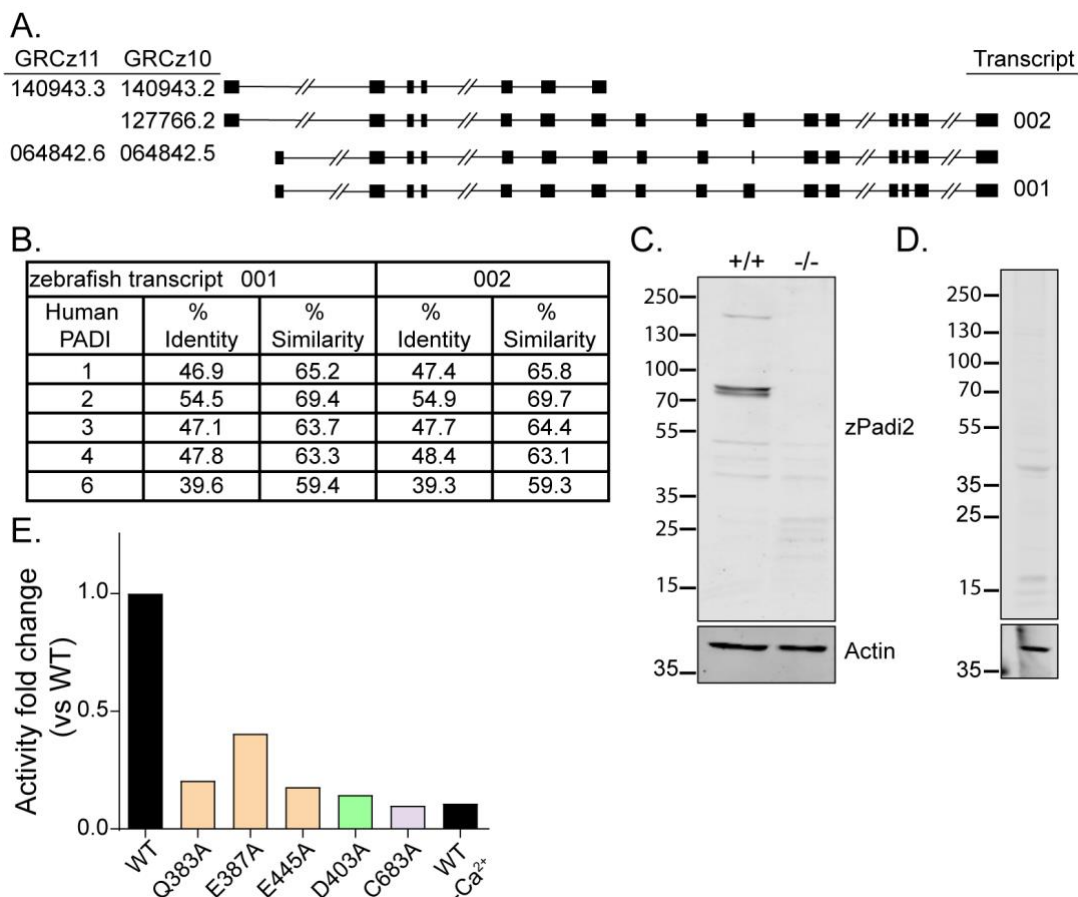
Fig 2.1: Zebrafish Padi2 model characterization. (A) Schematics of *padi2* transcripts, with exons represented by solid boxes and introns by connected lines (dashes indicate shortening of relative length for display purposes). Left, list of the corresponding last 7 digits of a transcript's Ensembl ID from GRCz11 and GRCz10 genome assemblies (full Ensemble IDs listed in materials and methods). Right, list of the names used to reference the cloned transcripts discussed in this paper. (B) Amino acid sequence identity and similarity of both Padi2 variants with human PADIs. Pairwise sequence alignment done using EMBOSS water. (C) Full western blot (from Fig 2.2D) of pooled larvae for zebrafish Padi2 and actin. Wild-type and *padi2*^{-/-} lysates were probed. Representative blot of 4 western blots. (D) Western blot of pooled wild-type larvae

probed with pre-immune serum and Actin. (E) Citrullination activity of Padi2 002 and

individual point mutations in select calcium-coordinating and catalytic amino acids

(colors correspond to highlighted residues in Fig 2.2A). Fold change of enzymatic

activity normalized to wild-type Padi2 002. Data represent 2 independent experiments

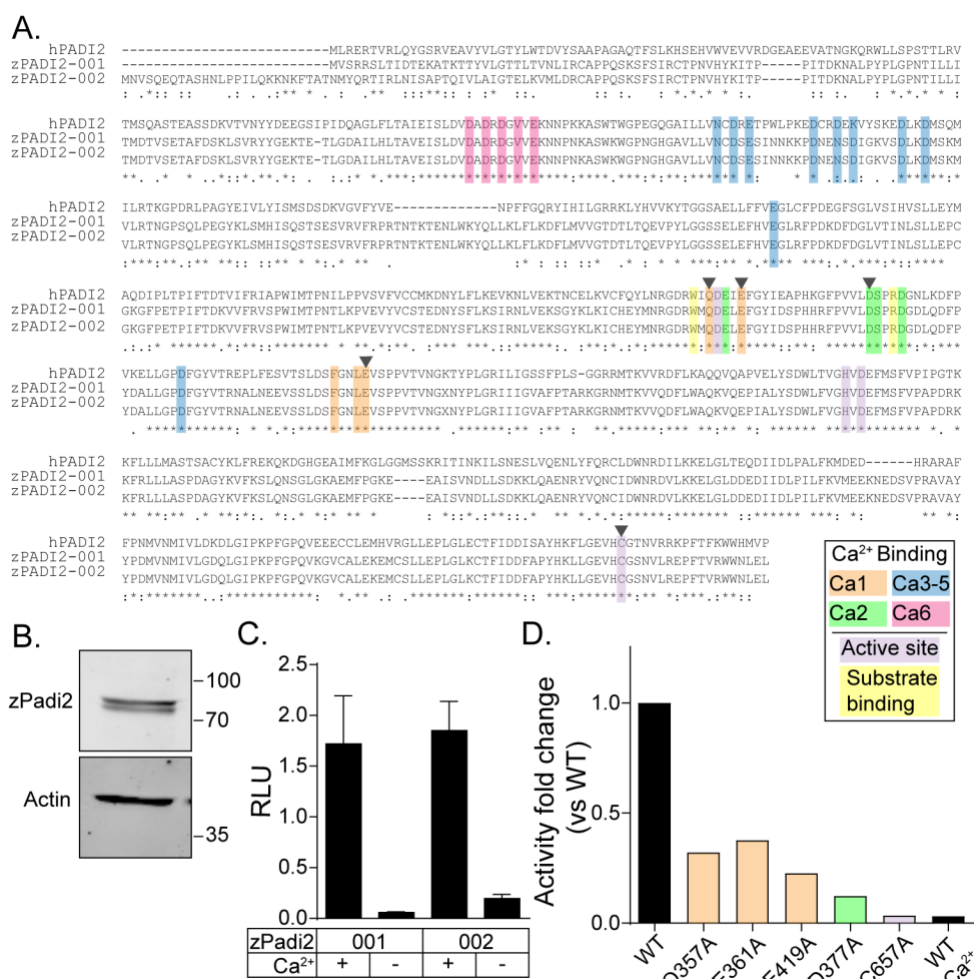and wild-type values are also represented in Fig 2.2C.

Fig 2.2: Zebrafish Padi2 has calcium dependent arginine-deiminase activity. (A) Full amino acid sequences of human PADI2 and predicted zebrafish Padi2 splice variants (001 and 002). Amino acids are highlighted to demonstrate calcium coordination, catalytic residues, and substrate-binding residues. Black arrow heads indicate amino acids referred to in D and Fig 2.1E. (B) Representative western blot of pooled larvae probed for zebrafish Padi2 and Actin (representative of 4 experiments). (C) Citrullination activity of bacterially expressed zebrafish Padi2 001 and 002 total lysate with and without calcium. Absorbance of light was measured and expressed as mean ($\pm$ SEM) relative light units (RLU) normalized for protein level. Data represent

three independent experiments. (D) Citrullination activity of Padi2 001 and individual point mutations in calcium coordinating and catalytic amino acids (colors correspond to highlighted residues in A). Fold change of enzymatic activity is shown relative to wild-type Padi2 001. Data represent 2 independent experiments and wild-type values are also represented in C.

and catalysis [3, 22], with binding of Ca1 and Ca2 being essential for hPADI4 activity [3]. We found that zebrafish Padi2 activity was also calcium dependent (Fig 2.2C). Additionally, alanine point mutations of the amino acids predicted to be necessary for Ca1 and Ca2 binding [3] diminished citrullination activity of zebrafish Padi2 (Fig 2.2D and Fig 2.1E). We confirmed that zebrafish Padi2 uses a conserved cysteine essential for catalysis, as mutation of this cysteine to alanine abolished activity (Fig 2.2D and Fig 2.1E). These data indicate that zebrafish Padi2 is a canonical PADI that has similar function as mammalian PADI enzymes.

Generation of a *padi2* zebrafish mutant using CRISPR/Cas9 gene editing

We next sought to generate a zebrafish *padi* mutant line that could be used to investigate the effects of a loss of citrullination activity on zebrafish development and disease. To generate a *padi2* loss of function allele, we employed CRISPR/Cas9 gene editing with a gRNA targeted to exon 7 (Fig 2.3A) and identified a mutant line with a 20 base pair deletion (Fig 2.3B and 2.3C). This mutation, referred to here as *padi2*$^{-/-}$, caused a predicted frameshift mutation resulting in an early stop. We confirmed that the *padi2*$^{-/-}$ larvae have reduced levels of *padi2* mRNA with RT-qPCR of individual *padi2*$^{+/-}$ incrossed progeny (Fig 2.3D). Using our antibody, we also confirmed *padi2*$^{-/-}$ larvae are devoid of Padi2 protein (Fig 2.3E and Fig 2.1D). We used the citrullination assay on lysate from whole wild-type larvae to detect calcium-dependent citrullination activity Importantly, we demonstrated that *padi2*$^{-/-}$ zebrafish lysates lack citrullination activity, even in the presence of excess calcium (Fig 2.3F), indicating that Padi2 is likely the only protein with detectable citrullination activity in zebrafish larvae.
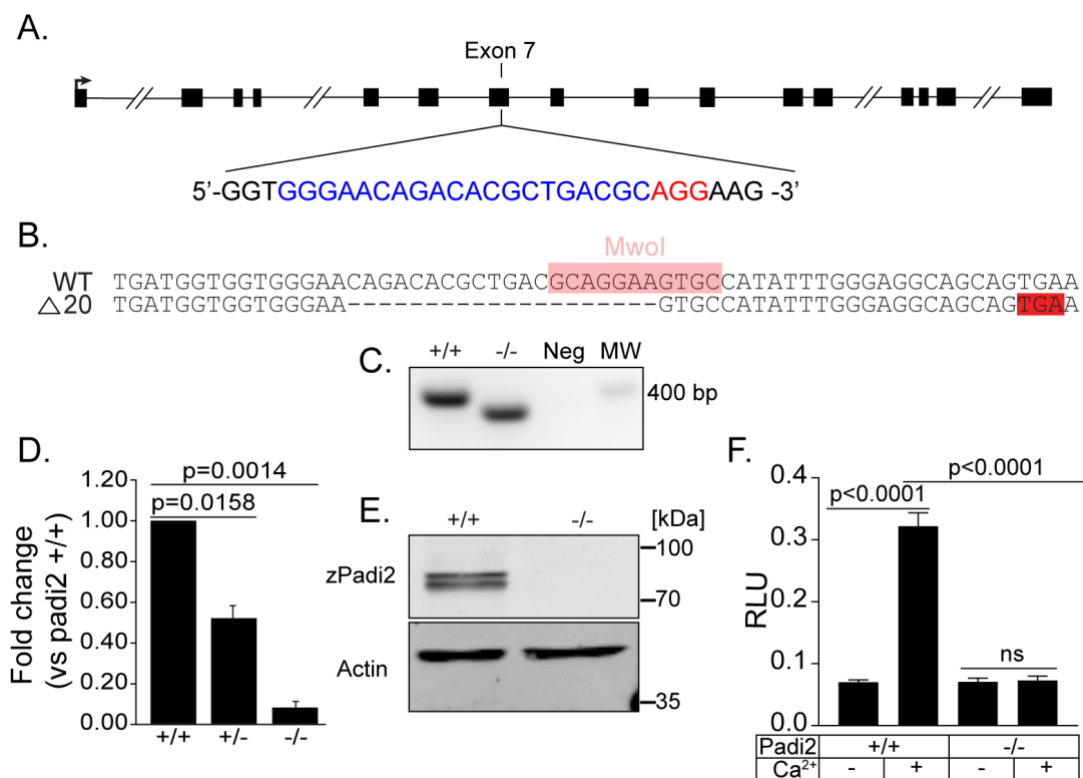
Fig 2.3: Generation and confirmation of a *padi2* mutant. (A) Schematic of *padi2*

gene with exon 7 gRNA sequence highlighted for CRISPR/Cas9 mutagenesis. gRNA

sequence in blue, PAM site in red. (B) Sequence alignment of wild-type and *padi2*^{-/-} 20

bp mutation in exon 7. MwoI restriction site for genotyping highlighted in pink, predicted

early stop codon highlighted in red. (C) PCR amplification of DNA from a single 2 dpf

embryo results in a molecular weight shift of a ~400 bp amplicon in *padi2*^{-/-} compared to

wild-type cousins. Neg, water-negative control; MW, Invitrogen 1 Kb Plus Molecular

DNA Ladder. (D) RT-qPCR of *padi2* exon5/6 on individual larvae from a *padi2*^{+/-} incross.

Data are from three pooled independent experiments with the means and SEM reported

and a one sample t test performed. (E) Representative western blot for zebrafish Padi2

and Actin from pooled larvae (representative of 4 experiments). (F) Relative citrullination

activity of pooled zebrafish lysates, normalized to wild-type no-calcium condition. Data

are from three independent experiments with the means and SEM reported and a

paired t test performed.

padi2 mutant larvae have increased numbers of neuromuscular junctions

Previous studies have indicated that PADIs are necessary for normal development and fertility [23-25]. Interestingly, we found that the Padi2-deficient zebrafish did not have any gross morphological defects and had normal viability of the larvae; crossings of this mutant line statistically followed expected Mendelian ratios (Fig 2.4). _padi2_$^{-/-}$ fish developed to adulthood and produced maternally zygotic mutants. Previous morpholino data implicated Padi2 in angiogenesis [26]. However, in this mutant line we did not observe any defects in blood vessel development. Using the _Tg(flk:mCherry)_ line to mark the vasculature, we observed that _padi2_$^{-/-}$ larvae have normal intersegmental vessel (ISV) formation at approximately 48 hours post fertilization (hpf) (Fig 2.5A). ISV length, quantified by averaging the lengths of five ISV centered around the cloaca for each individual larva was not significantly different in _padi2_-/- larvae and their control _padi2_$^{+/+}$ siblings, indicating normal vasculature in this zebrafish _padi2_ mutant line (Fig 2.5B).

The mammalian PADI2 is the predominate isozyme in skeletal muscle and nervous system [27-29]. To further characterize the mutant line, we examined the effects of the mutation on muscle development in zebrafish. We visualized slow and fast-twitch muscles in the trunk of 5 days post fertilization (dpf) larvae by staining for the myosin heavy chain and phalloidin (Fig 2.5C and 2.5D). Both skeletal muscle fibers appeared morphologically normal in the _padi2_$^{-/-}$ larvae. Next, to examine neuromuscular synapses in the trunk of 5 dpf larvae, we immunostained for presynaptic vesicles (α-SV2) and acetylcholine receptors (AChR) (α-BTX) (Figure 2.5E). Quantification of these puncta indicated that _padi2_$^{-/-}$ larvae have increased neuromuscular junctions (Fig 2.5F).

A.

Genotype	+/+	+/-	-/-
Total number	298	609	290
Percentage	25%	51%	24%

B.

Genotype	+/+	+/-	-/-
Total number	41	56	29
Percentage	33%	44%	23%

Fig 2.4: Homozygous *padi2* mutants are viable: (A) Genotype frequency at 5 dpf of incrossed heterozygotes. (B) Genotype frequency of adult offspring of incrossed heterozygotes. Data are from four and six clutches, respectively, and analyzed by Chi-squared tests.
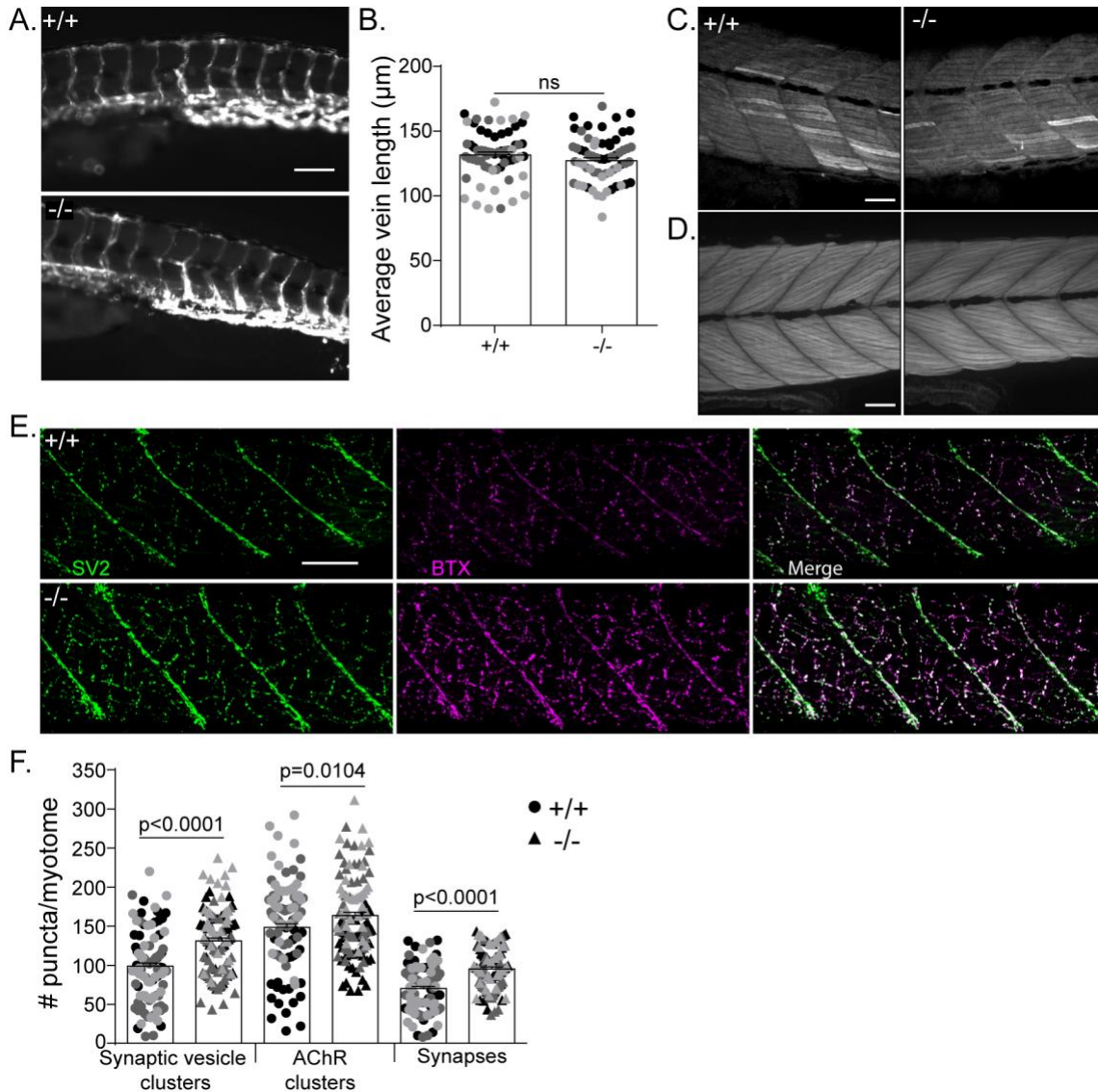
Fig 2.5: *padi2* mutants have increased neuromuscular junctions. (A)

Representative images of the vasculature of 2 dpf larvae from a *Tg(flk:mcherry);padi2*^{+/-}

incross. Scale bar=100 μm. (B) Plot representing the average length in μm of five

intersegmental vessels centered around the cloaca from each larva. Data from three

pooled independent experiments with the lsmeans $\pm$ SEM reported and analyzed by

ANOVA. Each point represents individual larva and are color coded by experimental

replicates. n=62 larvae for each genotype. ns= not significant. (C) Representative

images of slow-muscle fibers immunostained with α-MyHC antibody (F59) in the trunk of 5 dpf larvae (n= 43 +/+, 49 -/-, from 3 independent experiments). Scale bar=50 μm. (D) Representative images of the trunk of phalloidin-stained 5 dpf larvae for visualization of F-actin in fast-muscle fibers (n= 46 +/+, 48 -/-, from 3 independent experiments). C-D, Scale bar=50 μm. Wild-type cousin (left) and *padi2*^{-/-} (right). (E) Neuromuscular junctions are labeled with α-SV2 (green, presynaptic vesicles), α-BTX (red, postsynaptic AChRs), and merge (synapses) in wild-type cousins (top) and *padi2*^{-/-} (bottom) larvae at 5 dpf. Scale bar=50 μm. (F) Quantification of the number of SV2 puncta, AChR puncta, and synapses in a single myotome in the trunks of larvae. Data are from three pooled independent experiments with the lsmeans ($\pm$) SEM and p values calculated by ANOVA reported. Each symbol represents a single myotome and are color coded by experimental replicates. Measurements were taken from 2 myotomes per larva with wild-type n=100 from 50 larvae, and n=114 from 57 *padi2*^{-/-} larvae.

Discussion

      Here we report a zebrafish *padi2* mutant line with impaired calcium-dependent citrullination activity. While mammalian *Padi* mutant models have been established, these models are limited, at least in part by the presence of multiple *Padi* genes and the possibility of genetic compensation. Zebrafish possess a single Padi enzyme, and therefore, are an ideal tool for studying the function of citrullination and its effect on development, physiology, and disease. We found that Padi2 has conserved features of its activity, including conserved amino acids for calcium coordination and catalysis. In this study, we found that Padi2-deficient zebrafish have aberrant neuromuscular junctions.

      Previous studies have shown that Padi2 is expressed in central synapses [30], however the role of citrullination in synapse development or function remains largely unknown. Our results indicate that loss of Padi2 results in an increased number of neuromuscular junctions. Further motor neuron-muscle recordings will be necessary in order to address whether Padi2 is required for proper synapse activity or rather if NMJ numbers represent an indirect effect of Padi2's role in motoneuron development. Future behavioral analysis of early zebrafish larvae movement should also be done to determine if *padi2* mutant NMJ numbers has functional consequences, as a recent report by Falcao *et al.* showed PADI2 knockout mice displayed decreased object-recognition memory, as well as impaired motor-coordination behaviors [31]. Additionally, Falcao *et al.* demonstrated a developmental role of PADI2 in efficient oligodendrocyte differentiation and proper axon myelination. While it is known that PADI2 is the major PADI isozyme of the nervous system in mammals [1, 4, 32, 33], our data combined with

this mouse study implicate a potential role for Padi2 in glial cells, presynaptic signaling, synaptogenesis, and synaptic elimination, which should be investigated in future studies.

Unlike in zebrafish, the establishment of a fully citrullination-depleted mammalian model is not feasible as mammals have five distinct *Padi* genes [1]. Additionally, in mammalian studies, two of the PADI enzymes are required for development. The highly abundant egg and early embryo PADI6 is essential for embryonic development as mutations in the gene lead to female sterility in both mice and humans [23, 34-37]. PADI1 facilitates early embryo gene activation through the citrullination of histone tails and is necessary for development past the 4-cell stage in mice [24, 25]. Our finding that zebrafish *padi2*^{-/-} females produced viable offspring was surprising. One possible explanation for this result could be that PADI1 and PADI6 exert their developmental effects through other mechanisms not dependent on deiminase activity. For example, PADI6 is known to have lost some of its calcium binding amino acids and lacks deiminase activity [38]. Alternatively, the viability of the zebrafish *padi2* mutant suggests that zebrafish Padi2 provides a simple model for the mammalian PADI2 enzyme, as *Padi2*-deficient mice are also viable [17]. Indeed, the zebrafish Padi is more closely related to mammalian PADI2 than the other mammalian PADI enzymes, which are hypothesized to have arisen via gene duplications [1, 4]. Through mutations, mammalian PADIs could have acquired their restricted tissue patterns and specialization during the later evolution of biological complexity in vertebrates. The simplicity of the zebrafish model makes this *padi2* mutant a valuable animal model for

the study of this isolated ancestral protein of the mammalian PADI with the broadest tissue distribution and substrate specificity [1, 4].

A major concern in mammalian studies of knockout PADI proteins is the unexamined potential for genetic compensation by other *Padi* genes. Indeed, several mouse studies observed modulated expression of other PADI isozymes when PADI2 was overexpressed [16, 39]. Work with PADI2 knockout mice showed upregulation of PADI6 in inappropriate tissues [40] and PADI4 citrullination of myelin basic protein [18]. Particularly, treatment of a mouse model of MS (experimental autoimmune encephalomyelitis, EAE) with 2-chloroacetamidine, a PADI2 and PADI4 inhibitor, attenuated the disease [19], while the PADI2 knockout mouse still developed EAE [17]. This work led to the conclusion that citrullination is not essential for the development of EAE, while later studies demonstrated that in PADI2-deficient mice citrullination activity remained due to PADI4 activity [18, 19]. The use of the zebrafish model in future studies will allow for the isolation of the role of Padi2 and, to some extent, citrullination in disease pathogenesis, eliminating the potential of redundancies between PADI2 and PADI4 observed in mouse models.

In summary, we have developed a Padi- and citrullination-deficient vertebrate model in zebrafish. *padi2* null zebrafish larvae lack *padi2* mRNA, Padi2 protein, and deiminase activity. Zebrafish are an attractive disease model due to their amenability to imaging of *in vivo* dynamics and cell-cell interactions, their use in high throughput screens of preclinical therapeutics, as well as, sharing over 80% of the human disease related genes [41]. Many zebrafish disease models have been developed for the investigation of cancer [42], multiple sclerosis [43-45], and rheumatoid arthritis [46], in

which PADIs have been implicated in disease pathogenesis. A citrullination-deficient vertebrate model provides a powerful tool for future studies of the role of citrullination in development, disease, and the identification of PADI targets.

Materials and methods

Zebrafish maintenance and handling

All protocols in this study were approved by the University of Wisconsin-Madison Animal Care and Use committee (IACUC). Adult zebrafish were maintained on a 14h:10h light/dark schedule. Fertilized embryos were transferred and maintained in E3 buffer at 28.5°C. Adult AB and NHGRI-1 [47] fish were obtained from the Zebrafish International Resource Center (ZIRC) and utilized in this study. Zebrafish are monitored for any complications or discomfort, after which the affected animal is immediately euthanized. Euthanization is done by placing the zebrafish into 0.05% Tricaine (diluted in E3 water) buffered with sodium bicarbonate to a pH 7 for 10 to 15 minutes. Fish are monitored for lack of movement and breathing at which point they are placed in a latex container for disposal. Larvae (3 dpf or older) are placed in cold water (4°C) for at least 20 minutes following loss of operculum movement. Sedation of adult zebrafish was done by placing the animal in 0.014% tricaine in fish water buffered with sodium bicarbonate to a pH 7 for about 3-5 minutes to guarantee anesthetization. Upon completion of fin tissue collection, anesthetized fish are placed into tanks with fresh water and observed for 2-3 minutes to ensure they maintain normal behavior.

Zebrafish and Human PADI alignment

Sequence alignments were done using EMBOSS water [20]. Transcripts listed in Table 1.

Table 1. Annotated PADI transcripts used in this study.

Name	Trancscript ID	Genome assembly
zPadi2 202	ENSDART00000140943.3	GRCz11
zPadi2 203	ENSDART00000140943.2	GRCZ10
zPadi2 201	ENSDART00000064842.6	GRCz11
zPadi2 201	ENSDART00000064842.5	GRCz10
zPadi2 202	ENSDART00000127766.2	GRCz10
hPADI1 201	ENST00000375471.4	GRCh38
hPADI2 202	ENST00000375486.8	GRCh38
hPADI3 201	ENST00000375460.3	GRCh38
hPADI4 201	ENST00000375448.4	GRCh38
hPADI6 201	ENST00000619609.1	GRCh38

Generation of a padi2 mutant line and genotyping

Zebrafish CRISPR/Cas9 injections were done as previously performed in our lab [48, 49]. guide RNA (gRNA) was designed using CHOPCHOP [50] for zebrafish Padi2 (ENSDARG00000044167).

Exon 7 target sequence: GGGAACAGACACGCTGACGC

The pT7 gRNA vector (Addgene 46759) was digested with BsmBI, BglII, and SalI and diluted to 5 ng/ul. Oligos were annealed in annealing buffer (40 mM Tris pH8.0, 20 mM MgCl2, 50 mM NaCl, 1 mM EDTA pH 8.0) by lowering the temperature 1°C every 30 seconds from 95°C to 4°C. Annealed oligos and cut pT7 gRNA were ligated using Quick Ligase (New England Biolabs) and transformed into DH5a competent *E. coli* cells (Thermo Fisher Scientific). Single colonies were selected and sequenced with an M13

primer. Positive plasmid was linearized with BamHI (New England Biolabs) and *in vitro*

transcribed using the MAXIscript T7 kit (Ambion) followed by RNA cleanup by

miRVANA kit (Invitrogen). The gRNA and Cas9 protein (New England Biolabs) were

injected into a one-cell stage embryo from the NHGRI-1 zebrafish line with a 2 nl

injection. The final injection mix consisted of ~50 ng/ul gRNA and ~300 nM Cas9. To

confirm, genomic DNA was extracted from 2 days post fertilization (dpf) embryos,

amplified using the primers listed below, and separated on a 3% metaphor gel (Lonza).

Padi2 F: CTGATACATGGCACAACCTACG

Padi2 R: GAAAACCAGCAAGCAGAGAAAGTT

Sequences of F0 mosaic cuts were confirmed by TOPO cloning and sequencing.

Clutches of larvae with confirmed CRISPR cuts were grown to adulthood. Adult F0

CRISPR injected fish were screened for germline mutations by testing their individual

outcrossed offspring (2-5 dpf) using the primers listed above and Indel Detection and

Amplicon Analysis (IDAA) [51]. Sequences were analyzed using Peak Studio [52].

Mutation sequence was confirmed by TOPO cloning and sequencing.

Heterozygous *padi2* zebrafish were maintained by outcrossing to AB wild-type

background zebrafish and genotyped by genomic DNA isolated from fin clips and

amplified using the primers listed above. PCR product was either separated on a 2%

agarose gel for 3 hours or digested overnight with MwoI (New England Biolabs).

qRT-PCR

RNA and DNA were extracted from individual 2 dpf embryos from a *padi2+/-*

incross using TRIZOL (Invitrogen) following the manufacturers protocol. Embryos were

genotyped using GoTaq (Promega) as described above and 2-3 embryos of each

genotype were used for cDNA production using Superscript III First Strand Synthesis System with Oligo(dT) (Thermo Fisher Scientific). qPCR was performed using FastStart Essential Green Master (Roche) and a LightCycler96 (Rocher). Primers are listed for *padi2* and *ef1a* below. Data were normalized to *ef1a* using the ∆∆Ct method [53] and represented as fold change over wild-type embryos.

Padi2 exon5 qRT-PCR F: TAATGGCCATGGTGCAGTTC

Padi2 exon6 qRT-PCR R: ATGGTCCATTAGTGCGCAAC

Ef1a qRT-PCR F: TGCCTTCGTCCCAATTTCAG

EF1a qRT-PCR R: TACCCTCCTTGCGCTCAATC

Generation of zebrafish *padi2* clones and point mutations

Padi2 splice variants were amplified with Pfu Turbo DNA polymerase (Agilent) from cDNA using In-Fusion primers listed below. PCR products and a pCS2+8 vector [54] (Addgene) were digested with XbaI and BamHI (Promega) and ligated at room temperature using Takara ligation kit for long fragments.

Padi2 cloning R, with XbaI: GGATCG TCTAGATTACAGCTCCAGGTTCCACC

Padi2 cloning F transcript 002: CGATCCGGATCCATGAATGTTTCGCAGGAGC

Padi2 cloning F transcript 001: CGATCCGGATCCATGGTGTCCCGTCGATCTCTTAC

Both cDNA transcripts were cloned into pTRCHisA vector (Invitrogen) for N-terminal polyhistidine (his) tagging and expression in *E. coli* (BL21(DE3)pLysS Competent cells) using primers listed below. Constructs were inserted into the vector cut with BamHI and HindIII (Promega) using In-Fusion HD cloning kit (Clonetech). Point mutations were made with complementary primers (listed below) in pTRCHisA-padi2 vectors using QuikChange II Site-Directed Mutagenesis Kit (Agilent).

Catalytic C→A F: GTGAAGTTCACGCCGGGTCCAATGTTC

Catalytic C→A R: GAACATTGGACCCGGCGTGAACTTCAC

Ca1 binding Q→A F: ATCGCTGGATGGCGGATGAGCTTGAGTT

Ca1 binding Q→A R: AACTCAAGCTCATCCGCCATCCAGCGAT

Ca1 binding E→A F: GGATGAGCTTGCGTTTGGTTACATTG

Ca1 binding E→A R: CAATGTAACCAAACGCAAGCTCATCC

Ca1 binding E→A F: TTTCGGTAATCTGGCGGTCAGTCCACCA

Ca1 binding E→A R: TGGTGGACTGACCGCCAGATTACCGAAA

Ca2 binding D→A F: TGTTGTCCTGGCTTCTCCTCGTGAT

Ca2 binding D→A R: ATCACGAGGAGAAGCCAGGACAACA

Antibody production and western blotting

The anti-zebrafish Padi2 antibody was generated in rabbits using combined full length 001 and 002 variants fused to 6x poly-histidine in the pTRCHisA vector. Each immunogen was purified from BL21 *E. coli* lysates using a nickel-nitrilotriacetic acid superflow resin (Qiagen) then combined and sent to Covance for anti-serum productions. For western blotting, 50-100 2 dpf larvae were pooled and deyolked in calcium-free Ringer's solution with gentle disruption with a p200 pipette. Larvae were washed twice with phosphate-buffered saline (PBS) and stored at -80°C until samples were lysed by sonication in 20mM Tris pH 7.6, 0.1% Triton-X-100, 0.2 mM Phenylmethylsulfonyl fluoride (PMSF), 1 µg/mL Pepstatin, 2 µg/mL Aprotinin, and 1 µg/mL Leupeptin at 3 µL per larvae while on ice and clarified by centrifugation. Protein concentrations were determined using a bicinchoninic acid protein assay kit (Thermo Fisher Scientific), according to the manufacturer's instructions. Equal amounts of total

protein were loaded on 6-20% gradient SDS-polyacrylamide gels and transferred to nitrocellulose. Anti-serum was used at 1:500 dilution. Western blots were imaged with an Odyssey Infrared Imaging System (LI-COR Biosciences, Omaha, NW). For citrullination analysis by western of whole zebrafish lysates, methods for the citrullination colorimetric assay were followed, as described below, with the addition of dilution buffer in place of BAEE (N_α-Benzoyl-L-arginine ethyl ester hydrochloride in 100 mM Tris pH 7.4). The reaction was stopped after 90 minutes by boiling samples in SDS-PAGE sample buffer.

In vitro citrullination colorimetric assay

Zebrafish Padi2 constructs and point mutations were expressed in BL21 _E. coli_ cells. Lysates were prepared on ice by sonication in 20mM Tris pH 7.6, 0.1% Triton-X-100, 0.2 mM Phenylmethylsulfonyl fluoride (PMSF), 1 µg/mL Pepstatin, 2 µg/mL Aprotinin, and 1 µg/mL Leupeptin and clarified by centrifugation. Bacterial lysates were aliquoted and frozen at -80°C. Lysates from zebrafish larvae were prepared as described above for western blotting and used at equivalent amounts. Assay performed as previously described [21]. In short, 12.5µL lysate was incubated with 12.5 µL 4X reaction buffer (400 mM Tris pH 7.4, ± 80 mM $CaCl_2$, 20 mM DTT), 12.5 µL 80 mM BAEE (N_α-Benzoyl-L-arginine ethyl ester hydrochloride in 100 mM Tris pH 7.4), 12.5 µL dilution buffer (10 mM Tris pH 7.6, 150 mM NaCl, 2mM DTT) for 1 hour at 37°C. Reaction was stopped by the addition of 33 µM EDTA final concentration. Reactions were diluted 1:10 for an 8 mM BAEE final concentration and 50 µL aliquots were done in triplicate in a 96-well plate. 150 µL colorimetric buffer (composed of 1 mL buffer A (80 mM Diacetyl monoxime, 2 mM Thiosemicarbazide) and 3 mL buffer B (3 M Phosphoric

Acid, 6 M Sulfuric acid, 2 mM Ammonium iron (III) sulfate)) were added to each well and incubated at 95°C for 15 minutes, absorption was read at 540 nM. Relative light units were normalized to western blot densitometry using Odyssey Infrared Imaging System (LI-COR Biosciences, Omaha, NE).

Immunofluorescence, imaging, and analysis

Images always shown with anterior to the left. Immunostaining was performed on the offspring from incrossed adult F2 wild-type and *padi2*-/- sibling zebrafish.

5 dpf larvae were fixed in 4% pfa, 0.125 M sucrose, and 1X PBS overnight. For visualization of slow muscles, larvae were washed 3 times with 0.1% PBS-tween20 and incubated in 0.1% w/v collagenase type 1A (Sigma) in PBS at 37°C for 1.5 hours followed by 3 washes in PBSTD (0.3% TritonX, 1% DMSO in PBS). Larvae were blocked for 2 hours at room temperature (RT) in PBSTD with 2% BSA and 4% goat serum. Monoclonal mouse anti-myosin heavy chain (F59) (DSHB) [55] was used at 1:20 in block buffer and incubated overnight in 4°C. Larvae were washed five times in PBSTD and secondary Dylight 488 donkey anti-mouse IgG antibodies (Rockland Immunochemicals) were used at 1:250 in block buffer overnight at 4°C. Final five washes were done in PBSTD. Images were acquired on a spinning disk confocal (CSU-X; Yokogawa) on a Zeiss Observer Z.1 inverted microscope and an EMCCD evolve 512 camera (Photometrics) with a Plan-Apochromat NA 0.8/20x air objective, z-stacks, 1 μm optical sections, 512x512 resolution. Images were Z-projected with using Zen 2.3 lite software.

For visualization of fast muscle, fixed fish were washed with PBS 3 times followed by three washes in PBS with 0.1% tween-20. Larvae were permeabilized with

PBS 2% PBSTx (20% Triton-X-100 in 1X PBS) for 1.5 hours with gentle rocking. Fish

were then incubated with Rhodamin-phalloidin (Invitrogen) diluted 1:100 in 2% PBSTx

at 4°C overnight. Fish were rinsed in fresh 2% PBSTx followed by several washes in

0.2% PBSTx. Imaging was performed on the spinning disk microscope with a Plan-

Apochromat NA 0.8/20x air objective (centered on cloaca) with 1 µm optical sections.

For neuromuscular junction visualization, fix was washed off with three PBS

washes. The skin was peeled with fine forceps (Dumont #55 dumostar, Fine Science

Tools) starting above the swim bladder and removed down to the fin. Skinned larvae

were incubated in 0.1% w/v collagenase type 1A at RT for 15 minutes with gentle

rocking followed by three washes in PBS. For visualization of acetylcholine receptors

(AChR), fish were incubated for 30 minutes at RT 10 µg/ml alexa 594 conjugated a-

bungarotoxin (Thermo Fisher Scientific) diluted in incubation buffer (IB: 0.1% sodium

azide, 2% BSA, 0.5% Triton-X-100 in PBS, pH7.4). Embryos were rinsed three times in

IB. Mouse anti-synaptic vesicle glycoprotein 2A (SV2) (DSHB) [56] was used at 1:50 in

IB overnight at 4°C. Larvae were washed five times in IB and incubated with secondary

antibody at 1:250 in IB for 4 hours at RT or 4°C overnight. Final washes were done in IB

before imaging on a spinning disk microscope with an EC Plan-NeoFluaR NA 0.75/40x

air objective (Zeiss) (centered around the cloaca with 2x1 tile images and 1 µm optical

sections). To quantify colocalization of signal, maximum intensity projections were

analyzed in FIJI using the plugin ComDet v3.7 for spot localization. Particles were

threshold as approximate size being 5 pixels, intensity threshold for SV2 between 4-5

and α-BTX between 2-3 and a 6 pixel max distance between particles.

https://github.com/ekatrukha/ComDet/wiki

Tg(flk:mcherry) [57]*;padi2* +/- incrossed larvae were imaged at 2dpf on a Zeiss zoomscope (EMS3/SyCoP3; Zeiss; Plan-NeoFluar Z objective-50x magnification) with an Axiocam Mrm CCD camera using ZEN pro 2012 software (Zeiss). Larvae were individually genotyped post imaging. Analysis was done blinded using FIJI. The lengths of five intersegmental vessels centered around the cloaca were measured and averaged per larvae.

Statistical analysis

For all statistical analyses, at least three independent experiments were conducted. For data in Fig 2E, analysis was done using one-way ordinary analysis of variance (ANOVA) with a Holm's-Sidak's multiple comparisons test. To examine mutant survival, mendelian ratio was confirmed for both larvae and adult offspring from a heterozygous incross by Chi-squared tests. For neuromuscular synapse quantifications, data were pooled from the independent replicates and results were summarized in terms of least-squared adjusted means and standard errors. Results were analyzed using (ANOVA) with a Tukey's multiple comparisons test. Graphical representation shows individual data points color coded to reflect replicates. Statistical analysis and graphical representations were done using R version 3.4 and GraphPad Prism version 6.

Acknowledgements

References

1.   Vossenaar ER, Zendman AJ, van Venrooij WJ, Pruijn GJ. PAD, a growing family of citrullinating enzymes: genes, features and involvement in disease. Bioessays. 2003;25(11):1106-18.

2.   Rogers GE, Harding HW, Llewellyn-Smith IJ. The origin of citrulline-containing proteins in the hair follicle and the chemical nature of trichohyalin, an intracellular precursor. Biochim Biophys Acta. 1977;495(1):159-75.

3.   Arita K, Hashimoto H, Shimizu T, Nakashima K, Yamada M, Sato M. Structural basis for Ca(2+)-induced activation of human PAD4. Nat Struct Mol Biol. 2004;11(8):777-83.

4.   Rebl A, Kollner B, Anders E, Wimmers K, Goldammer T. Peptidylarginine deiminase gene is differentially expressed in freshwater and brackish water rainbow trout. Mol Biol Rep. 2010;37(5):2333-9.

5.   Witalison EE, Thompson PR, Hofseth LJ. Protein Arginine Deiminases and Associated Citrullination: Physiological Functions and Diseases Associated with Dysregulation. Curr Drug Targets. 2015;16(7):700-10.

6.   Spengler J, Lugonja B, Ytterberg AJ, Zubarev RA, Creese AJ, Pearson MJ, et al. Release of Active Peptidyl Arginine Deiminases by Neutrophils Can Explain Production of Extracellular Citrullinated Autoantigens in Rheumatoid Arthritis Synovial Fluid. Arthritis Rheumatol. 2015;67(12):3135-45.

7.   Gyorgy B, Toth E, Tarcsa E, Falus A, Buzas EI. Citrullination: a posttranslational modification in health and disease. Int J Biochem Cell Biol. 2006;38(10):1662-77.

8.   Chang X, Han J, Pang L, Zhao Y, Yang Y, Shen Z. Increased PADI4 expression in blood and tissues of patients with malignant tumors. BMC Cancer. 2009;9:40.

9. Schellekens GA, de Jong BA, van den Hoogen FH, van de Putte LB, van Venrooij WJ. Citrulline is an essential constituent of antigenic determinants recognized by rheumatoid arthritis-specific autoantibodies. J Clin Invest. 1998;101(1):273-81.

10. Wigerblad G, Bas DB, Fernades-Cerqueira C, Krishnamurthy A, Nandakumar KS, Rogoz K, et al. Autoantibodies to citrullinated proteins induce joint pain independent of inflammation via a chemokine-dependent mechanism. Ann Rheum Dis. 2016;75(4):730-8.

11. Engdahl C, Bang H, Dietel K, Lang SC, Harre U, Schett G. Periarticular Bone Loss in Arthritis Is Induced by Autoantibodies Against Citrullinated Vimentin. J Bone Miner Res. 2017;32(8):1681-91.

12. Bawadekar M, Shim D, Johnson CJ, Warner TF, Rebernick R, Damgaard D, et al. Peptidylarginine deiminase 2 is required for tumor necrosis factor alpha-induced citrullination and arthritis, but not neutrophil extracellular trap formation. J Autoimmun. 2017;80:39-47.

13. Shelef MA, Sokolove J, Lahey LJ, Wagner CA, Sackmann EK, Warner TF, et al. Peptidylarginine deiminase 4 contributes to tumor necrosis factor alpha-induced inflammatory arthritis. Arthritis Rheumatol. 2014;66(6):1482-91.

14. Moscarello MA, Mastronardi FG, Wood DD. The role of citrullinated proteins suggests a novel mechanism in the pathogenesis of multiple sclerosis. Neurochem Res. 2007;32(2):251-6.

15. Wood DD, Bilbao JM, O'Connors P, Moscarello MA. Acute multiple sclerosis (Marburg type) is associated with developmentally immature myelin basic protein. Ann Neurol. 1996;40(1):18-24.

16. Musse AA, Li Z, Ackerley CA, Bienzle D, Lei H, Poma R, et al. Peptidylarginine deiminase 2 (PAD2) overexpression in transgenic mice leads to myelin loss in the central nervous system. Dis Model Mech. 2008;1(4-5):229-40.

17. Raijmakers R, Vogelzangs J, Raats J, Panzenbeck M, Corby M, Jiang H, et al. Experimental autoimmune encephalomyelitis induction in peptidylarginine deiminase 2 knockout mice. J Comp Neurol. 2006;498(2):217-26.

18. Wood DD, Ackerley CA, Brand B, Zhang L, Raijmakers R, Mastronardi FG, et al. Myelin localization of peptidylarginine deiminases 2 and 4: comparison of PAD2 and PAD4 activities. Lab Invest. 2008;88(4):354-64.

19. Moscarello MA, Lei H, Mastronardi FG, Winer S, Tsui H, Li Z, et al. Inhibition of peptidyl-arginine deiminases reverses protein-hypercitrullination and disease in mouse models of multiple sclerosis. Dis Model Mech. 2013;6(2):467-78.

20.   Smith TF, Waterman MS. Identification of common molecular subsequences. J Mol Biol. 1981;147(1):195-7.

21.   Nakayama-Hamada M, Suzuki A, Kubota K, Takazawa T, Ohsaka M, Kawaida R, et al. Comparison of enzymatic properties between hPADI2 and hPADI4. Biochem Biophys Res Commun. 2005;327(1):192-200.

22.   Slade DJ, Fang P, Dreyton CJ, Zhang Y, Fuhrmann J, Rempel D, et al. Protein arginine deiminase 2 binds calcium in an ordered fashion: implications for inhibitor design. ACS Chem Biol. 2015;10(4):1043-53.

23.   Esposito G, Vitale AM, Leijten FP, Strik AM, Koonen-Reemst AM, Yurttas P, et al. Peptidylarginine deiminase (PAD) 6 is essential for oocyte cytoskeletal sheet formation and female fertility. Mol Cell Endocrinol. 2007;273(1-2):25-31.

24.   Kan R, Jin M, Subramanian V, Causey CP, Thompson PR, Coonrod SA. Potential role for PADI-mediated histone citrullination in preimplantation development. BMC Dev Biol. 2012;12:19.

25.   Zhang X, Liu X, Zhang M, Li T, Muth A, Thompson PR, et al. Peptidylarginine deiminase 1-catalyzed histone citrullination is essential for early embryo development. Sci Rep. 2016;6:38727.

26.   Khajavi M, Zhou Y, Birsner AE, Bazinet L, Rosa Di Sant A, Schiffer AJ, et al. Identification of Padi2 as a novel angiogenesis-regulating gene by genome association studies in mice. PLoS Genet. 2017;13(6):e1006848.

27.   Watanabe K, Senshu T. Isolation and characterization of cDNA clones encoding rat skeletal muscle peptidylarginine deiminase. J Biol Chem. 1989;264(26):15255-60.

28.   Watanabe K, Akiyama K, Hikichi K, Ohtsuka R, Okuyama A, Senshu T. Combined biochemical and immunochemical comparison of peptidylarginine deiminases present in various tissues. Biochim Biophys Acta. 1988;966(3):375-83.

29.   Kubilus J, Baden HP. Purification and properties of a brain enzyme which deiminates proteins. Biochim Biophys Acta. 1983;745(3):285-91.

30.   Bayes A, Collins MO, Reig-Viader R, Gou G, Goulding D, Izquierdo A, et al. Evolution of complexity in the zebrafish synapse proteome. Nat Commun. 2017;8:14613.

31.   Falcao AM, Meijer M, Scaglione A, Rinwa P, Agirre E, Liang J, et al. PAD2-Mediated Citrullination Contributes to Efficient Oligodendrocyte Differentiation and Myelination. Cell Rep. 2019;27(4):1090-102 e10.

32.	Keilhoff G, Prell T, Langnaese K, Mawrin C, Simon M, Fansa H, et al. Expression pattern of peptidylarginine deiminase in rat and human Schwann cells. Dev Neurobiol. 2008;68(1):101-14.

33.	Magnadottir B, Hayes P, Hristova M, Bragason BT, Nicholas AP, Dodds AW, et al. Post-translational protein deimination in cod (Gadus morhua L.) ontogeny novel roles in tissue remodelling and mucosal immune defences? Dev Comp Immunol. 2018;87:157-70.

34.	Xu Y, Shi Y, Fu J, Yu M, Feng R, Sang Q, et al. Mutations in PADI6 Cause Female Infertility Characterized by Early Embryonic Arrest. Am J Hum Genet. 2016;99(3):744-52.

35.	Qian J, Nguyen NMP, Rezaei M, Huang B, Tao Y, Zhang X, et al. Biallelic PADI6 variants linking infertility, miscarriages, and hydatidiform moles. Eur J Hum Genet. 2018;26(7):1007-13.

36.	Maddirevula S, Coskun S, Awartani K, Alsaif H, Abdulwahab FM, Alkuraya FS. The human knockout phenotype of PADI6 is female sterility caused by cleavage failure of their fertilized eggs. Clin Genet. 2017;91(2):344-5.

37.	Wang X, Song D, Mykytenko D, Kuang Y, Lv Q, Li B, et al. Novel mutations in genes encoding subcortical maternal complex proteins may cause human embryonic developmental arrest. Reprod Biomed Online. 2018;36(6):698-704.

38.	Raijmakers R, Zendman AJ, Egberts WV, Vossenaar ER, Raats J, Soede-Huijbregts C, et al. Methylation of arginine residues interferes with citrullination by peptidylarginine deiminases in vitro. J Mol Biol. 2007;367(4):1118-29.

39.	McElwee JL, Mohanan S, Horibata S, Sams KL, Anguish LJ, McLean D, et al. PAD2 overexpression in transgenic mice promotes spontaneous skin neoplasia. Cancer Res. 2014;74(21):6306-17.

40.	van Beers JJ, Zendman AJ, Raijmakers R, Stammen-Vogelzangs J, Pruijn GJ. Peptidylarginine deiminase expression and activity in PAD2 knock-out and PAD4-low mice. Biochimie. 2013;95(2):299-308.

41.	Howe K, Clark MD, Torroja CF, Torrance J, Berthelot C, Muffato M, et al. The zebrafish reference genome sequence and its relationship to the human genome. Nature. 2013;496(7446):498-503.

42.	Kirchberger S, Sturtzel C, Pascoal S, Distel M. Quo natas, Danio?-Recent Progress in Modeling Cancer in Zebrafish. Front Oncol. 2017;7:186.

43.	Kulkarni P, Yellanki S, Medishetti R, Sriram D, Saxena U, Yogeeswari P. Novel Zebrafish EAE model: A quick in vivo screen for multiple sclerosis. Mult Scler Relat Disord. 2017;11:32-9.

44.	Munzel EJ, Becker CG, Becker T, Williams A. Zebrafish regenerate full thickness optic nerve myelin after demyelination, but this fails with increasing age. Acta Neuropathol Commun. 2014;2:77.
45.	Chung AY, Kim PS, Kim S, Kim E, Kim D, Jeong I, et al. Generation of demyelination models by targeted ablation of oligodendrocytes in the zebrafish CNS. Mol Cells. 2013;36(1):82-7.

46.	Askary A, Smeeton J, Paul S, Schindler S, Braasch I, Ellis NA, et al. Ancient origin of lubricated joints in bony vertebrates. Elife. 2016;5.

47.	LaFave MC, Varshney GK, Vemulapalli M, Mullikin JC, Burgess SM. A defined zebrafish line for high-throughput genetics and genomics: NHGRI-1. Genetics. 2014;198(1):167-70.

48.	LeBert D, Squirrell JM, Freisinger C, Rindy J, Golenberg N, Frecentese G, et al. Damage-induced reactive oxygen species regulate vimentin and dynamic collagen-based projections to mediate wound repair. Elife. 2018;7.

49.	LeBert DC, Squirrell JM, Rindy J, Broadbridge E, Lui Y, Zakrzewska A, et al. Matrix metalloproteinase 9 modulates collagen matrices and wound repair. Development. 2015;142(12):2136-46.

50.	Montague TG, Cruz JM, Gagnon JA, Church GM, Valen E. CHOPCHOP: a CRISPR/Cas9 and TALEN web tool for genome editing. Nucleic Acids Res. 2014;42(Web Server issue):W401-7.

51.	Yang Z, Steentoft C, Hauge C, Hansen L, Thomsen AL, Niola F, et al. Fast and sensitive detection of indels induced by precise gene targeting. Nucleic Acids Res. 2015;43(9):e59.

52.	McCafferty J, Reid R, Spencer M, Hamp T, Fodor A. Peak Studio: a tool for the visualization and analysis of fragment analysis files. Environ Microbiol Rep. 2012;4(5):556-61.

53.	Livak KJ, Schmittgen TD. Analysis of relative gene expression data using real-time quantitative PCR and the 2(-Delta Delta C(T)) Method. Methods. 2001;25(4):402-8.

54.	Gokirmak T, Campanale JP, Shipp LE, Moy GW, Tao H, Hamdoun A. Localization and substrate selectivity of sea urchin multidrug (MDR) efflux transporters. J Biol Chem. 2012;287(52):43876-83.

55.	Miller JB, Crow MT, Stockdale FE. Slow and fast myosin heavy chain content defines three types of myotubes in early muscle cell cultures. J Cell Biol. 1985;101(5 Pt 1):1643-50.

56.	Buckley K, Kelly RB. Identification of a transmembrane glycoprotein specific for secretory vesicles of neural and endocrine cells. J Cell Biol. 1985;100(4):1284-94.

57.   Wang Y, Kaiser MS, Larson JD, Nasevicius A, Clark KJ, Wadman SA, et al. Moesin1 and Ve-cadherin are required in endothelial cells during in vivo tubulogenesis. Development. 2010;137(18):3119-28.

Chapter 3

Regeneration following tail transection requires Padi2 activity in the zebrafish fin fold model

Netta Golenberg and Anna Huttenlocher

Author contributions: NG performed all experiments

Abstract

Previous studies in multiple systems have shown the importance of early calcium signaling in regeneration but the mechanism by which it promotes regeneration is still unclear. Epimorphic regeneration proceeds through the formation of the blastema, a stem-cell like signaling cell population that is responsible for promoting proliferation and patterning during limb regeneration. Peptidylarginine deiminases are a family of calcium-dependent enzymes that deiminate proteins in a process called citrullination. By examining Padi2, and it's citrullination activity, we found a localized population of cells in the notochord bead with citrullinated histones and this citrullination is Padi2-dependent in zebrafish larvae. Interestingly, zebrafish larvae lacking Padi2 and citrullination activity displayed a defect in regeneration. This was accompanied by persistent neutrophil presence at a wound. While the notochord bead still forms in the Padi2 mutants, essential regeneration-Hedgehog signaling and proliferation are perturbed in Padi2-deficient larvae. Our results show that citrullination by Padi2 is required for proper formation of a stem-cell like signaling site, proper leukocyte recruitment, and efficient regeneration following wounding.

Introduction

Simple animal models of regeneration are powerful systems to analyze the molecular signals required for efficient regeneration. After amputation, wound healing and regeneration progress through similar steps across systems [1]. Immediately after wounding, early signals activate a series of regenerative steps beginning with the wound-healing phase. This phase is defined by the migration and formation of the wound epithelium as well as immune cell activation and recruitment to a wound [2]. The wound epithelium promotes the formation of a mass of stem-cell like cells called the blastema which is required for proliferation and restoration of the lost tissue [3]. Improper activation or regulation of these tightly controlled steps results in improper regeneration. Increased cytosolic calcium early in wound healing has been linked to later regenerative proliferation [4-6]. Here we investigate the mechanism by which intracellular calcium promotes regeneration.

The calcium-dependent family of enzymes, peptidylarginine deiminases (PADIs or PADs) catalyze the deimination of a peptidyl-arginine to the neutrally-charged, non-coded amino acid, citrulline, in a reaction called citrullination [7]. PADIs bind 5-6 calcium ions for enzymatic activity and require a high intracellular-calcium concentration for full activation [8]. Citrullination of histone proteins and chromatin modifiers are necessary for the maintenance of pluripotency through the promotion of an open chromatin state and gene expression [9-11]. Dysregulation of PADIs' expression and activity is associated with numerous autoimmune disorders, cancers, neurodegenerative disorders.

To investigate the role of citrullination in regeneration and wound healing, we explored the link between histone citrullination and stem cells and discovered a population of cells with wound-induced citrullination of histone H4R3 in the regenerative structure referred to as the notochord bead. Loss of the only deaminating enzyme in the zebrafish, Padi2, resulted in the absence of this wound-induced histone citrullination and impaired fin regeneration. Additionally, Padi2 mutant zebrafish had excessive and sustained neutrophil recruitment to a wound. Late-regenerative proliferation was reduced in Padi2 mutant larvae, indicating that citrullination is necessary for proper wound resolution and regeneration.

Results

Wounding induces localized histone citrullination

Due to the role of citrullinated histones in maintaining pluripotency [10, 11], we evaluated whether histone citrullination affected regeneration of the zebrafish fin. To first determine whether zebrafish Padi2 citrullinates histones in zebrafish, we used whole larvae lysate treated *ex vivo* with calcium and examined citrullinated histone H4 levels. Whole larvae lysate from wild-type larvae showed calcium-dependent citrullination of histone H4 (H4cit3) on a western blot but deimination is not observed in *padi2*^{-/-} lysate (Fig 3.1A), indicating that Padi2 is likely the only enzyme with detectable histone citrullination activity in zebrafish larvae. As has previously been shown, caudal fin transection results in a dramatic increase in intracellular calcium concentrations at a wound [5] and may be sufficient to promote citrullination. Visualization of histone H4
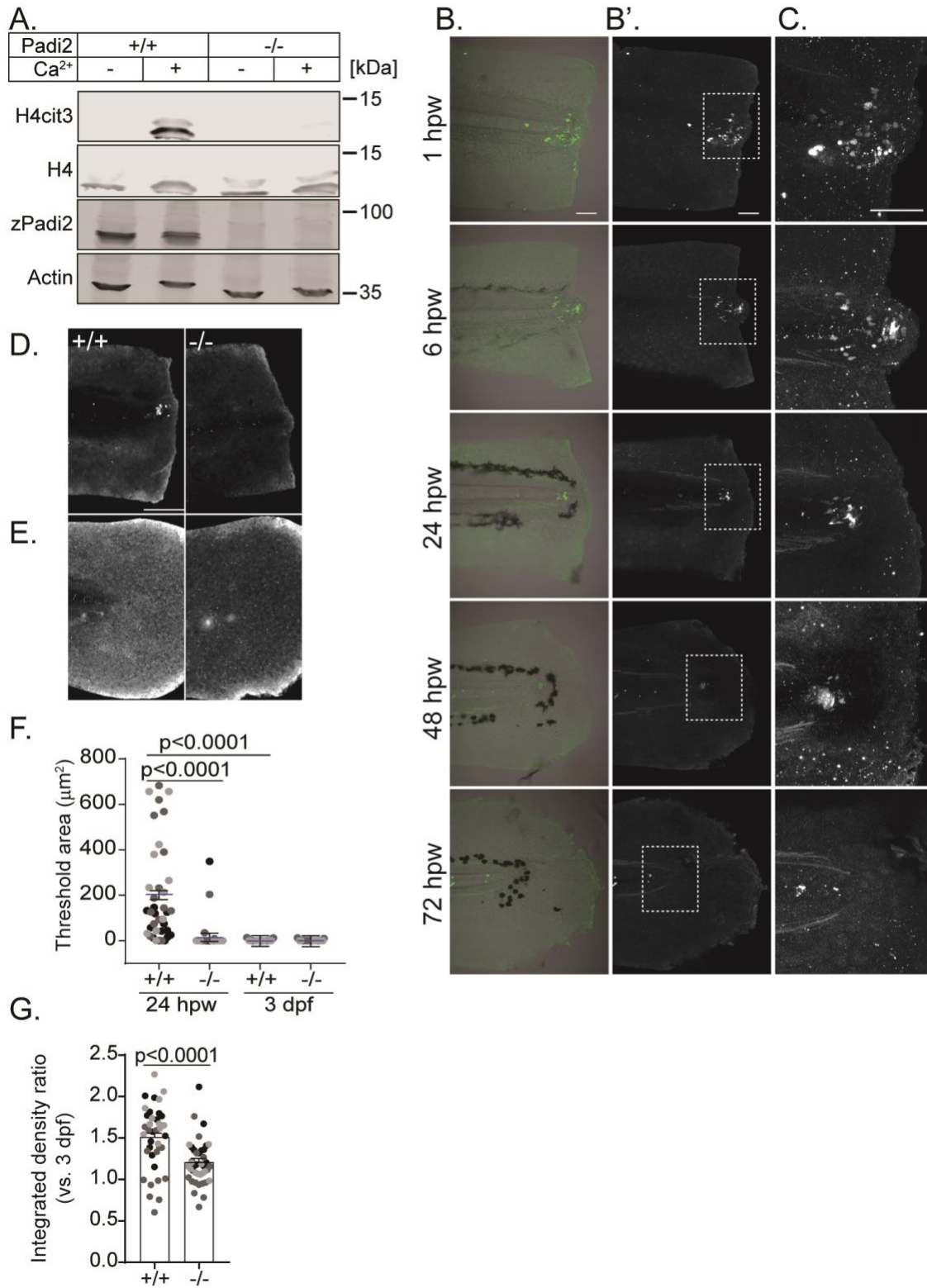
Fig 3.1: Tail transection stimulates Padi2-dependent histone H4 citrullination. (A)

Representative western blot of *padi2^{-/-}* and wild-type cousin lysates showing protein

levels of: citrullinated Histone4 (H4cit3), total Histone4 (H4), total Padi2 (zPadi2), and total actin (actin) (representative of 2 experiments). (B) Representative images of H4cit3 staining in tail transected fins at 20x magnification. Merge images with brightfield are shown in B for orientation in the fin, single channel H4cit3 shown in B'. Box denotes region imaged at 60x magnification in (C). B-C, Representative images from 2 independent experiments. (D) Representative images of H4cit3 staining in 24 hpw wild-type cousin (left) and *padi2*$^{-/-}$ (right). (E) Representative images of H4cit3 staining in 3 dpf unwounded control larvae. (F) Quantification of threshold area of H4cit3 signal at the notochord from (D) and (E). (G) Quantification of H4cit3 integrated density in 24 hpw larvae compared to 3 dpf controls. Data are from three pooled independent experiments with the lsmeans ($\pm$) SEM reported and p values were calculated by ANOVA. Datapoints are colored by experimental replicate. D-G, 24 hpw n= 38 +/+ and 41 -/-, 3 dpf n=25 both genotypes. Scale bars= 100 μm in B, D, and 50 μm in C.

citrullination upon caudal fin amputation in wild-type zebrafish revealed signal exclusively within a localized group of cells in the notochord bead, a region previously described as the regeneration blastema (Fig 3.1B and 3.1C) [12]. High-magnification imaging revealed histone H4 citrullination within individual cells as early as 1-hour post wounding (hpw) and this citrullination persisted up to 48 hpw as a compact signal (Fig 3.1C). Histone H4 citrullination was absent from the regenerated fin by 72 hpw (Fig 3.1B and 3.1C). Histone H4 deimination is wound dependent as no signal was observed in unwounded larvae (Fig 3.2). We confirmed the specificity of this wound-induced histone citrullination with immunofluorescence in *padi2*^{-/-} larvae at 24 hpw. In the *padi2*^{-/-} larvae, wounding failed to induce histone H4 citrullination above unwounded levels, in contrast to their wild-type cousins (Fig 3.1D-G). Previous reports have shown that this region of cells act as a required wound-signaling center, potentially as a regeneration-required blastema structure (Rojas-Munoz, Romero 2018). Our data indicate that histone citrullination may have a role in proper wound healing and regeneration.

Padi2 is required for efficient epimorphic regeneration

To directly investigate the role of citrullination in regeneration, we employed the larval caudal fin regeneration model in a Padi2 and citrullination-deficient zebrafish mutant. To assay caudal fin regeneration, 2.5 dpf larvae were transected through the notochord as previously described by Rojas-Munoz *et al.* without wounding the caudal vein [12]. Larvae were allowed to regenerate the lost tissue for 3 days. Regeneration was assessed by measuring the fin length from the blood circulation loop to the edge of the regenerated or developing fin along the notochord axis (Fig 3.3A). Regeneration
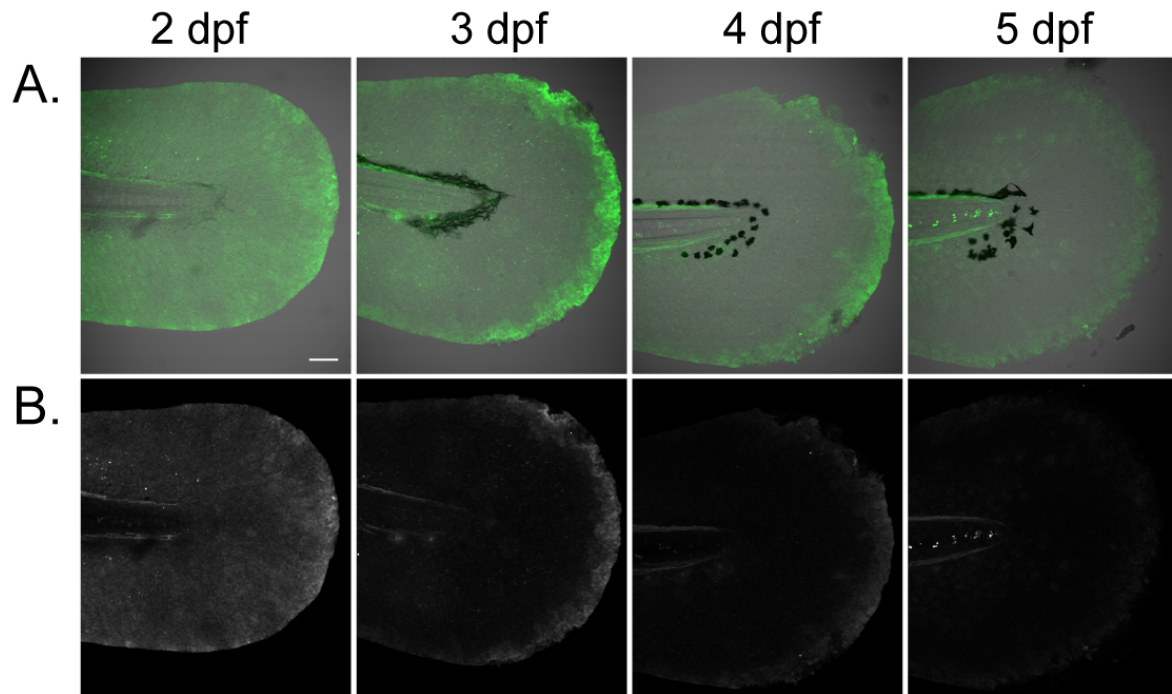
Fig 3.2: Histone H4 citrullination is not observed in developmental larval fins. (A)
Representative images of unwounded fins through development with histone H4cit3
staining in green merged with brightfield and (B) H4cit3 staining alone (single replicate).
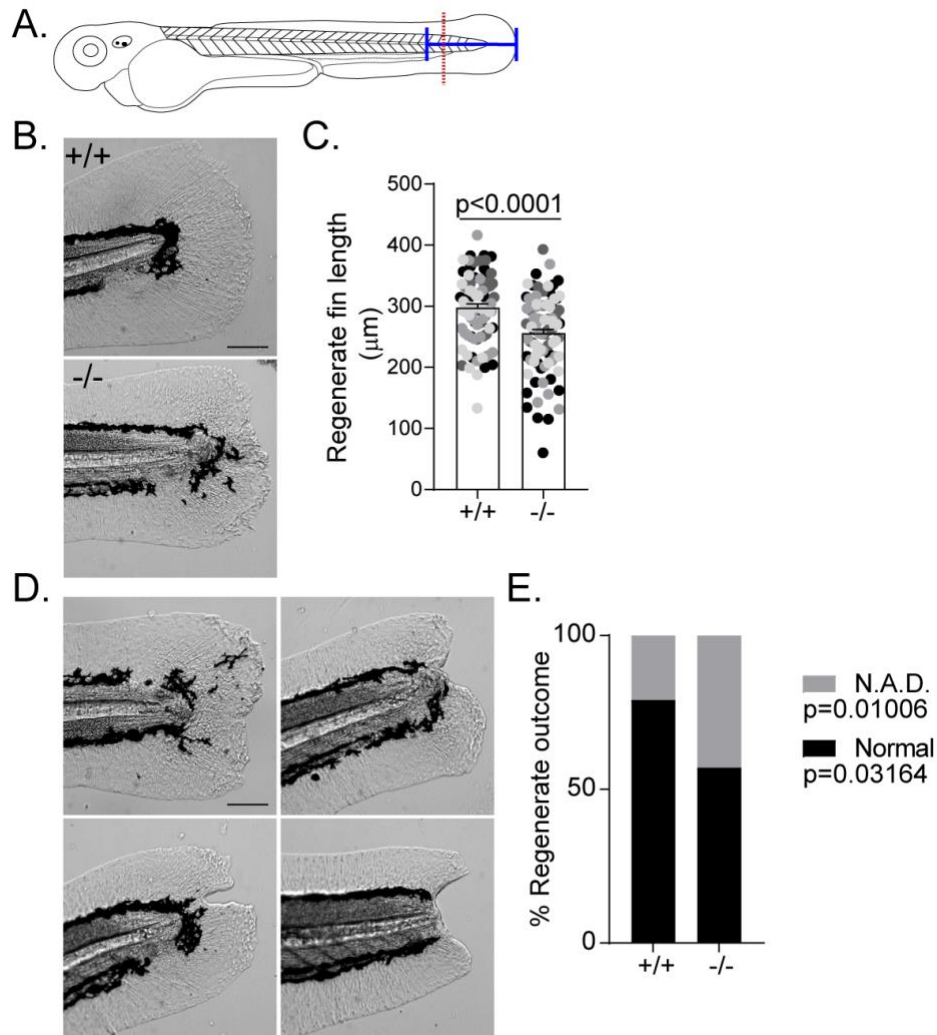Scale bar= 100 μm.

Fig 3.3: Padi2 is required for regeneration. (A) Schematic of regeneration assay. Tail

transections were performed through the notochord (amputation site indicated with red

dotted line) at 2.5 dpf. Regeneration and developmental fin lengths were measured from

the blood circulation to the end of the fin (blue solid line). (B) Representative images of

regeneration at 3 dpw. (C) Quantification of regenerate fin length. (D) Representative

images of the notochord adjacent defect (N.A.D). (E) Quantification of regenerate

outcome. All data are from four pooled independent experiments with the lsmeans and

SEM reported and p values calculated by ANOVA with n= 90 +/+, 95 -/-. Scale bars=

100 μm.

was impaired in the Padi2-decifient larvae when compared to wild-type cousins (Fig 3.3B and 3.3C). *padi2-/-* larvae, had a slight, but significant increase in their fin length at 5 dpf during unwounded development as compared to wild-type cousins (Fig 3.4), indicating Padi2 may have independent roles in fin development and regeneration. Interestingly, we observed a unique phenotype in these regenerated fins, with regeneration specifically impaired in the region posterior to the notochord (Fig 3.3D). We will refer to this phenotype as a notochord adjacent defect or N.A.D. This defect was observed in significantly more of the *padi2-/-* larvae compared to their wild-type cousins (Fig 3.3E).

Padi2 is required for proper leukocyte recruitment to a wound

Wounding induces the early recruitment and eventual resolution of leukocytes to the site of tissue damage and improper leukocyte recruitment can result in impaired regeneration [13]. Citrullination has been shown to affect the immune response in a number of diseases [14], with direct evidence for deimination of leukocyte chemotactic cues [15-17]; therefore, we examined leukocyte response to a wound in Padi2-deficient larvae. To visualize neutrophil response to a wound, we used *padi2-/-* and wild-type cousin larvae with mCherry-labeled neutrophil nuclei (*Tg(lyzc:H2B-mCherry)*) and counted these nuclei within the region posterior to the blood circulation loop (Fig 3.5A). Padi2-decifient larvae had increased neutrophil recruitment to a wound early at 6hpw, and this increase persisted at 24hpw (Fig 3.5B and 3.5C). Neutrophils failed to resolve from the wound in *padi2* mutant larvae by 48 hpw, when we see few neutrophils still present in wild-type wounds (Fig 3.5D and 3.5E). Total neutrophil numbers, although
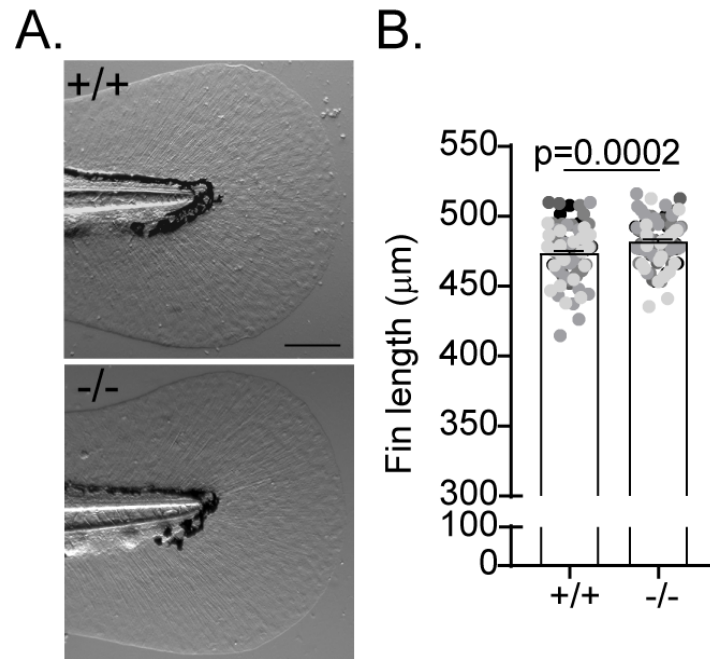
Fig 3.4: Padi2-deficient larvae have increased developmental fin length. (A)

Representative images of 5 dpf developmental fins. (B) Quantification of developmental

fin length from four independent experiments. Lsmeans and SEM reported and p-value

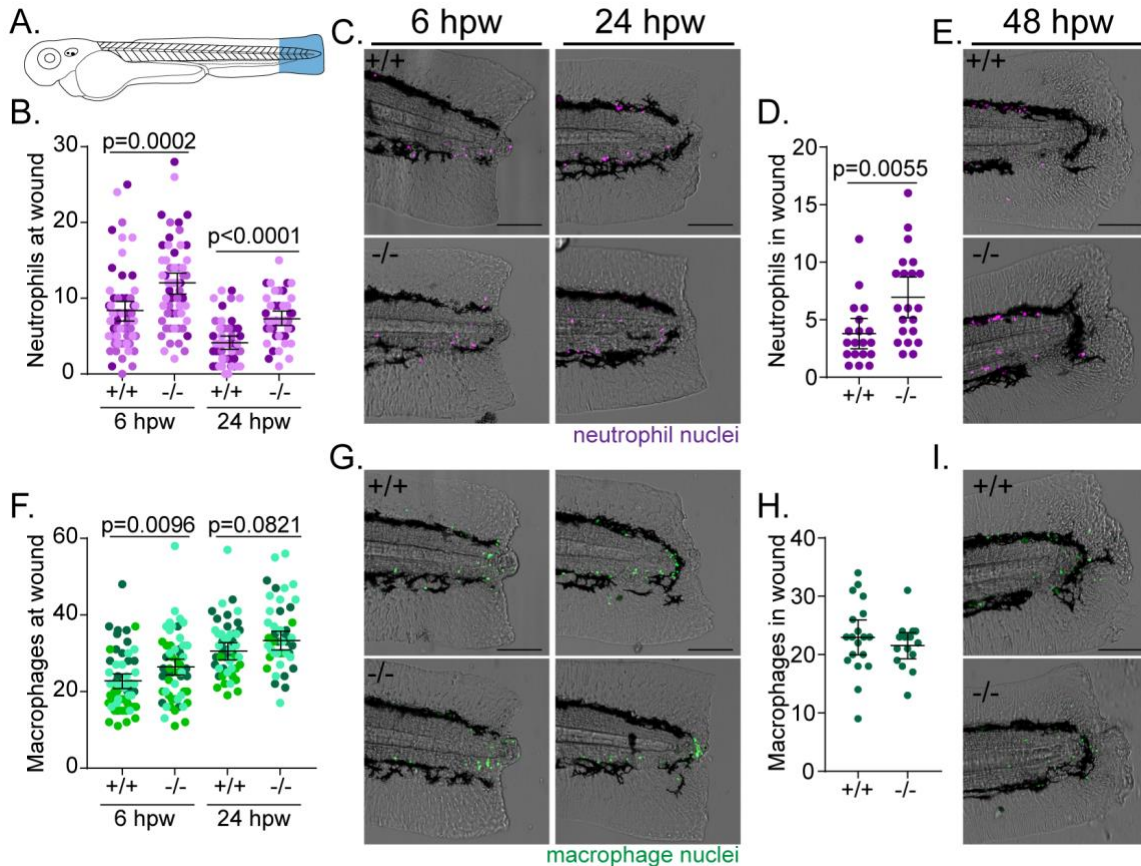calculated by ANOVA with n= 109 +/+, 108 -/-. Scale bar= 100 μm.

Fig 3.5: *padi2* mutants have increased numbers of neutrophils recruited to a tail transection. (A). Schematic of leukocyte quantification region (in blue) at a wound. Quantification (B) and representative images (C) of mCherry-labeled neutrophil nuclei (*Tg(lyzC:H2B-mCherry)*) at a wound at 6 hpw and 24 hpw. 6 hpw, n= 62 +/+, 57 -/- and 24 hpw, n= 50 +/+, 47 -/-. Quantification (D) and representative images (E) of mCherry-labeled neutrophil nuclei at a wound at 48 hpw. Single replicate with n=19 +/+, 21 -/-. Quantification (F) and representative images (G) of GFP-labeled macrophage nuclei (*Tg(mpeg1:H2B-GFP)*) at a wound at 6 hpw and 24 hpw. 6 hpw, n=61 +/+, 55 -/- and 24 hpw, n= 48 +/+, 44 -/-. Quantification (H) and representative images (I) of GFP-labeled macrophage nuclei at a wound at 48 hpw with n=19 +/+, 15 -/-. Data in B and F are from three pooled independent experiments with the lsmeans ($\pm$) SEM and p values

calculated by ANOVA reported. Datapoints represent single larvae and are colored by

experimental replicate. Data in D and H are from single replicates and p values

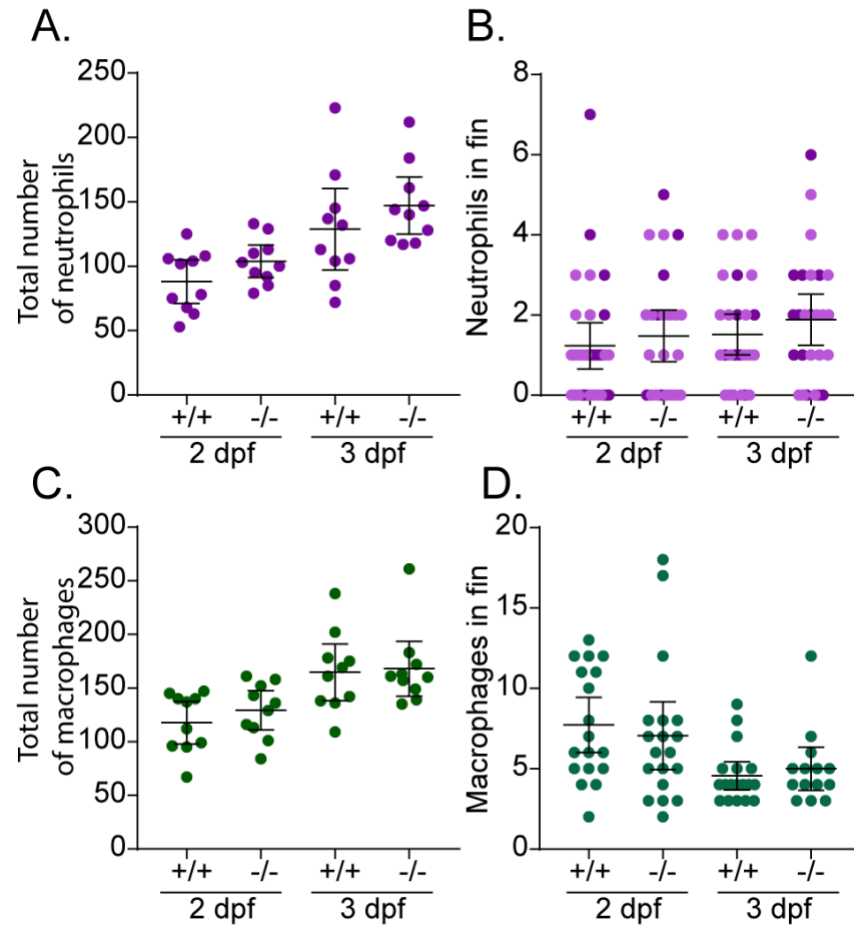calculated by t test. Scale bars= 100 μm.

Fig 3.6: Leukocyte development is normal in Padi2 mutant larvae. (A)

Quantification of neutrophils from whole larvae. Single replicate, n=10 larvae for each

time and genotype. (B) Quantification of neutrophils in developmental, unwounded fins.

Pooled from two independent experiments, n=30 +/+, 25 -/- at 2 dpf and n=27 +/+, 26 -/-

at 3 dpf. (C) Quantification of macrophages from whole larvae. Single replicate, n=10

larvae for each condition. (D) Quantification of macrophages in developmental,

unwounded fins. Single replicate with n=18 +/+, 19 -/- at 2 dpf and n= 18 +/+, 14 -/- at 3

dpf. All p values were calculated by t test, scale bars= 100 μm.

slightly higher in *padi2* mutants, were not significantly different than their wild-type

cousins (Fig 3.6A). Even with this slight increase, mutant larvae did not have increased

neutrophils within the unwounded fin, indicating that these neutrophils are not

improperly activated in unwounded larvae (Fig 3.6B).

To assess macrophage dynamics at a wound, larvae with GFP-labeled

macrophage nuclei (*Tg(mpeg1:H2B-GFP)*) were wounded. As observed with

neutrophils, there was a slight increase in macrophages at a wound in the *padi2*$^{-/-}$

larvae, although this difference did not persist (Fig 3.5F-I). Again, macrophages were

equally recruited to the unwounded fin in both genotypes and there was no difference in

total number of macrophages in the larvae (Fig 3.6C and 3.6D). Of note, macrophages

were observed to be recruited to the periphery of the notochord bead (Fig 3.5G). These

data indicate Padi2 may have a role in regeneration potentially through a mechanism of

leukocyte recruitment, particularly with persistent neutrophils.

Padi2-deficient larvae have impaired wound-induced proliferation

During tail regeneration we observed the formation of the notochord bead.

Previously, this has been reported as an early blastema, although little direct evidence

exists for this observation. *Xenopus* tadpole tail regeneration as well as zebrafish work,

have shown the formation of this notochord bead is necessary for Hedgehog expression

which is required for proper regeneration [18-20]. These studies indicate this region may

be acting as a signaling center to promote regeneration. Morphologically, both wild-type

cousins and Padi2-deficient larvae formed the notochord bead structure early after

wounding (Fig 3.7A), although the function of these cells may be perturbed as we

observed a loss of citrullinated histones within this region (Fig 3.1D-G). Similarly, the
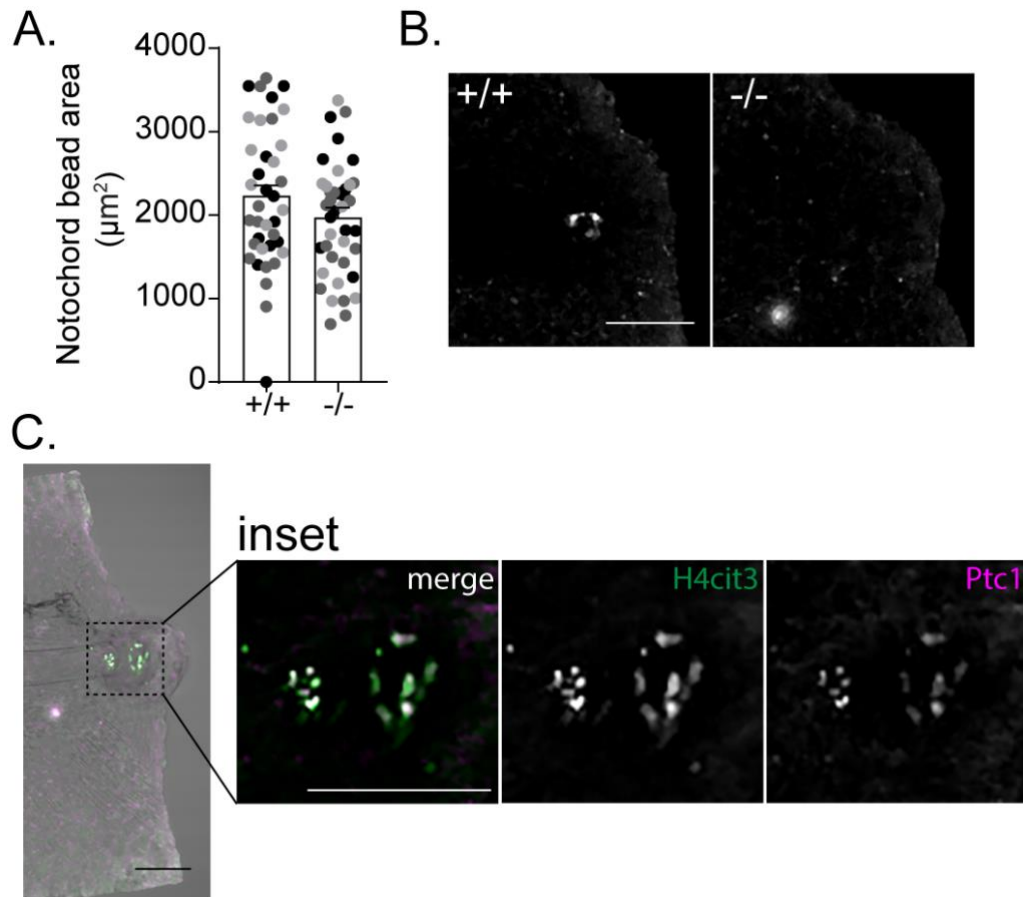
Fig 3.7: Padi2 is required for proper Hedgehog signaling in the notochord bead

(A) Quantification of the notochord bead area at 24 hpw. Data are from three pooled

independent experiments with the lsmeans ($\pm$) SEM reported and p values calculated

by ANOVA. Datapoints represent individual larvae and are colored by experimental

replicate. n= 38 +/+ and 41 -/-. (B) Representative images of Patched-1 (Ptc1)

immunostained fins at 24 hpw. (C) Representative image of wild-type 24 hpw fin

immunostained with α-H4cit3 in green and α-Ptc1 in magenta. Single replicate. Scale

bars= 100 μm.

notochord bead expression of the Hedgehog signaling target, Patched1 (Ptc1), was lost in the *padi2^-/-* larvae at 24 hpw, as determined by immunostaining (Fig 3.7B). Notably, Ptc1 signal colocalized with a majority of the histone H4cit3 signal observed in wild-type wounded fins (Fig 3.7C). These data indicate that Padi2's activity is required for proper downstream signaling through Hedgehog in the notochord bead.

An essential aspect of epimorphic regeneration is the blastema's proliferative capacity to restore lost cells. To examine the underlying mechanism responsible for this regeneration defect, cell proliferation was examined with a six-hour EdU pulse from 60-66 hpw. Mutant larvae had a considerably greater number of EdU-positive cells within the developmental fin than wild-type larvae (Fig 3.8A and 3.8B), confirming the increase in *padi2^-/-* larvae developmental fin growth (Fig 3.3), Upon wounding, wild-type larvae had an almost 4-fold increase in proliferative cells within the regenerating fin compared to the unwounded fins, however, Padi2-decifient larvae, failed to induce proliferation to the same degree after wounding (Fig 3.8C and 3.8D).

Apoptotic cells can induce neighboring cells to proliferate to replace the dying cells [21-23]. To determine whether Padi2-decifient larvae fail to induce cell proliferation upon wounding due to a defect in apoptosis activation, immunostaining for active-Caspase 3 was performed in wounded fins at 66 hpw. While there was a slight trend toward increased apoptosis in *padi2^-/-* larvae, there was no significant difference in apoptotic signals (Fig 3.8E and 3.8F) compared to wild-type. Additionally, we observed equal levels of apoptosis during development in age-matched larvae (Fig 3.9). These results indicate that differences in apoptosis are not the underlying cause of failed regeneration in *padi2* mutant larvae.
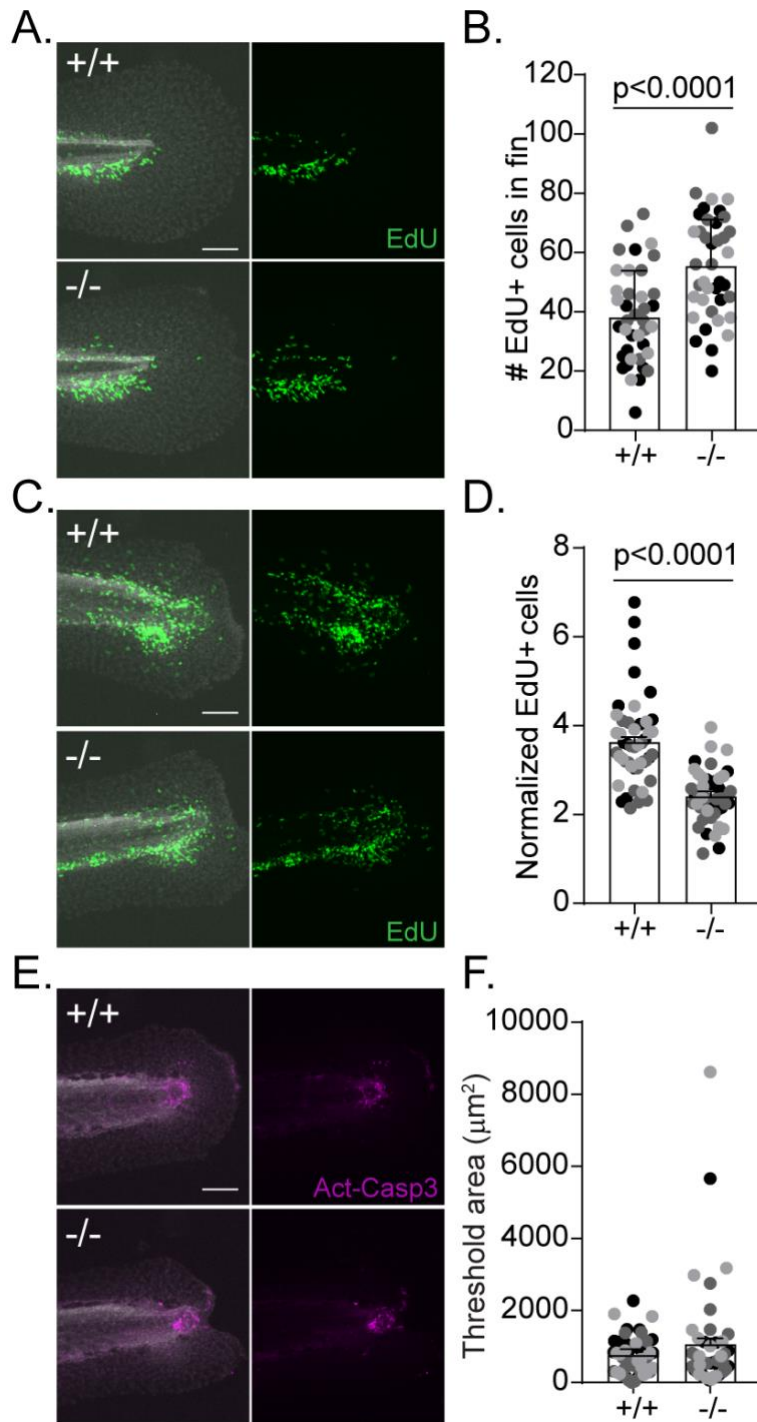
Fig 3.8: Wound-induced proliferation is perturbed in Padi2-deficient larvae. (A),(C)

Representative images of 6-hour EdU pulsed larvae in (A) developmental, unwounded

or (C) 60-66 hpw fins. Merged images of EdU in green and DAPI in white on the left, and single EdU image on the right. (B),(D) Quantification of EdU-positive cells in the fin. (E) Representative images of active-Caspase3 labeled fins at 66 hpw. Merged images of active-Caspase3 in magenta and DAPI in white on the left, and single active-Caspase3 channel on the right. (F) Quantification of active-Caspase3 threshold area in *padi2*$^{-/-}$ and wild-type fins. All data are from three pooled independent experiments with the lsmeans and SEM reported and p values calculated by ANOVA with n= 39 larvae each, no wound and n= 47 larvae each at 66 hpw. Scale bar= 100 μm.
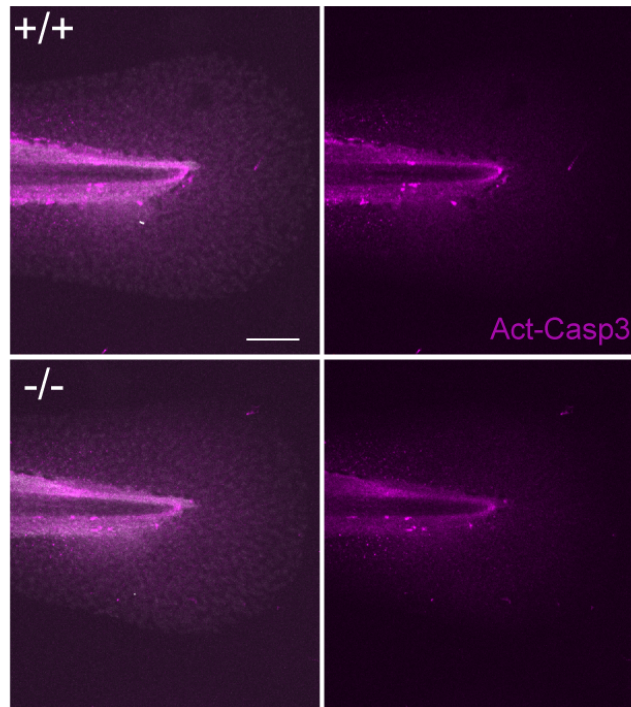
Fig 3.9: Apoptosis is not activated in unwounded fins. Representative images of

unwounded fins of aged matched 5 dpf larvae. Merged images of active-Caspase3 in

magenta and DAPI in white on the left, and single active-Caspase3 channel on the right.

Scale bar= 100 μm.

Altogether, *padi2*-mutant zebrafish have improper leukocyte dynamics to a wound, histone citrullination, and wound-induced proliferation leading to impaired fin regeneration.

Discussion

In this study we identified an important role for Padi2 and histone citrullination in zebrafish fin regeneration. While calcium is essential for proper regeneration, its mechanism of action is still unknown. Here, we have shown that there is a localized increase in citrullinated histones within the notochord bead after wounding. While the notochord bead forms independently of Padi2, histone citrullination within this region along with downstream Hedgehog signaling is dependent on Padi2 expression. Loss of Padi2 results in improper regeneration, predominantly in the region adjacent to the notochord. Early leukocyte-mediated wound healing is also perturbed in *padi2*-mutant larvae, as increased and persistent neutrophil infiltration at the wound is observed. Finally, Padi2-deficient larvae do not demonstrate a wound-induced increase in proliferation, a process necessary for restoring the damaged tissue. This indicates that Padi2 is a positive regulator of wound healing.

Abnormal protein citrullination and the subsequent improperly regulated immune response have been implicated in the pathogenesis of a number of diseases, including cancers, rheumatoid arthritis, lupus, and neurological diseases [14]. Therefore, understanding the role of PADI and citrullination in the immune response is critical. Studies on autoimmune disorders show that citrullination is associated with excessive immune cell recruitment; therefore, our results showing increased neutrophils at a wound in citrullination-deficient larvae may be surprising. A recent report, however,

found that a PADI2 knockout mouse had an upregulation in leukocyte and neutrophil migration and chemotaxis expression pathways, while PADI4 knockout mouse had different effects, indicating independent roles for those two isozymes [24]. Our results also indicate that loss of citrullination in the wound environment leads to dysregulation of the leukocyte response.

Excessive, non-resolving inflammation is associated with poor wound healing. Therefore, we cannot dismiss neutrophil persistence at the wound in the *padi2*-mutant larvae as the cause of poor regeneration. This increase in neutrophils at a wound may be due to the higher numbers of total neutrophils observed in the *padi2$^{-/-}$* zebrafish; however, the unchanged activation of these cells in the unwounded fin indicates that the increase is likely due to a change in the wound cue. Citrullination of CXCL8, CXCL10, CXCL11, or CXCL12 causes loss or alteration of their inflammatory signaling [15, 25, 26]; therefore, loss of citrullination in *padi2*-mutant zebrafish may eliminate an inflammation dampening signal at the wound. We have shown that the interaction of Cxcl8 with its two receptors, Cxcr11 and Cxcr2, is carefully regulated to mediate neutrophil recruitment and reverse migration in response to a wound [27]. Citrullination of CXCL8 alters its binding and signaling through CXCR2 [15], making the citrullination of CXCL8 an attractive mechanism of regulation for bidirectional neutrophil motility. Similarly, citrullination of extracellular matrix (ECM) components such as collagen or fibronectin impair integrin binding and cell migration [28-30]; therefore, loss of Padi2 at the wound, could alternatively be directly affecting neutrophil migration by altering the wound ECM. Further studies should examine the citrullination-mediated cues during wounding to determine their temporal dynamics and their effects on leukocyte behavior.

Citrullination of histones and PADI association with chromatin is necessary for maintaining pluripotency [9-11]. It has been proposed that the blastema acts as a signaling source of stem-cell like cells that will proliferate and differentiate into multiple lineages in the fin. Here we provide evidence for a population of cells with histone citrullination in this region. These cells have previously been shown to be required for Hedgehog signaling and activation of other key regeneration pathways [18]. In our study, loss of histone citrullination results in the absence of early Hedgehog signaling and late-stage proliferation; therefore, we argue that Padi2 and histone citrullination are required for transforming these cells into a multipotent signaling center.

PADIs have been previously linked to wound healing in mice. Loss of PADI4 resulted in improved wound healing both in wild-type and diabetic mice through the loss of wound-induced NETosis [31]. Additionally, PADI4 and citrullinated-fibrin were upregulated in the clot-derived scab [32]. Zebrafish do not have a Padi4 orthologue, which may explain their high regenerative capacity. This work shows the importance of tight regulation of these pathways, as excessive inflammation is associated in a number of diseases, while we show here, loss of citrullination impairs wound healing. In addition to the negative wound healing role of PADI4, our work argues for future studies on a positive role and regulation of PADI2 in promoting wound healing.

Materials and methods

Zebrafish maintenance and handling

All protocols in this study were approved by the University of Wisconsin-Madison Animal Care and Use committee (IACUC). Adult fish were maintained on a light cycle of

14 hours of light and 10 hours of darkness. Fertilized embryos were maintained in E3 buffer at 28.5°C. Wild-type fish, type AB were used for all outcrosses. Previously published transgenic lines *Tg(mpeg1:H2B-GFP)* [33], *Tg(lyzc:H2B-mCherry)* [34], and the *padi2* mutant strain (discussed in chapter 2) were used in this study.

Regeneration assays

For regeneration assays, dechorionated larvae were transferred to 35 mm milk-coated plates. Larvae were washed twice in E3 and wounded in a final 0.24 mg/ml Tricaine (ethyl 3-aminobenzoate, Sigma)/E3 solution. Tail transections were performed on ~2.5 dpf larvae with a surgical blade (feather no 10) roughly 4 vacuolated cells from the posterior end of the notochord. Larvae were again washed 3 times with E3 and allowed to regenerate for 3 days post wounding (dpw) at which point larvae were fixed with 4% paraformaldehyde (PFA; Sigma-Aldrich)/PBS at 4°C overnight. Fins were imaged on Zeiss zoomscope (EMS3/SyCoP3; Zeiss; Plan-NeoFluar Z objective-112x magnification) with an Axiocam Mrm CCD camera using ZEN pro 2012 software (Zeiss). Regenerate length was measured from the edge of the blood vessel to the caudal edge of the tail fin using the FIJI image analysis software. Unwounded, 5 dpf larvae fin lengths were measured as a developmental control. The appearance of a notochord adjacent defect was scored on blinded images.

Immunofluorescence and imaging

Larvae were fixed in a solution of 1% NP-40, 0.5% Triton-X, and 1.5% PFA in PBS at 4°C overnight. The following day fix was replaced with a block solution of 2.5% BSA, 0.5% Tween-20, 5% goat serum in PBS. Samples were blocked for at least 2.5 hours at room temperature followed by the addition of poly-clonal rabbit anti-histone H4

(citrulline 3) antibody (EMD Millipore) used at 1:100 and incubated overnight at 4°C. For time course experiments, samples were kept in block at 4°C until the final sample was prepared at which time all samples had fresh block added and were blocked at room temperature before the addition of the primary antibody. Samples were washed 3 times in PBS at room temperature for 5 minutes each and secondary Dylight 488 donkey anti-rabbit IgG antibodies (Rockland Immunochemicals) were used at 1:250 in block buffer overnight at 4°C. Finally, 4 washes were done in PBS. Images were acquired on a laser-scanning confocal microscope (FluoView FV1000; Olympus) with an NA 0.75/20x or PLANAPO NA 1.45/60x oil objective and FV10-ASW software (Olympus). 20x images used for quantification were acquired as Z-stacks with 25, 1 um optical slices at 640x640 resolution.

Leukocyte Imaging

$padi2^{+/-}$ adults were crossed to AB wild-type zebrafish labeled with macrophage nuclei *Tg(mpeg1: H2B-GFP)* or neutrophil nuclei *Tg(lyzc:H2B-mCherry)*. Adult positive $padi2^{+/-}$ were incrossed and raised to adulthood. Experiments were performed on wild-type cousins and $padi2^{-/-}$ larvae as a result of incrossed adult transgenic siblings. Wounding was performed as described above and larvae were fixed with 1.5% PFA in 0.1 M PIPES (Sigma-Aldrich), 1 mM $MgSO_4$ (Sigma-Aldrich), and 2 mM EGTA (Sigma-Aldrich) overnight at 4°C. Wounds were imaged on a Zeiss zoomscope (EMS3/SyCoP3; Zeiss; Plan-NeoFluar Z objective-112x magnification) with an Axiocam Mrm CCD camera using ZEN pro 2012 software (Zeiss). Leukocyte numbers were counted by hand in the region past the blood circulatory loop. Whole larvae images were acquired on a spinning disk confocal (CSU-X; Yokogawa) on a Zeiss Observer Z.1 inverted

microscope and an EMCCD evolve 512 camera (Photometrics) with a Plan-Apochromat NA 0.8/20x air objective (5 μm optical sections, 5x1 tiles, 2355x512 resolution). Total neutrophil numbers were determined using Imaris (Bitplane) with the spots function as defined by a 10 μm diameter in the XY plane and a Z-diameter of 20 μm. Total macrophage numbers were counted by hand using Z-projected images in Zen 2.3 lite software. For all total leukocyte quantifications, leukocytes within the yolk sac and heart were excluded.

EdU and apoptosis labeling

Proliferation in the fin was measured using Click-iT Plus EdU Imaging Kit (Life Technologies). Larvae were incubated in 10 μM EdU (5-ethynyl-2'-deoxyurdine) solution in E3 for 6 hours with slight agitation. Wounded fish were incubated from 60-66hpw along with age matched unwounded controls. Larvae were fixed in 4% PFA in PBS overnight at 4°C and stored in methanol at -20°C until staining. Staining protocol was followed according to manufacturer's instructions. EdU-stained larvae were also incubated with rabbit anti-active Caspase3 antibody (BD Biosciences) at 1:200 in block (PBS, 1% DMSO, 1% BSA, 0.05% Triton-X, 1.5% goat serum) visualized with secondary Dylight 550, and 0.01 mg/mL DAPI (4',6-diamidino-2-phenylindole; Sigma). Immunofluorescence images were acquired on a spinning disk confocal (CSU-X; Yokogawa) on a Zeiss Observer Z.1 inverted microscope with an EMCCD evolve 512 camera (Photometrics) and a Plan-Apochromat NA 0.8/20x air objective, as Z-stacks, 3 μm optical sections, and with 512x512 resolution.

Western blot

For western blotting, 50-100 ~2 dpf larvae were pooled and deyolked in calcium-free Ringer's solution with gentle disruption with a p200 pipette. Larvae were washed twice with phosphate-buffered saline (PBS) and stored at -80°C until samples were lysed by sonication in 20mM Tris pH 7.6, 0.1% Triton-X-100, 0.2 mM Phenylmethylsulfonyl fluoride (PMSF), 1 µg/mL Pepstatin, 2 µg/mL Aprotinin, and 1 µg/mL Leupeptin at 3 µL per larvae while on ice. Samples were clarified by centrifugation. For citrullination analysis by western of whole zebrafish lysates, 12.5 µL lysate was incubated with 12.5 µL 4X reaction buffer (400 mM Tris pH 7.4, ± 80 mM $CaCl_2$, 20 mM DTT) and 25 µL dilution buffer (10 mM Tris pH 7.6, 150 mM NaCl, 2mM DTT) for 90 minutes at 37°C. Reactions were stopped by boiling samples in SDS-PAGE sample buffer and equivalent amounts were loaded on a 6-20% gradient SDS-polyacrylamide gels and transferred to nitrocellulose. zPadi2 rabbit anti-serum was used at 1:500 dilution, anti-Histone H4 (citrulline 3) (EMD-Millipore) at 1:50, anti-actin (ac15; Sigma) at 1:1000, and anti-Histone H4 (EMD-Millipore) at 1:1000. Western blots were imaged with an Odyssey Infrared Imaging System (LI-COR Biosciences, Omaha, NW).

Image analysis/processing

Image analysis was performed on FIJI. For experiments where fluorescence intensity was quantified, no adjustments were made to the images prior to analysis. For Histone H4cit3 analysis, a region of interest 92 x 93 pixels was centered around the notochord as determined by the corresponding brightfield image. Immunostained images were Z-projected and the integrated density in the region of interest (ROI) was determined. Images were thresholded using "Intermodes" and the total area within the ROI was determined for particles larger than 8 pixels. For display purposes of

representative images, images were processed to remove background using despeckling (Fig 3.10). Notochord bead area was determined in FIJI by outlining the region with deposited cells at the wound edge of the notochord as determined by examination of the optical brightfield slices.

For EdU analysis, images were 3D reconstructed on Imaris software (Bitplane). The number of EdU-positive cells were quantified in the fin region posterior of the blood circulatory loop with the spots function as defined by an XY-diameter of 7 µm and a Z-diameter of 14 µm. The leve of apoptosis activation at the wound was determined by outlining the fin past the blood circulation using the corresponding brightfield image. In FIJI, total threshold area for active-Caspase3 in the wound was determined using "Yen Dark" for particles larger than 3 pixels.

Statistical analysis

For experiments with at least three independent replicates, data were pooled and the results were summarized in terms of least-squared adjusted means and standard errors. Results were analyzed using one-way ordinary analysis of variance (ANOVA) with a Tukey's multiple comparisons test. Experiments with fewer than three independent experimental replicates were analyzed by t test. Categorical data in Fig 3.3E was analyzed by logistic regression ANOVA. Graphical representation shows individual data points color coded to corresponding replicates. Statistical analyses and graphical representations were done using R version3.4 and GraphPad Prism version6.
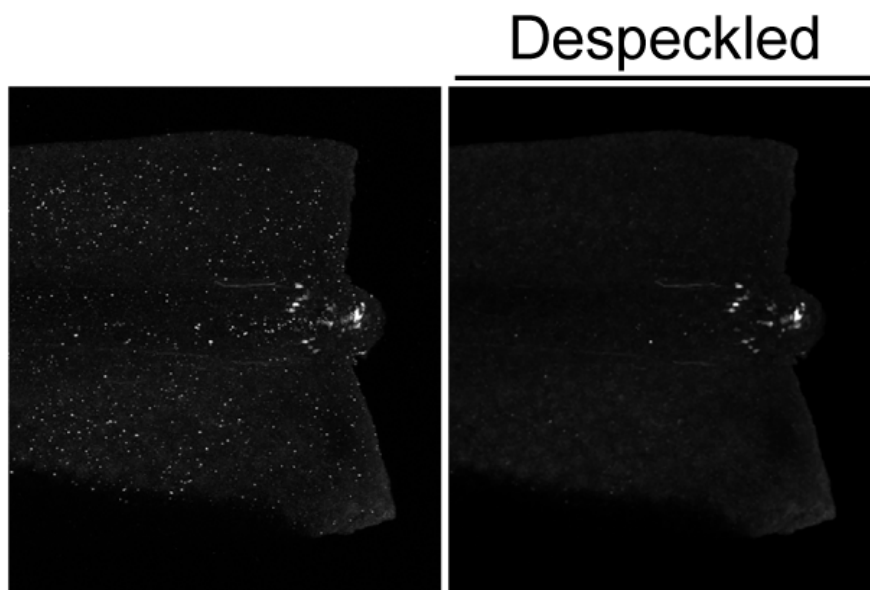
Fig 3.10: Post-Imaging processing of Histone H4 citrullination images. H4cit3 staining in wounded wild-type fin on the left, with post-imaging despeckled processing on the right.

References

1.   Yokoyama H. Initiation of limb regeneration: the critical steps for regenerative capacity. Dev Growth Differ. 2008;50(1):13-22.

2.   Roehl HH. Linking wound response and inflammation to regeneration in the zebrafish larval fin. Int J Dev Biol. 2018;62(6-7-8):473-7.

3.   Whitehead GG, Makino S, Lien CL, Keating MT. fgf20 is essential for initiating zebrafish fin regeneration. Science. 2005;310(5756):1957-60.

4.   Globus M, Vethamany-Globus S, Kesik A. Control of blastema cell proliferation by possible interplay of calcium and cyclic nucleotides during newt limb regeneration. Differentiation. 1987;35(2):94-9.

5.   Yoo SK, Freisinger CM, LeBert DC, Huttenlocher A. Early redox, Src family kinase, and calcium signaling integrate wound responses and tissue regeneration in zebrafish. J Cell Biol. 2012;199(2):225-34.

6.   Lagoudakis L, Garcin I, Julien B, Nahum K, Gomes DA, Combettes L, et al. Cytosolic calcium regulates liver regeneration in the rat. Hepatology. 2010;52(2):602-11.

7.   Vossenaar ER, Zendman AJ, van Venrooij WJ, Pruijn GJ. PAD, a growing family of citrullinating enzymes: genes, features and involvement in disease. Bioessays. 2003;25(11):1106-18.

8.   Arita K, Hashimoto H, Shimizu T, Nakashima K, Yamada M, Sato M. Structural basis for Ca(2+)-induced activation of human PAD4. Nat Struct Mol Biol. 2004;11(8):777-83.

9.   Wiese M, Bannister AJ, Basu S, Boucher W, Wohlfahrt K, Christophorou MA, et al. Citrullination of HP1gamma chromodomain affects association with chromatin. Epigenetics Chromatin. 2019;12(1):21.

10.   Christophorou MA, Castelo-Branco G, Halley-Stott RP, Oliveira CS, Loos R, Radzisheuskaya A, et al. Citrullination regulates pluripotency and histone H1 binding to chromatin. Nature. 2014;507(7490):104-8.

11.   Xiao S, Lu J, Sridhar B, Cao X, Yu P, Zhao T, et al. SMARCAD1 Contributes to the Regulation of Naive Pluripotency by Interacting with Histone Citrullination. Cell Rep. 2017;18(13):3117-28.

12.   Rojas-Munoz A, Rajadhyksha S, Gilmour D, van Bebber F, Antos C, Rodriguez Esteban C, et al. ErbB2 and ErbB3 regulate amputation-induced proliferation and migration during vertebrate regeneration. Dev Biol. 2009;327(1):177-90.

13.   Wilgus TA, Roy S, McDaniel JC. Neutrophils and Wound Repair: Positive Actions and Negative Reactions. Adv Wound Care (New Rochelle). 2013;2(7):379-88.

14.   Witalison EE, Thompson PR, Hofseth LJ. Protein Arginine Deiminases and Associated Citrullination: Physiological Functions and Diseases Associated with Dysregulation. Curr Drug Targets. 2015;16(7):700-10.

15.   Proost P, Loos T, Mortier A, Schutyser E, Gouwy M, Noppen S, et al. Citrullination of CXCL8 by peptidylarginine deiminase alters receptor usage, prevents proteolysis, and dampens tissue inflammation. J Exp Med. 2008;205(9):2085-97.

16.   Loos T, Opdenakker G, Van Damme J, Proost P. Citrullination of CXCL8 increases this chemokine's ability to mobilize neutrophils into the blood circulation. Haematologica. 2009;94(10):1346-53.

17.   Yoshida K, Korchynskyi O, Tak PP, Isozaki T, Ruth JH, Campbell PL, et al. Citrullination of epithelial neutrophil-activating peptide 78/CXCL5 results in conversion from a non-monocyte-recruiting chemokine to a monocyte-recruiting chemokine. Arthritis Rheumatol. 2014;66(10):2716-27.

18.   Romero MMG, McCathie G, Jankun P, Roehl HH. Damage-induced reactive oxygen species enable zebrafish tail regeneration by repositioning of Hedgehog expressing cells. Nat Commun. 2018;9(1):4010.

19.   Taniguchi Y, Watanabe K, Mochii M. Notochord-derived hedgehog is essential for tail regeneration in Xenopus tadpole. BMC Dev Biol. 2014;14:27.

20.   McHedlishvili L, Epperlein HH, Telzerow A, Tanaka EM. A clonal analysis of neural progenitors during axolotl spinal cord regeneration reveals evidence for both spatially restricted and multipotent progenitors. Development. 2007;134(11):2083-93.

21.   Brock CK, Wallin ST, Ruiz OE, Samms KM, Mandal A, Sumner EA, et al. Stem cell proliferation is induced by apoptotic bodies from dying cells during epithelial tissue maintenance. Nat Commun. 2019;10(1):1044.

22.   Sun G, Irvine KD. Regulation of Hippo signaling by Jun kinase signaling during compensatory cell proliferation and regeneration, and in neoplastic tumors. Dev Biol. 2011;350(1):139-51.

23.   Tseng AS, Adams DS, Qiu D, Koustubhan P, Levin M. Apoptosis is required during early stages of tail regeneration in Xenopus laevis. Dev Biol. 2007;301(1):62-9.

24.   Liu Y, Lightfoot YL, Seto N, Carmona-Rivera C, Moore E, Goel R, et al. Peptidylarginine deiminases 2 and 4 modulate innate and adaptive immune responses in TLR-7-dependent lupus. JCI Insight. 2018;3(23).

25.   Struyf S, Noppen S, Loos T, Mortier A, Gouwy M, Verbeke H, et al. Citrullination of CXCL12 differentially reduces CXCR4 and CXCR7 binding with loss of inflammatory and anti-HIV-1 activity via CXCR4. J Immunol. 2009;182(1):666-74.

26.   Loos T, Mortier A, Gouwy M, Ronsse I, Put W, Lenaerts JP, et al. Citrullination of CXCL10 and CXCL11 by peptidylarginine deiminase: a naturally occurring posttranslational modification of chemokines and new dimension of immunoregulation. Blood. 2008;112(7):2648-56.

27.   Powell D, Tauzin S, Hind LE, Deng Q, Beebe DJ, Huttenlocher A. Chemokine Signaling and the Regulation of Bidirectional Leukocyte Migration in Interstitial Tissues. Cell Rep. 2017;19(8):1572-85.

28.   Shelef MA, Bennin DA, Mosher DF, Huttenlocher A. Citrullination of fibronectin modulates synovial fibroblast behavior. Arthritis Res Ther. 2012;14(6):R240.

29.   Yuzhalin AE, Gordon-Weeks AN, Tognoli ML, Jones K, Markelc B, Konietzny R, et al. Colorectal cancer liver metastatic growth depends on PAD4-driven citrullination of the extracellular matrix. Nat Commun. 2018;9(1):4783.

30.   Sipila K, Haag S, Denessiouk K, Kapyla J, Peters EC, Denesyuk A, et al. Citrullination of collagen II affects integrin-mediated cell adhesion in a receptor-specific manner. FASEB J. 2014;28(8):3758-68.

31.   Wong SL, Demers M, Martinod K, Gallant M, Wang Y, Goldfine AB, et al. Diabetes primes neutrophils to undergo NETosis, which impairs wound healing. Nat Med. 2015;21(7):815-9.

32.   Coudane F, Mechin MC, Huchenq A, Henry J, Nachat R, Ishigami A, et al. Deimination and expression of peptidylarginine deiminases during cutaneous wound healing in mice. Eur J Dermatol. 2011;21(3):376-84.

33.   Miskolci VS, J.M.; Rindy, J.; Vincent, W.J.B.; Sauer, J.D.; Gibson, A.; Eliceiri, K.W.; Huttenlocher, A. Distinct inflammatory and wound healing responses to complex caudal fin injuries of larval zebrafish. Elife. 2019.

34.   Yoo SK, Lam PY, Eichelberg MR, Zasadil L, Bement WM, Huttenlocher A. The role of microtubules in neutrophil polarity and migration in live zebrafish. J Cell Sci. 2012;125(Pt 23):5702-10.

Chapter 4

Conclusions and Future Directions

The research in this dissertation has focused on investigating the role of Padi2 and citrullination during development, disease, and wound healing. In this work, we developed of the first Padi-null, citrullination-deficient *in vivo* model. Using this model, we uncovered a role for citrullination in leukocyte recruitment and blastema-dependent proliferation. In the future, this work could have important clinical impacts on autoimmune diseases and the treatment of wounds.

Development and characterization of a Padi2-deficient model

In chapter 2 we presented our study of citrullination and peptidylarginine deiminases in the zebrafish model. Through CRISPR/Cas9 mutagenesis, a zebrafish line with a 20 basepair *padi2* deletion was isolated and maintained. Using this zebrafish line we determined that Padi2 is the only enzyme in the zebrafish proteome with citrullination activity. The Padi2-deficient larvae had normal gross morphology and survival. Mutant larvae had normal musculature but improper neuromuscular synapse numbers and impaired behavioral responses to stimuli and decreased spontaneous movement initiation.

In mammalian systems, there are five reported PADI enzymes, each with distinct substrates, functions, and tissue localization [1]. Our data align with previous reports that the single teleost enzyme is the ancestral protein of the PADI family with the mammalian isozymes arising due to gene duplication [1]. We found conserved amino acids and regions necessary for calcium coordination, substrate binding, and catalysis in the zebrafish Padi enzyme first reported in mammalian PADI4 and PADI2 [2-4].

While mammalian PADIs have roles in skin homeostasis, the innate immune system, and the nervous system, the fact that our citrullination-deficient model was viable and developmentally normal was intriguing. This raised the question, is zebrafish Padi2 functionally equivalent to all five mammalian isozymes or is it rather an orthologue of mammalian PADI2 and, therefore, has similar functions to PADI2 only? PADI1 and PADI6 are required for female fertility, with mutations in either gene resulting in embryos that do not divide past the 4-cell stage, a phenotype we do not observe in our citrullination-deficient zebrafish [5, 6]. While more work is needed to dissect the function of zebrafish Padi2, our model enables research into the role of citrullination during a window in development that has previously not been accessible.

The ability to study Padi2 at this developmental stage led to our discovery that loss of Padi2 results in unregulated, excessive neuromuscular synapse formation in the larval trunk and defects in the initiation of movements. Further work is needed to show that this synapse abnormality is directly responsible for the movement defect observed in *padi2* mutants. While Padi2 is known to be expressed in the presynaptic complex in mice and zebrafish, we do not know yet if the observed zebrafish movement defect is due to improper synapse function, abnormal synapse numbers, or if our neuromuscular and movement defects are independent of one another. In the future, electrophysiology should be performed to assess both neuron and muscle recordings to better characterize the functional output of the neuromuscular junctions in the mutant larvae.

Recently published work showed that PADI2 activity is necessary for proper oligodendrocyte differentiation and function [7]. Additionally, PADI2 knockout mice had similar behavioral defects as those we observed in the zebrafish larvae [7]. There are

established fluorescently-labeled zebrafish lines for oligodendrocytes and neurons [8-10]. In the future, these lines should be used to create cell-specific expression of zebrafish Padi2 in oligodendrocytes, motor neurons, and microglia followed with visualization of neuromuscular junction development and assessment of behaviors to allow for further dissection of the cell requirement for Padi2 activity in these mutant phenotypes. Examining the nervous system function during development in the absence of citrullination will be clinically relevant as pathological citrullination has been found in Alzheimer's disease and multiple sclerosis [11-13]. Zebrafish models for these diseases exist [14-17], making our zebrafish mutant a key advancement for studying the role of citrullination and for the identification of specific PADI substrates in these diseases.

The role of Padi2 and citrullination in regeneration

In chapter 3, we explored the role of citrullination during fin regeneration using our *padi2* mutant zebrafish line and found that Padi2-deficient larvae had impaired fin regrowth following tail transection. Future work is needed to identify Padi2's direct mechanism during regeneration. Our study uncovered two possible roles for citrullination during regeneration. First, *padi2* mutant larvae had increased and sustained neutrophil presence at the wound which could be the cause of the regeneration delay. Secondly, we observed impaired cell proliferation in the *padi2* mutants, indicating an underlying defect in blastema function. These citrullination-deficient larvae lacked damage-induced histone citrullination and hedgehog signaling in a specialized population of cells.

We observed that Padi2 is necessary for regulating neutrophil migration to the wound site. Excessive or persistent neutrophil infiltration at a wound impairs wound healing and regeneration, emphasizing the importance of understanding how neutrophil recruitment and resolution are regulated. In the future, live imaging of neutrophil migration in a wounded fin will allow us to dissect whether citrullination is required for neutrophil recruitment or neutrophil resolution. Cell tracking of migrating neutrophils will allow us to determine whether the increased neutrophil numbers at the wound in the Padi2-deficient larvae reflect a continuous recruitment of new neutrophils to the wound or are due to a failure in properly recruited neutrophils to leave the wound site. Additionally, to determine if the observed regeneration defect in the Padi2 mutant larvae is a biproduct of the excessive neutrophil presence at the wound, we could impair neutrophil migration out of the hematopoietic tissue by crossing the *padi2* mutant to our previously published neutrophil specific dominant-negative Rac2^{D57N} zebrafish line (*tg(mpx:mCherry-Rac2^{D57N})*) [18]. If a lack of neutrophil recruitment to a wound is sufficient to restore regeneration when compared to wildtype; *mpx:mCherry-Rac2^{D57N}* larvae, this will provide evidence that citrullination mediates wound healing through promoting proper neutrophil dynamics at a wound.

Previous work from our laboratory identified a mechanism for neutrophil recruitment and resolution in which Cxcl8 binding to its chemokine receptors, Cxcr1 and Cxcr2, mediated these two phases of migration [19]. Citrullination of chemokines, including citrullination of human CXCL8, has been reported [20]. Citrullination of CXCL8 impaired cleavage to its more potent chemoattractant form [20]. *In vitro* assays demonstrated that citrullinated CXCL8 increases its binding efficiency to CXCR1, but

not CXCR2 when compared to the full length CXCL8 [20]. In the context of our *in vivo* model, we propose that citrullination of Cxcl8 dampens excessive Cxcl8 signaling produced at the wound and limits neutrophil recruitment through competition for Cxcr1 binding. Once at a wound, neutrophils will then favor Cxcr2 binding to the cleaved form of Cxcl8 to promote chemokinesis and eventual neutrophil resolution [19].

We hypothesize that in the *padi2* mutant larvae, citrullination is lost at the wound, resulting in the loss of the Cxcl8 signal dampening mechanism. Future work should focus on the identification of a cleaved form of Cxcl8 in the zebrafish as well as citrullination sites through mass spectrometry. Recruitment activity could be assessed in the zebrafish through protein injections into the otic vesicle and quantification of the degree of neutrophil recruitment to cleaved Cxcl8 or citrullinated Cxcl8. Eventually, point mutations could be made to any identified citrullination sites within the zebrafish Cxcl8 and neutrophil dynamics to a wound can be examined. We cannot rule out that citrullination of other chemokines or extracellular matrix components may also affect neutrophil recruitment and should also be explored.

We proposed another mechanism by which Padi2 is required for regeneration through the promotion of a stem-cell like population of cells necessary to promote wound-proliferation. Recent works have linked citrullination of histones and chromatin modifiers to open chromatin conformation and expression of pluripotency genes in stem cells [21-23]. Our work identified a wound-induced Padi2-dependent citrullination of histones within a discrete population of cells. Loss of histone citrullination in the *padi2* mutants was accompanied with a decrease in wound proliferation. We hypothesize that this histone citrullination promotes a naïve state within these cells and the formation of a

population of stem-cell like cells in the premature blastema to support later regenerative proliferation and regrowth.

While it is known that the blastema is required for regeneration, the source of these blastema cells remains unknown. Previous hypotheses for the source of blastemal cells include formation through the transdifferentiation of terminally differentiated cells into a stem-cell population to repopulate multiple cell types, a population of lineage restricted cells that proliferate to restore the individual cell types, or a source of quiescent stem-cells activated after wounding [24-27]. The zebrafish model is especially advantageous for determining the origin of these cells due to the ease of imaging within the transparent tissue and the availability of a wide number of labeled cell lines including keratinocytes, fibroblasts, and neurons, all present within the fin [28-30]. In the future, using fluorescently labeled lines, we could investigate which cell lineage contributes to the population of cells with citrullinated histones after wounding.

Neurons and the spinal cord are necessary for proper regeneration as shown in multiple limb regeneration models [31, 32]. Our work demonstrated that neuromuscular junctions were abnormal in the developing larvae. Future work using mosaic expression of fluorescently-labeled regenerating sensory neurons in the *padi2* mutant fin should be done to assess whether Padi2 altered regeneration through a role in the nervous system. For all candidate blastema sources, cell-specific rescues of Padi2 can be made in the mutant genetic background to determine if the specific cell rescue is sufficient to restore histone citrullination activity and proper regeneration.

A final question regarding the mechanism of citrullination's regulation on regeneration is how Padi2 is activated at the wound. While several mechanisms for citrullination regulation exist, calcium coordination is the most attractive candidate. Following wounding there is a large influx of calcium which raises the intracellular calcium concentration [33-36]. We hypothesize that this wound-induced calcium activates Padi2 citrullination after wounding. Further studies should explore the source of calcium or enzymatic activation of Padi2. While several calcium inhibitors exist, they can be toxic when they are exposed to an entire organism. Our lab has shown that immediately following wounding there is a large wave of calcium followed by calcium flashes in individual cells. Quickly after wounding (~5-8 minutes), the fin contracts and there is sustained calcium signal at the wound edge and in slightly proximal regions. In the future, we intend to test whether wound contraction activates a second calcium signal at the wound through the opening of stretch-activated channels and whether these channels provide the calcium activation for Padi2-mediated histone citrullination at the wound.

Long term work should focus on the examination of an evolutionary role of PADI2 in regeneration through other animal wound models. For example, the *Xenopus* model also has a single Padi enzyme; therefore, use of this model could be used to determine if tadpole tail regeneration occurs through a similar citrullination-dependent mechanism. Similar examination should then be done in the non-regenerating adult *Xenopus* wounds to determine if this mechanism is lost after development [37]. While mammals have limited regenerative capacity, the mammalian liver is able to proliferate and recover lost tissue weight [38]. Examination of citrullination in a murine liver

regeneration model could help determine if there is a universal role for PADI2 in regenerating tissues. To investigate whether PADI2 promotes hepatocyte plasticity, PADI2 could be ectopically expressed in mature hepatocytes to determine if PADI2 is able to promote dedifferentiation and proliferation. Additionally, to determine if PADI2 has a positive role in healing, the degree or rate of liver regeneration could be measured in injured livers that have exogenous expression of PADI2 in the liver progenitor cells. Eventually, this work should move to non-regenerating mammalian wounds to determine if exogenous PADI2 activation can improve mammalian wound healing.

In summary, we believe that the Padi- and citrullination-deficient zebrafish model we developed will be a powerful system in the study of citrullination in diseases and wound healing. The complexity of the mammalian PADIs limits the ability to identify therapeutic targets in the context of citrullination-implicated diseases, including cancers, rheumatoid arthritis, and multiple sclerosis. Examining these disease models in the *padi2* mutant zebrafish will allow for dissection of the role of citrullination in disease pathogenesis and inflammation and will provide a model to test preclinical therapeutics. Additionally, citrullination in disease has been associated with inflammation and a negative role for PADI4 has been reported in wound healing [39-41]. Our work demonstrates the importance of understanding the regulation and balance of pro- and anti-regenerative processes. We argue that, in addition to understanding how to ameliorate immune response to excessive or improper citrullination, harnessing PADI2 activity to promote proliferation could have great implications on improving human wound healing.

References

1.   Vossenaar ER, Zendman AJ, van Venrooij WJ, Pruijn GJ. PAD, a growing family of citrullinating enzymes: genes, features and involvement in disease. Bioessays. 2003;25(11):1106-18.

2.   Arita K, Hashimoto H, Shimizu T, Nakashima K, Yamada M, Sato M. Structural basis for Ca(2+)-induced activation of human PAD4. Nat Struct Mol Biol. 2004;11(8):777-83.

3.   Liu YL, Tsai IC, Chang CW, Liao YF, Liu GY, Hung HC. Functional roles of the non-catalytic calcium-binding sites in the N-terminal domain of human peptidylarginine deiminase 4. PLoS One. 2013;8(1):e51660.

4.   Slade DJ, Fang P, Dreyton CJ, Zhang Y, Fuhrmann J, Rempel D, et al. Protein arginine deiminase 2 binds calcium in an ordered fashion: implications for inhibitor design. ACS Chem Biol. 2015;10(4):1043-53.

5.   Esposito G, Vitale AM, Leijten FP, Strik AM, Koonen-Reemst AM, Yurttas P, et al. Peptidylarginine deiminase (PAD) 6 is essential for oocyte cytoskeletal sheet formation and female fertility. Mol Cell Endocrinol. 2007;273(1-2):25-31.

6.   Zhang X, Liu X, Zhang M, Li T, Muth A, Thompson PR, et al. Peptidylarginine deiminase 1-catalyzed histone citrullination is essential for early embryo development. Sci Rep. 2016;6:38727.

7.   Falcao AM, Meijer M, Scaglione A, Rinwa P, Agirre E, Liang J, et al. PAD2-Mediated Citrullination Contributes to Efficient Oligodendrocyte Differentiation and Myelination. Cell Rep. 2019;27(4):1090-102 e10.

8.   Hines JH, Ravanelli AM, Schwindt R, Scott EK, Appel B. Neuronal activity biases axon selection for myelination in vivo. Nat Neurosci. 2015;18(5):683-9.

9.   Flanagan-Steet H, Fox MA, Meyer D, Sanes JR. Neuromuscular synapses can form in vivo by incorporation of initially aneural postsynaptic specializations. Development. 2005;132(20):4471-81.

10.   Uemura O, Okada Y, Ando H, Guedj M, Higashijima S, Shimazaki T, et al. Comparative functional genomics revealed conservation and diversification of three enhancers of the isl1 gene for motor and sensory neuron-specific expression. Dev Biol. 2005;278(2):587-606.

11.   Wood DD, Bilbao JM, O'Connors P, Moscarello MA. Acute multiple sclerosis (Marburg type) is associated with developmentally immature myelin basic protein. Ann Neurol. 1996;40(1):18-24.

12. Moscarello MA, Wood DD, Ackerley C, Boulias C. Myelin in multiple sclerosis is developmentally immature. J Clin Invest. 1994;94(1):146-54.

13. Ishigami A, Ohsawa T, Hiratsuka M, Taguchi H, Kobayashi S, Saito Y, et al. Abnormal accumulation of citrullinated proteins catalyzed by peptidylarginine deiminase in hippocampal extracts from patients with Alzheimer's disease. J Neurosci Res. 2005;80(1):120-8.

14. Kulkarni P, Yellanki S, Medishetti R, Sriram D, Saxena U, Yogeeswari P. Novel Zebrafish EAE model: A quick in vivo screen for multiple sclerosis. Mult Scler Relat Disord. 2017;11:32-9.

15. Munzel EJ, Becker CG, Becker T, Williams A. Zebrafish regenerate full thickness optic nerve myelin after demyelination, but this fails with increasing age. Acta Neuropathol Commun. 2014;2:77.

16. Chung AY, Kim PS, Kim S, Kim E, Kim D, Jeong I, et al. Generation of demyelination models by targeted ablation of oligodendrocytes in the zebrafish CNS. Mol Cells. 2013;36(1):82-7.

17. Saleem S, Kannan RR. Zebrafish: an emerging real-time model system to study Alzheimer's disease and neurospecific drug discovery. Cell Death Discov. 2018;4:45.

18. Deng Q, Yoo SK, Cavnar PJ, Green JM, Huttenlocher A. Dual roles for Rac2 in neutrophil motility and active retention in zebrafish hematopoietic tissue. Dev Cell. 2011;21(4):735-45.

19. Powell D, Tauzin S, Hind LE, Deng Q, Beebe DJ, Huttenlocher A. Chemokine Signaling and the Regulation of Bidirectional Leukocyte Migration in Interstitial Tissues. Cell Rep. 2017;19(8):1572-85.

20. Proost P, Loos T, Mortier A, Schutyser E, Gouwy M, Noppen S, et al. Citrullination of CXCL8 by peptidylarginine deiminase alters receptor usage, prevents proteolysis, and dampens tissue inflammation. J Exp Med. 2008;205(9):2085-97.

21. Wiese M, Bannister AJ, Basu S, Boucher W, Wohlfahrt K, Christophorou MA, et al. Citrullination of HP1gamma chromodomain affects association with chromatin. Epigenetics Chromatin. 2019;12(1):21.

22. Christophorou MA, Castelo-Branco G, Halley-Stott RP, Oliveira CS, Loos R, Radzisheuskaya A, et al. Citrullination regulates pluripotency and histone H1 binding to chromatin. Nature. 2014;507(7490):104-8.

23. Xiao S, Lu J, Sridhar B, Cao X, Yu P, Zhao T, et al. SMARCAD1 Contributes to the Regulation of Naive Pluripotency by Interacting with Histone Citrullination. Cell Rep. 2017;18(13):3117-28.

24.   Brockes JP, Kumar A. Comparative aspects of animal regeneration. Annu Rev Cell Dev Biol. 2008;24:525-49.

25.   Knopf F, Hammond C, Chekuru A, Kurth T, Hans S, Weber CW, et al. Bone regenerates via dedifferentiation of osteoblasts in the zebrafish fin. Dev Cell. 2011;20(5):713-24.

26.   Tu S, Johnson SL. Fate restriction in the growing and regenerating zebrafish fin. Dev Cell. 2011;20(5):725-32.

27.   Singh SP, Holdway JE, Poss KD. Regeneration of amputated zebrafish fin rays from de novo osteoblasts. Dev Cell. 2012;22(4):879-86.

28.   LeBert D, Squirrell JM, Freisinger C, Rindy J, Golenberg N, Frecentese G, et al. Damage-induced reactive oxygen species regulate vimentin and dynamic collagen-based projections to mediate wound repair. Elife. 2018;7.

29.   Gong Z, Ju B, Wang X, He J, Wan H, Sudha PM, et al. Green fluorescent protein expression in germ-line transmitted transgenic zebrafish under a stratified epithelial promoter from keratin8. Dev Dyn. 2002;223(2):204-15.

30.   Sagasti A, Guido MR, Raible DW, Schier AF. Repulsive interactions shape the morphologies and functional arrangement of zebrafish peripheral sensory arbors. Curr Biol. 2005;15(9):804-14.

31.   Rieger S, Sagasti A. Hydrogen peroxide promotes injury-induced peripheral sensory axon regeneration in the zebrafish skin. PLoS Biol. 2011;9(5):e1000621.

32.   Kumar A, Brockes JP. Nerve dependence in tissue, organ, and appendage regeneration. Trends Neurosci. 2012;35(11):691-9.

33.   Xu S, Chisholm AD. A Galphaq-Ca(2)(+) signaling pathway promotes actin-mediated epidermal wound closure in C. elegans. Curr Biol. 2011;21(23):1960-7.

34.   Shannon EK, Stevens A, Edrington W, Zhao Y, Jayasinghe AK, Page-McCaw A, et al. Multiple Mechanisms Drive Calcium Signal Dynamics around Laser-Induced Epithelial Wounds. Biophys J. 2017;113(7):1623-35.

35.   Yoo SK, Freisinger CM, LeBert DC, Huttenlocher A. Early redox, Src family kinase, and calcium signaling integrate wound responses and tissue regeneration in zebrafish. J Cell Biol. 2012;199(2):225-34.

36.   Franklin BM, Voss SR, Osborn JL. Ion channel signaling influences cellular proliferation and phagocyte activity during axolotl tail regeneration. Mech Dev. 2017;146:42-54.

37.	Sanchez Alvarado A, Tsonis PA. Bridging the regeneration gap: genetic insights from diverse animal models. Nat Rev Genet. 2006;7(11):873-84.

38.	Gilgenkrantz H, Collin de l'Hortet A. Understanding Liver Regeneration: From Mechanisms to Regenerative Medicine. Am J Pathol. 2018;188(6):1316-27.

39.	Makrygiannakis D, af Klint E, Lundberg IE, Lofberg R, Ulfgren AK, Klareskog L, et al. Citrullination is an inflammation-dependent process. Ann Rheum Dis. 2006;65(9):1219-22.

40.	Wong SL, Demers M, Martinod K, Gallant M, Wang Y, Goldfine AB, et al. Diabetes primes neutrophils to undergo NETosis, which impairs wound healing. Nat Med. 2015;21(7):815-9.

41.	Coudane F, Mechin MC, Huchenq A, Henry J, Nachat R, Ishigami A, et al. Deimination and expression of peptidylarginine deiminases during cutaneous wound healing in mice. Eur J Dermatol. 2011;21(3):376-84.

Appendix

Loss of Padi2 improves zebrafish survival during *Aspergillus fumigatus* infection

Netta Golenberg, Emily E. Rosowski, Chad J. Johnson, Jeniel E. Nett, Nancy P. Keller, and Anna Huttenlocher

Author contributions: NG performed and analyzed experiments. EER performed hindbrain infections of *Aspergillus.* NPK provided *Aspergillus* spores. JEN provided *Candida* and CJJ prepared *Candida* yeast. AH designed experiments.

Results

Neutrophil extracellular traps (NETs) are comprised of a network of DNA and granule proteins extruded by neutrophils in response to large pathogens that cannot be engulfed by cells of the innate immune system [1, 2]. PADI4 and its citrullination of histones have been reported to contribute to the formation to NETs to select stimuli [3]. The fungus, *Aspergillus* is an interesting pathogen to study because it infects a host as a spore and then germinates within the body to produce large hyphal structures [4]. To examine the role of Padi2 in zebrafish *Aspergillus* infection, *padi2* mutants and wild-type larvae were infected with spores of the patient-derived *Aspergillus fumigatus* strain CEA10 in the larval hindbrain. Larval survival was monitored for 7 days post infection (dpi). While both mutant and wild-type larvae survived mock PBS hindbrain injections, wild-type larvae succumbed to infection at a greater proportion than $padi2^{-/-}$ larvae (Fig 4.1A). In fact, the hazard ratio revealed that wildtype larvae were ~7 times more likely to die following CEA10 infection than Padi2-deficient larvae. To determine whether this trend was strain specific, we infected related larvae with another patient derived *A. fumigatus* strain, Afs35, which is more consistently pathogenic. While we did see death in the *padi2* mutant larvae following Afs35 infection, wild-type larvae had an even greater amount of death following infection, with wild-type larvae having ~3 times the risk of death compared to $padi2^{-/-}$ larvae (Fig 4.1B).

NETs play a crucial role in preventing the dissemination of infection during sepsis but this dramatic inflammatory response also carries detrimental results. Both circulating histones and the proteases associated with NETs contribute to resident tissue damage [2]. Extracellular histones can act as a chemokine promoting the release of
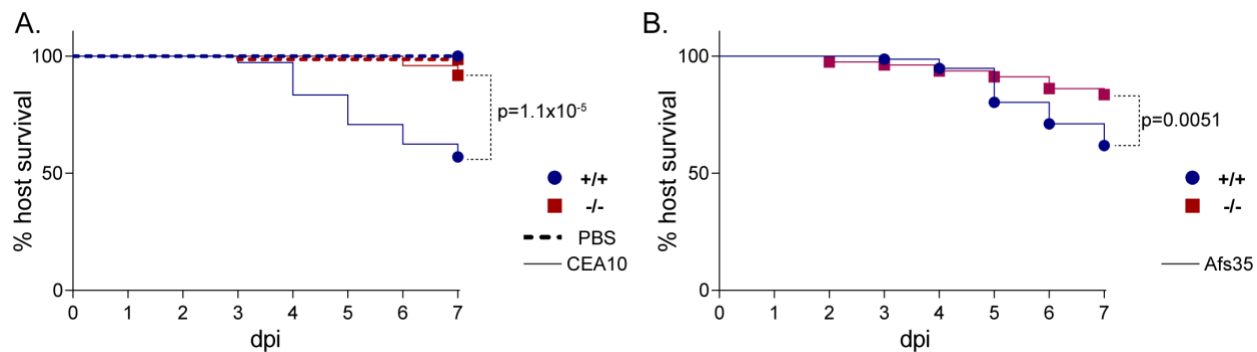
Fig 4.1: Padi2 mutants have increased survival advantage during Aspergillus fumigatus infection. (A) Unrelated wildtype and *padi2⁻/⁻* larvae were infected with *A. fumigatus* (CEA10) and larval survival was monitored. Hazard ratio: 7.169. Data represents three independent pooled experiments with n= 72 wildtype and n= 70 and 73 for -/- PBS or *A. fumigatus* infected larvae. Average injection CFUs: 38. (B) Wildtype cousins and *padi2⁻/⁻* larvae were infected with *A. fumigatus* (Afs35) and larval survival was monitored. Hazard ratio: 2.551. Data represents three independent pooled experiments with n= 76 +/+, 79 -/-. Average injection CFUs: 34.

proinflammatory cytokines and inducing apoptosis of nearby cells. Direct *in vivo*
evidence has shown DNAse treatment during sepsis attenuated tissue damage and
improved survival [5, 6].

Our hypothesis, based on our preliminary data, is that *Aspergillus* infection
promotes NET formation which causes resident tissue damage leading to increased
zebrafish death. We, therefore, postulate that the *padi2* mutants are able to fight
infection using NET-independent macrophage and neutrophil functions. Additionally, the
loss of citrullination in these mutants inhibits these larvae's ability to form NETs,
increasing their survival by reducing tissue damage. Interesting future experiments
should monitor pathogen survival in the host over time using CFU counts to determine
whether these zebrafish have differential clearance rates of the fungal spores.
Additionally, mammalian PADI4 is thought to be responsible for citrullination-dependent
NET formation [3]; therefore, it will be important to determine if zebrafish NET formation
is Padi2-dependent. This can be done either by examining extracellular-neutrophil DNA
as previously described [7] or by imaging using immunofluorescent markers to visualize
colocalization of the granule protein myeloperoxidase with neutrophil DNA in the brain
as shown in Fig 4.2 following infection with the fungal pathogen *Candida albicans*.
Staining for granule protein and neutrophil DNA allowed for the visualization of intact
nuclei and NETosing neutrophils (Fig 4.2A). In brains with a high amount of
germination, a large network of neutrophil DNA and myeloperoxidase was seen
associated with fungal hyphae, and the DNA was captured coating hyphae (Fig 4.2B).
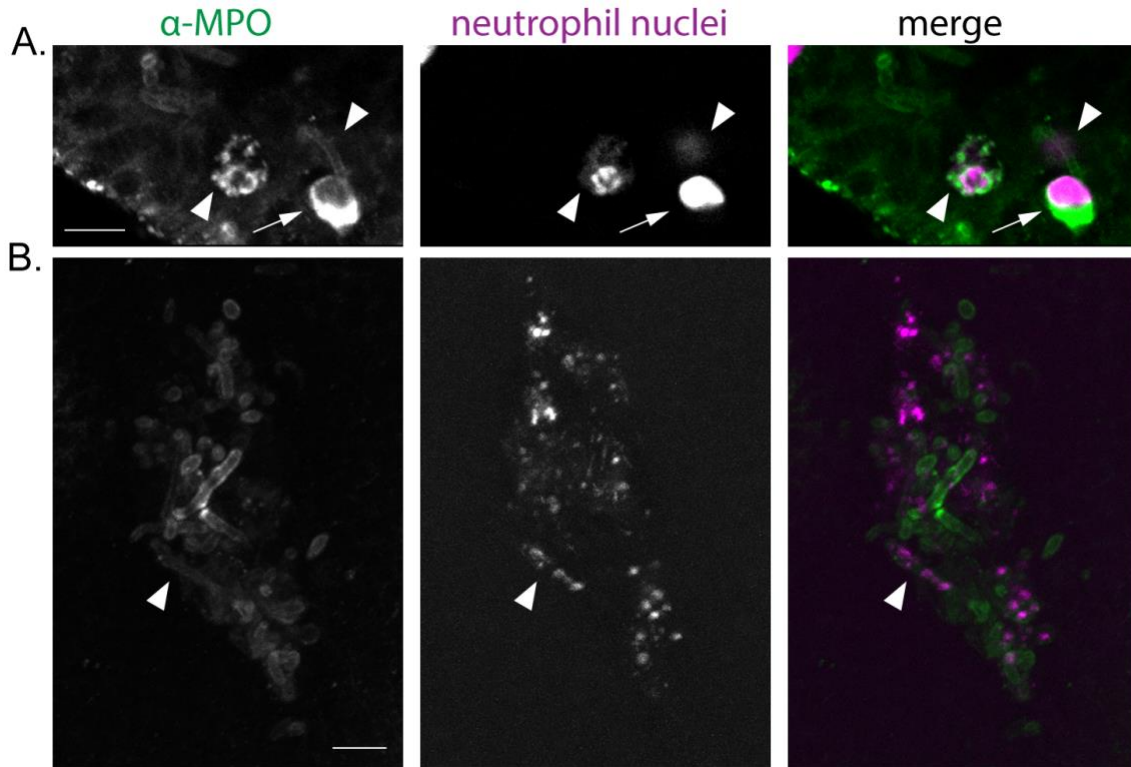While this work has been done on zebrafish infected with another fungal pathogen,

Fig 4.2: NETs are observed in wildtype larvae brains infected with Candida albicans Representative images of dissected brains from mCherry-labeled neutrophil nuclei transgenic larvae (*Tg(lyzc:H2B-mCherry)*) infected with Candida albicans immunostained for α-zebrafish myeloperoxidase (MPO). Scale bars= 10 μm. Arrow indicates healthy neutrophil and arrow heads indicate NETs. (A) Single plane image and (B) maximum Z- projection from two independent larval brains representative of 7 imaged brains from a single replicate.

Candida albicans, it would be interesting to do similar work in *Aspergillus* infected brains.

Materials and methods

Fungal infection and CFU counts

Aspergillus fumigatus CEA10 strain TFYL49.1 and Afs35 were used in this study. Spores were grown and injected into the hindbrain of 2 days post fertilization (dpf) larvae as previously described [8]. For survival, larvae were maintained in individual wells of a 96-well plate and survival was monitored for the next seven days post infection. Infectious doses were prepared to consist of ~30 spores per larvae. Actual initial spore doses were determined by single larvae colony forming units (CFU) on day 0 of infection and are reported in the figure legends. CFUs were determined by placing single larvae in a 1.5 microcentrifuge tube with 90 μL of 1xPBS containing 500 μg/mL Kanamycin and 500 μg/mL Gentamycin and were homogenized in a mini bead beater at maximum speed for 15 seconds. The entire volume was plated on a 10 cm Gut Microbiota Medium (GMM) plate and incubated for two days at 37°C at which point CFUs were counted and recorded. For each experiment, at least 8 larvae were individually plated for the initiation CFU dose.

Larval brain immunofluorescence

Candida albicans infections were done as previously described [9] with hindbrain microinjections as performed as described above [8]. Infectious doses were prepared to consist of 10-20 yeast per injection. 2-day post infection zebrafish were fixed in 4% paraformaldehyde and 0.125 M sucrose in PBS for a couple of hours at room

temperature. Larvae were washed three times with PBS and the larval brain was dissected and collected. Larval brains were incubated in collagenase (0.1% w/v in 0.1M phosphate buffer) for 2 hours at room temperature. Brains were washed with an incubation buffer (0.2% BSA, 2% goat serum, 0.5% Triton-X, and 1% DMSO in PBS), twice quickly, followed by three-30 minute washes, and with a final 60 minute block. A primary polyclonal rabbit anti-zebrafish myeloperoxidase antibody [10] was added to the samples at 1:50 dilution and incubated overnight at 4°C. Washes were done in incubation buffer and Dylight 488 anti-rabbit IgG secondary antibody as added for 4 hours at room temperature. Brains were mounted onto glass slides in vectashield. Images were acquired on a laser-scanning confocal microscope (FluoView FV1000; Olympus) with an NA 0.75/20x or UPlanFLN NA 1.30/40x oil objective and FV10-ASW software (Olympus).

Statistical analyses

For larval survival data, 3 independent replicates were pooled and analyzed by Cox proportional hazard regression analysis, with experimental replicates included as a group variable. P values and hazard ratios are reported. The hazard ratio represents the relative risk of death between two conditions. Experimental replicates with less than 10% death in the wildtype condition for *A. fumigatus* CEA10 infections were excluded. Statistical analyses and graphical representations were done in R version 3.4 and GraphPad Prism version 6.

References

1.   Brinkmann V, Reichard U, Goosmann C, Fauler B, Uhlemann Y, Weiss DS, et al. Neutrophil extracellular traps kill bacteria. Science. 2004;303(5663):1532-5.

2.   Li RHL, Tablin F. A Comparative Review of Neutrophil Extracellular Traps in Sepsis. Front Vet Sci. 2018;5:291.

3.   Holmes CL, Shim D, Kernien J, Johnson CJ, Nett JE, Shelef MA. Insight into Neutrophil Extracellular Traps through Systematic Evaluation of Citrullination and Peptidylarginine Deiminases. J Immunol Res. 2019;2019:2160192.

4.   Dagenais TR, Keller NP. Pathogenesis of Aspergillus fumigatus in Invasive Aspergillosis. Clin Microbiol Rev. 2009;22(3):447-65.

5.   Mai SH, Khan M, Dwivedi DJ, Ross CA, Zhou J, Gould TJ, et al. Delayed but not Early Treatment with DNase Reduces Organ Damage and Improves Outcome in a Murine Model of Sepsis. Shock. 2015;44(2):166-72.

6.   Czaikoski PG, Mota JM, Nascimento DC, Sonego F, Castanheira FV, Melo PH, et al. Neutrophil Extracellular Traps Induce Organ Damage during Experimental and Clinical Sepsis. PLoS One. 2016;11(2):e0148142.

7.   Johnson CJ, Davis JM, Huttenlocher A, Kernien JF, Nett JE. Emerging Fungal Pathogen Candida auris Evades Neutrophil Attack. MBio. 2018;9(4).

8.   Knox BP, Deng Q, Rood M, Eickhoff JC, Keller NP, Huttenlocher A. Distinct innate immune phagocyte responses to Aspergillus fumigatus conidia and hyphae in zebrafish larvae. Eukaryot Cell. 2014;13(10):1266-77.

9.   Brothers KM, Newman ZR, Wheeler RT. Live imaging of disseminated candidiasis in zebrafish reveals role of phagocyte oxidase in limiting filamentous growth. Eukaryot Cell. 2011;10(7):932-44.

10.   Mathias JR, Perrin BJ, Liu TX, Kanki J, Look AT, Huttenlocher A. Resolution of inflammation by retrograde chemotaxis of neutrophils in transgenic zebrafish. J Leukoc Biol. 2006;80(6):1281-8.